ASPECTS OF GLENOID COMPONENT WEAR AND DISASSEMBLY IN THE NOTTINGHAM TOTAL SHOULDER ARTHROPLASTY

Doctor of Philosophy Thesis

Gyorgy Kocsis

September 2018



The University of Nottingham

UNITED KINGDOM · CHINA · MALAYSIA

Abstract

Introduction

Glenoid component wear and loosening is the Achilles heel of total shoulder replacement. Analysis of failed, revised implants may give an insight into the causes of component failure.

The Nottingham Total Shoulder Arthroplasty System (NTSA) is an anatomical prosthesis design with an UHMWPE bearing captured onto a metal glenoid baseplate. The two most frequent modes of failure were component loosening and polyethylene bearing disassembly from the metal glenoid baseplate.

Component loosening is complex; an insight into the mechanisms is provided by a comprehensive literature review. As polyethylene wear plays a central role in the process, volumetric assessment of the NTSA glenoid liner wear rate and scanning electron microscopy were carried out in this study. For 3D scanning of ex vivo implants, the use of coherence scanning interferometry (white light scanner) was proposed, acquiring 3D images without contact, ionising radiation or extensive surface preparation.

A potential mechanism for the UHMWPE bearing disassembly from the metal glenoid baseplate - vacuum forces between the glenoid liner and the artificial humeral head components - is suggested from this work.

Methods

Polyethylene glenoid liner wear analysis

Twenty-four Nottingham total shoulder replacement metal-back glenoid liners were explanted from revision shoulder arthroplasty cases. A Phase Vision Quartz DBE 800 scanner was used to scan the explanted polyethylene liners. The images of worn liners were registered to the reference image. Differences in wear and wear rate were quantified and central and non-central wear groups were distinguished.

A Hitachi S-2600N Variable Pressure Scanning Electron Microscope (VPSEM) was used.

Vacuum phenomenon

New NTSA components were mounted on a materials test machine, surrounded by bovine synovial fluid which was restrained by a commercially available latex condom. Forces were measured continuously as the components were quickly distracted from each other.

The force that may lead to glenoid disassembly was approximated using cyclic testing. The glenoid component of the NTSA system was mounted on the tensile test machine and the polyethylene liner was repeatedly pushed outwards, along an axis perpendicular to the plane of the baseplate, using 40N, 60N, 80N and 300N of force.

Results

Polyethylene glenoid liner wear analysis

The central wear group had a polyethylene wear rate of 115 ± 55mm^3/year (mean ± SD). The non-central group showed a wear rate of 112 ± 42 mm^3/year (mean ± SD), which was not significantly different from the central wear group (p=0.426) Polyethylene liners with rapid edge wear showed a wear rate of 545 mm^3/year. Scanning electron microscopy images showed that the polyethylene was wearing in laminar flakes which indicated fatigue wear.

Vacuum phenomenon

The vacuum tests showed a peak force of 50.4N (SD 3.8) from which an average of 10.2N (SD 0.015) was attributed to the resistance of the artificial capsule; thus, approximately 40N of vacuum force was present.

An SN (stress versus number of cycles) curve for push-out failure load for the plastic liner was prepared and failure at 12500 cycles was predicted for the vacuum forces that we observed in the actual vacuum forces measurements.

Conclusion

The volumetric wear rate was found to be faster than data suggested by previous studies on all polyethylene cemented glenoid components and

more than twice as fast as in the case of total hip replacement with the acetabular liner made of the same type of polyethylene. Use of coherence scanning interferometry is proposed for wear analysis.

Vacuum forces may play an important role in glenoid component disassembly in the NTSA system.

Acknowledgement

I thank my supervisors, Professor Angus Wallace, Professor Donal McNally and Professor Roger Bayston for their time, never-ending patience and support.

I thank Biomet UK for their support by providing me with original implant mechanical test results and implants for our tests.

Special thanks to Charlie Payne for his know-how in accomplishing the white-light scans.

I am very grateful to Mark Francis-Parry, manager in the Biomechanics lab for preparing the jigs and bobs.

I am indebted to the School of Veterinary Medicine and Science of the University of Nottingham for kindly providing me with bovine synovial fluid for the experiments.

Statement of originality

This thesis and the work described in it are my own work, except as may be otherwise indicated. The dissertation does not contain material that has already been used to any substantial extent for a comparable purpose.

The university standard form for declaration of originality has also been submitted as per relevant regulations.

Contents

Abstract 1

Acknowledgement 4

List of abbreviations 7

1.0 Introduction 8

2.0 General considerations 15

2.1 History of anatomical shoulder arthroplasty 15

2.2 Literature overview 20

3.0 Hypotheses and aims 78

3.1 Hypothesis 1. 78

3.2 Hypothesis 2. 78

4.0 Hypothesis 1. The vacuum phenomenon within a total shoulder replacement causing glenoid component dissociation – a novel observation 79

4.1 Introduction 79

4.2 Materials and methods 84

5.0 Hypothesis 2. Wear analysis of explanted conventional metal back polyethylene liners 103

5.1 Introduction 103

5.2 Materials and methods 106

5.3 Results 111

5.4 Discussion 120

5.5 Conclusions 124

6.0 Combined discussion of Hypotheses 125

7.0 References 133

List of abbreviations

AOANJRR	Australian Orthopaedic Association National Joint Replacement Registry
HA	Hyaluronic acid
MOM	Metal-on-Metal
NTSA	Nottingham Total Shoulder Arthroplasty
SN curve	Stress versus Number of Cycles curve
Ti	Titanium
TSA	Total Shoulder Arthroplasty
TSR	Total Shoulder Replacement
UK NJR	National Joint registry, United Kingdom
RSA	Radiostereometric analysis

Glossary of terms

Disassembly	Assembled components separate into parts
Dislocation	The ball of a joint leaves the socket
Dissociation	Two otherwise connected components of an artificial joint become uncoupled
Eccentric	Not positioned centrally
Metaphysis	The wider part at the end of the shaft of a long bone, adjacent to the growth plate

ASPECTS OF GLENOID COMPONENT WEAR AND DISASSEMBLY IN THE NOTTINGHAM TOTAL SHOULDER ARTHROPLASTY

1.0 Introduction

This PhD project was designed to investigate certain aspects of glenoid component failure in the Nottingham Total Shoulder Arthroplasty (NTSA) which is the most common cause of failure in total shoulder arthroplasty.[1, 2]

The Nottingham Total Shoulder Arthroplasty system was developed by the inventor – Professor Angus Wallace & his colleague Mr Lars Neumann with the Biomet Company in 1991. The first prototype was inserted in May 1991 and the first definitive Nottingham Total Shoulder replacement with an offset humeral head was inserted in October 1993. This device was chosen as the subject of this work, as a large, well maintained database is available at the Nottingham City Hospital, Nottingham University Hospitals, UK, as well as explants and imaging data.

The prosthesis was used for 16 years in the UK and Europe but the glenoid component was withdrawn from the market in 2009 (Personal communication with Professor Wallace) and marketing of this design was discontinued in 2010 when Biomet introduced the Comprehensive Shoulder System to replace it.

The main characteristics of the Nottingham TSR were:

1) The head was modular and could be mounted onto the stem with an offset peg which could be rotated in any direction, to optimise soft tissue balance and alignment
2) The metaphyseal part of the humeral stem was porous coated to achieve optimal fixation and eliminate stress shielding
3) The system was designed with conforming radii of humeral and glenoid components to avoid point wear of the polyethylene liner

4) Hydroxyapatite coating on the under-surface of the metal glenoid baseplate was applied to improve osteointegration onto the bony glenoid

5) The polyethylene liner was clipped on to the metal glenoid base plate using a newly designed capture mechanism.[3]



Figure 1. The Nottingham Total Shoulder Arthroplasty

The implanted device comprises the following components (Figure 1).

A) A Ti alloy glenoid baseplate is inserted and screwed onto the bony glenoid, after bone preparation, using two titanium alloy screws

B) The Ti alloy humeral stem has a reverse taper fitting onto which a cobalt chrome alloy head is mounted

C) An Ultra High Molecular Weight Polyethylene (UHMWPE) liner or bearing component which is clipped into:

D) The glenoid baseplate to articulate with the head component. This UHMWPE socket was designed to be fully congruent with the head component. The design of the baseplate and liner was intended to ensure that the liner is clipped solidly and irreversibly onto the metal glenoid baseplate.

The overall performance of the Nottingham TSR was assessed by looking at the survival, as part of this project. For the analysis the Nottingham Total Shoulder Replacement Database was used. Total shoulder arthroplasty cases were identified and selected. The survival analysis included 314 cases, which were all the primary total shoulder replacement cases carried out at the Nottingham City Hospital between 1997 and 2009. Some cases had to be excluded from the analysis: 86 patients for missing data, there were 9 unrelated deaths and 3 patients were lost to follow up. Survival statistics were prepared following the Kaplan-Meier method.

The Kaplan-Meier analysis is shown in Figure 2.

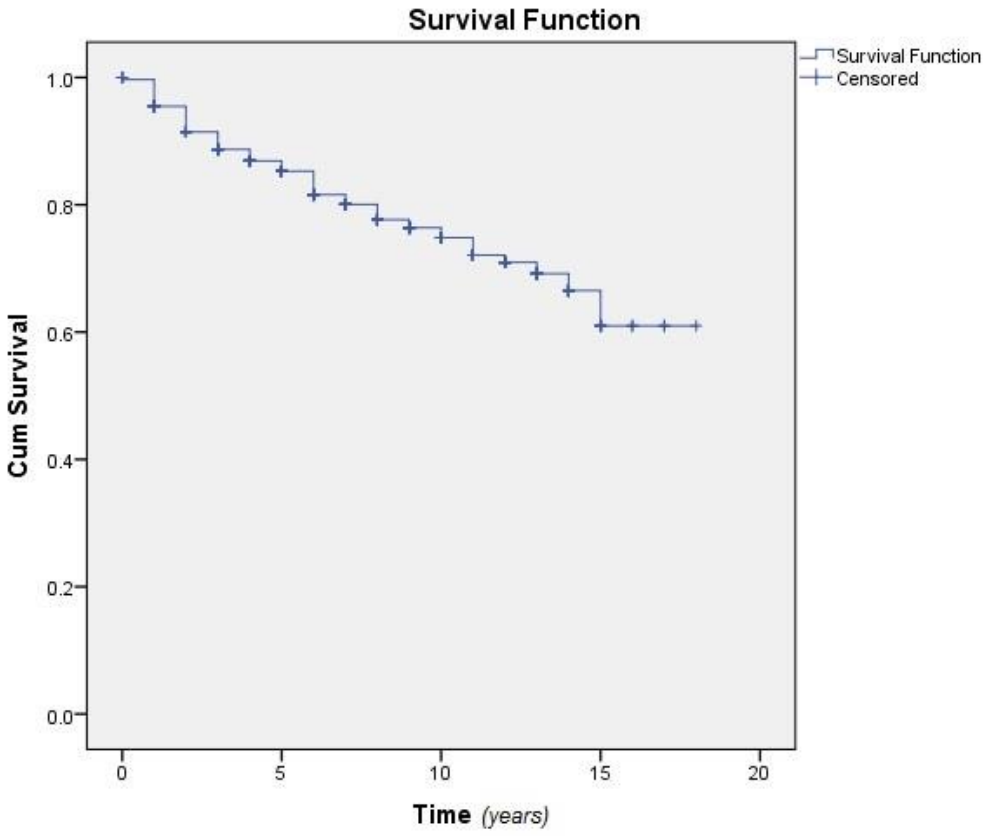


Figure 2. Survival analysis of the Nottingham total shoulder system; time measured in years

The statistical analysis was carried out using SPSS (IBM Analytics, Armonk, USA).

Implant survival seems to be inferior to desirable.[3] This may be due to a number of factors including the use of non-highly crosslinked polyethylene. This Research Programme aims to focus on the faults of this system rather than comparing the Nottingham TSRA system with the competitors of the time.

How do anatomical, or conventional total shoulder replacements fail?

The causes for revision in anatomical TSR systems have been analysed in the Australian Orthopaedic Association National Joint Replacement Registry (AOANJRR) (Table 1).[4]

Table ST25 Primary Total Conventional Shoulder Replacement by Reason for Revision

Reason for Revision	Number	Percent
Instability/Dislocation	194	24.2
Rotator Cuff Insufficiency	181	22.6
Loosening	132	16.5
Implant Breakage Glenoid Insert	88	11.0
Infection	50	6.2
Dissociation	29	3.6
Fracture	20	2.5
Incorrect Sizing	16	2.0
Pain	15	1.9
Arthrofibrosis	13	1.6
Metal Related Pathology	11	1.4
Wear Glenoid Insert	9	1.1
Malposition	8	1.0
Lysis	4	0.5
Other	32	4.0
TOTAL	**802**	**100.0**

Table 1. Causes for revision in conventional total shoulder arthroplasty in Australia for all TSA systems. Reproduced from AOANJRR.[4]

https://aoanjrr.sahmri.com/annual-reports-2017

Causes for revision have also been assessed by the National Joint Registry in the UK. The findings are summarised in Table 2.

Reason for revision	Total number of cases 168	Percentage
	Number of cases revised	
Infection	7	4.17
Instability	54	32.14
Cuff insufficiency	63	37.5
Aseptic loosening	15	8.93
Periprosthetic fracture	4	2.38

Table 2. Causes for revision in all Conventional total shoulder arthroplasty in the UK in 2017.[5] Reproduced from National Joint Registry 14th Report, 2017.
http://www.njrcentre.org.uk/njrcentre/Reports,PublicationsandMinutes/Annualreports/tabid/86/Default.aspx

Based on the UK figures it is not possible to differentiate between glenoid and humeral component-related problems. The Australian registry is more specific but still does not differentiate between loosening around the glenoid or the humeral component.

In the case of the Nottingham TSR the mechanisms for the failures of the glenoid component were aseptic loosening and bearing disassembly, bearing disassembly being the second in incidence, as discussed by Rosenberg et al.[3]

The actual outcome of the metal glenoid baseplate fixation to the glenoid bone interface is better described by removing the cases with component disassembly from the survival analysis, as shown in Figure 3.

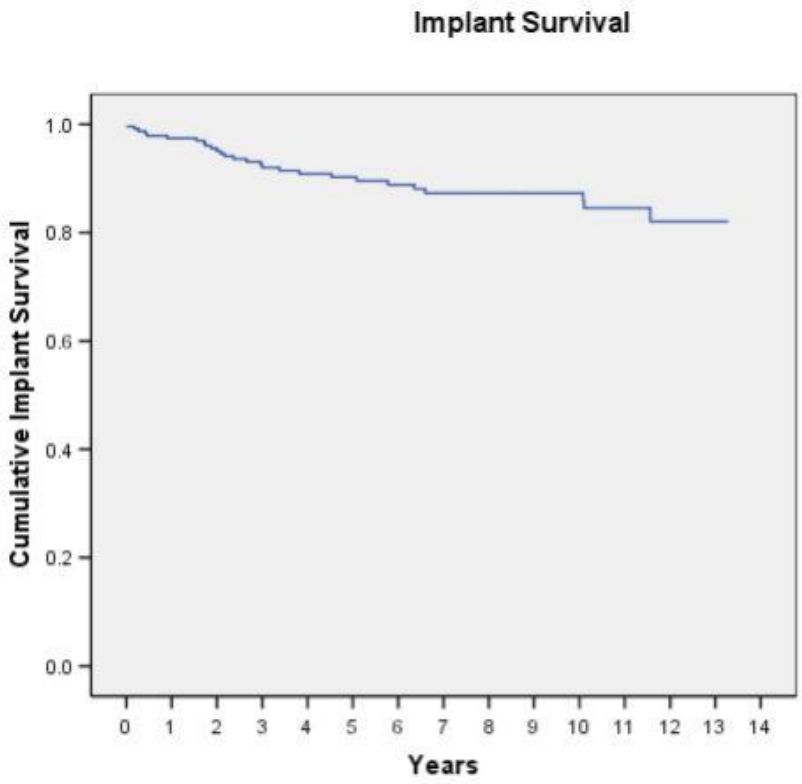


Figure 3. Kaplan Meier Glenoid Survival for Primary TSRs - hydroxyapatite coated uncemented glenoid components 1997 to 2010 (n=235). Unpublished data from W. A. Wallace, reproduced with permission.

Although pervasive conclusions must not be drawn, comparison of the latter survival figures is possible to current TSR data. The uncemented glenoid baseplate revision rate without the disassembly cases is 12.7%, whereas the overall revision rate of cemented TSA in the Australian cohort at 9 years is 6.3%.[4] This means that other than the high rate of disassembly, the survival figures of a metal back glenoid are still somewhat worse than those of the cemented equivalents. The primary reason for revision in the Nottingham cohort was aseptic loosening. Hence the assumption that aseptic loosening may contribute to this difference seems appropriate.

2.0 General considerations

2.1 History of anatomical shoulder arthroplasty

The story of shoulder arthroplasty should start with the innovative German surgeon, Themistocles Gluck. Gluck was born in Iasi, Moldavia (Moldova, now, in Romania) in 1853. Other than joint replacement, Gluck experimented with numerous surgical innovations, such as intramedullary fixation (with ivory cylinders), he used a steel plate to fix a broken femur and replaced part of a mandible. He also experimented with bone cements, including copper amalgam, plaster of Paris, and a stone putty (resin with pumice or gypsum). He described a number of surgical procedures for the larynx, trachea, lung, and inguinal hernias. It is interesting to note that he performed vessel sutures and venous grafts in the 1880s, which predated by many years the work of the American surgeon Alexis Carrel who received the Nobel prize for vascular repair in 1912.[6] Gluck tested his ideas in animal models before attempting them on humans. He designed and implanted artificial wrists, elbows, shoulders, hips, knees, and ankles. Although he experimented with other materials as well, because of its scope for integration Gluck eventually opted for cadaveric bone and ivory as raw material for his prostheses.

His shoulder prosthesis had an ivory humeral component fixed into the medullary canal of the humerus and this hooked into an ivory eye screwed into the glenoid.[7]

His results were overshadowed by early failure due to infection, a complication causing headaches to other pioneers of arthroplasty, such as Jules-Émile Péan.

Péan (1830-1898) was a French surgeon who lived in Paris. The first patient to receive a shoulder prosthesis from Péan was a 37 year old male patient with tuberculosis affecting his right shoulder and proximal humerus. As the patient refused amputation, Péan decided to replace the affected joint and bone segments. The new prosthesis was not designed by Péan, but was designed and constructed by a Parisian dentist. The stem was made of

platinum with screw holes distally. The head was a rubber ball, attached both to the shaft component and the glenoid by two platinum loops. Péan first resected the proximal half of the humerus and debrided all infected tissue. Once the infection settled, the prothesis was implanted as a second stage procedure, in 1882. The patient was claimed to be able to perform most every-day activities. A year later a discharging sinus appeared at the patient's elbow. Initially Péan tried to salvage the prosthesis joint by repeat attempts of surgical drainage, but eventually, about two years following the implantation the prosthesis had to be removed.[8] These failures removed the idea of total shoulder arthroplasty from mainstream thinking for decades.

In the 1950s various metal and plastic implants were designed and implanted.
From the scientific perspective, perhaps the most spectacular design was that of Frederick Krueger, in 1950. Krueger made acrylic moulds of proximal humeri to recreate original anatomy. His prosthesis was made of vitallium and had a medial and posterior offset. It was a stemmed design with holes through the stem for bone ingrowth.[9]
Some other designs were made of acrylic,[10, 11] polyamide[12] or of polyethylene.[13] Richard implanted humeral head acrylic prostheses for complex proximal humerus fractures otherwise more typically treated by bone resection. Functional results were poor in spite of attempts of rotator cuff reattachment to the acrylic humeral head.[10, 11] MacAusland used a polyamide prosthesis to treat a comminuted fracture dislocation of the proximal humerus with discouraging results.[12] The Royal National Orthopaedic Hospital in the UK reported their attempts to use four polyethylene proximal humeral prostheses implanted following tumour resection. The implants were secured with plates and screws to the distal humerus. All of the implants soon failed and one prosthesis fractured.[13] These plastic prostheses were eventually abandoned due to breakages and attrition caused by foreign body reactions.[14]

Charles S. Neer II[15] is generally considered to have started the modern era of shoulder replacements. He used a vitallium prosthesis to replace unreconstructably fractured proximal humeri. Later he expanded the indication for hemiarthroplasty to osteoarthritic shoulders. His early results were published in 1955. Neer introduced only minor modifications to his system over the coming years. Proper version of the prosthesis, sliding fulcrum with loose fitting glenoid - head interface and subscapularis repair were considered important. Until 1974 Neer almost exclusively performed non-cemented hemiarthroplasties.

In 1974 Neer introduced a total arthroplasty system. The Neer II humeral prosthesis was modified to conform to a glenoid component. The Neer III prosthesis was a constrained inverse prosthesis, but it was unsuccessful, and Neer eventually abandoned the idea of a constrained prosthesis.[16] Neer, in his famous paper in 1982 describes good results on a large patient series using polyethylene glenoid components.[16]

In 1982 Lettin and Scales published the results of 49 Stanmore total shoulder replacements from between 1969 and 1977.[17] The Stanmore prosthesis maintained the standard ball-and-socket gleno-humeral articulation, although with increased constraint. The functional improvement for the cohort was inconsistent and disappointing according to the authors, although an acceptable functional range of motion was achieved in most patients.

In the early 1990s a new generation of prosthetic joints was introduced. This generation of implants is often referred to as “second generation” (Biomet, Cofield, Global, for example). To try to match the dimensions of the native humeral head as well as the dimensions of the medullary canal, designers created implants with a wider choice of sizes. Most of these implants could not be adapted to suit the variations of the proximal humerus. The position of the stem (mostly press fit) determined the position of the head, often leading to mal-positioning the head in the horizontal and vertical planes compared to the original anatomy. This also affected the centre of rotation. The available head sizes often dictated the

surgeon to oversize the head. Long term results of this generation of prostheses were reported to be disappointing.[18]
Anatomical studies on the humeral head from the era found that the articular surface of the humerus was offset posteriorly and medially relative to the axis of the proximal metaphysis. Also, the head orientation in horizontal and vertical planes showed considerable variation.[19-21] The head - neck angle was also found to be variable.[22, 23]
The third generation of prostheses was introduced aiming to reproduce the original anatomy and through that the original biomechanics of the shoulder (Aequalis, for example).
The key concepts were resecting the humeral head precisely at the anatomical neck and adapting the implant to match retroversion. Reconstructing the original inclination, medial and posterior offset with an identical depth of head were considered crucial. Restoration of the individual lever arms of the rotator cuff muscles was attempted.[24]

As far as precise reproduction of the original humeral head special alignment is concerned, humeral head resurfacing, at least in theory, has very few rivals. Copeland's original (Mark I) cementless humeral component had a central peg which was locked with a screw from the lateral side of the proximal humerus. The system also had a polyethylene glenoid element stabilised by a cementless finned peg. The Mark-2 prosthesis was introduced in 1990. The securing screw was abandoned and the glenoid now had a metal backing and a fluted taper fit peg. Hydroxyapatite coating was added in 1993 to improve bone ingrowth, for the Mark III design.[25] Long term studies on shoulder hemiarthroplasty tended to report on glenoid erosion and pain which limited the use of hemiarthroplasties for OA.[26]
Neer introduced his glenoid component in 1972 to address glenoid erosion.[27] This was an oval-shaped all-polyethylene glenoid with a keel for cementing. Problems with radiolucent lines and loosening encouraged designers to seek alternative solutions. Cofield[28] introduced an uncemented TSR in 1986 (Cofield Total Shoulder System), which was followed by other uncemented systems, such as the Biomodular Shoulder and the 3M Modular

Shoulder. Cofield in his 1994 paper mentioned the problem of glenoid liner dissociation from the metal baseplate, and stressed that the two disassembly cases happened at 4 and 21 months post insertion, without any obvious wear to the liners. It is also mentioned in this paper that the polyethylene liner tended to wear very quickly.[28] In 2009, in another paper Cofield no longer recommended the use of the metal back implant, due to high long term failure rate.[29]

In spite of years of research, metal-backed components seem to perform inferiorly to cemented, polyethylene implants with respect to functional results and fixation. For the rapid wear of the polyethylene with this type of component Walch named four factors: 1) insufficient thickness of the polyethylene; 2) excessive thickness of the glenoid component; 3) rigidity due to the metal back; and 4) recurrence of posterior humeral subluxation despite re-orientation of the glenoid and balancing of the soft tissue[18]. Dissociation of the polyethylene from the metal base plate has also been extensively reported.

Further evolution of shoulder arthroplasty faces a new challenge. Rockwood in 2000 postulated that there were probably over 100 different shoulder prosthesis designs on the market.[30] Advances in the knowledge of shoulder biomechanics, but even more so, the differences in interpretation of these achievements has spawned a myriad of different designs, and this created new challenges in performance evaluation. Some manufacturers introduced designs that closely resembled other successful designs. To avoid a legal procedure, some minor changes were therefore introduced into the design, creating further confusion as to whether these changes in design could really be considered innovative. As time went by, comparison of a relatively small cohort of one prosthesis design to a relatively small cohort of another design became less and less meaningful. There was clearly great need for a tool that combined large scale data collection and structured interpretation, hence joint registries were born.

The 9 most relevant joint registries are from Norway, Sweden, New Zealand, Denmark, California, Australia, Emilia-Romagna (Northern Italy),

Germany and the United Kingdom. The idea of data merging and combined analysis further improves their potential.[31]

If Neer's original message is true, the future of shoulder arthroplasty leads towards more and more precise reconstruction of the original anatomy. The era of custom-made implants may be approaching.

2.2 Literature overview

2.2.1 The literature search method

Pubmed, Medline, Embase, Cochrane databases were searched.

Multi-field search:

- For shoulder prosthesis loosening in general

	"glenoid component"	and	"loosening"
Or	"shoulder replacement"	and	"loosening"
Or	"glenoid"	and	"loosening"
Or	"humeral component"	and	"loosening"
Or	"humeral stem"	and	"loosening"
Or	"glenoid"	and	"wear"
Or	"glenoid component"	and	"wear"

- For non-mechanical aspects of loosening

"biolog*" and "prosthesis" and "loosening" and "cell*"

Further material has been added from additional references identified in referenced articles or subject specific searches.

2.2.2 Epidemiology

Survival data of total shoulder arthroplasty have two types of problems. The follow up period is more than a decade long to create a large enough number for statistical analysis, but in addition the evolution of implants means that often the long-term outcome is based on a prosthesis which is no longer being marketed or the techniques used for insertion have changed. Most studies report on a relatively uniform, but small cohort from which a valid statistical analysis is difficult.

Although the UK National Joint Registry data collection on shoulder arthroplasty did not start until 1st April 2012, Report 14 holds data on 23,608 shoulder replacements.[5]

The total number of shoulder replacements has been increasing each year, from 2544 cases in 2012 to 5944 in 2016. The absolute number and the proportion of anatomical total shoulder replacements (TSA) was increasing each year, from 26.7% in 2012 to 32% in 2015; in 2016 the proportion of anatomical TSA showed a small decrease to 30.5% of the total including hemiarthroplasties and reverse polarity shoulder replacements.

Techniques with decreasing popularity included humeral hemiarthroplasty, resurfacing humeral hemiarthroplasty and resurfacing total shoulder arthroplasty. The statistics show an increasing usage of reversed polarity total shoulder replacement (Figure 4).

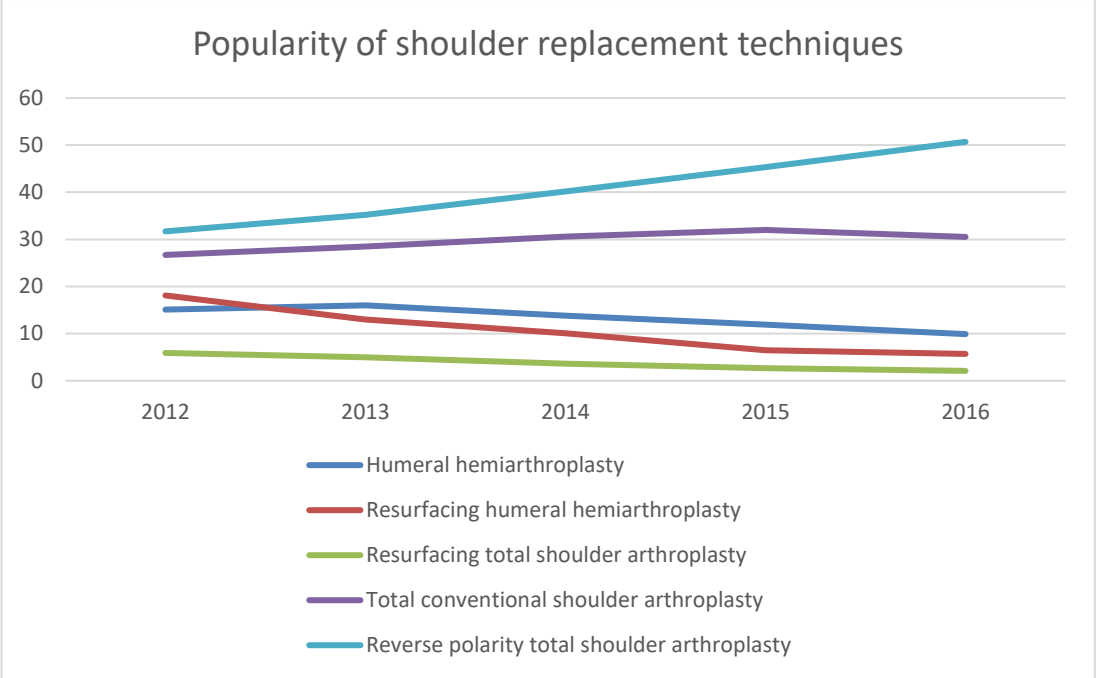


Figure 4. Total reversed polarity shoulder arthroplasty is gaining popularity over other techniques.[5] Reproduced from http://www.njrcentre.org.uk/njrcentre/Reports,PublicationsandMinutes/Annualreports/tabid/86/Default.aspx.

Conventional total shoulder replacement is unpopular for acute trauma cases. Out of the 2038 acute trauma cases in the registry only 29 cases were treated with anatomical TSA as opposed to 1041 cases treated with reversed polarity replacement.

The probability of revision is also presented by the registry for the first 4 years after implantation of different shoulder replacement techniques (Figure 5).

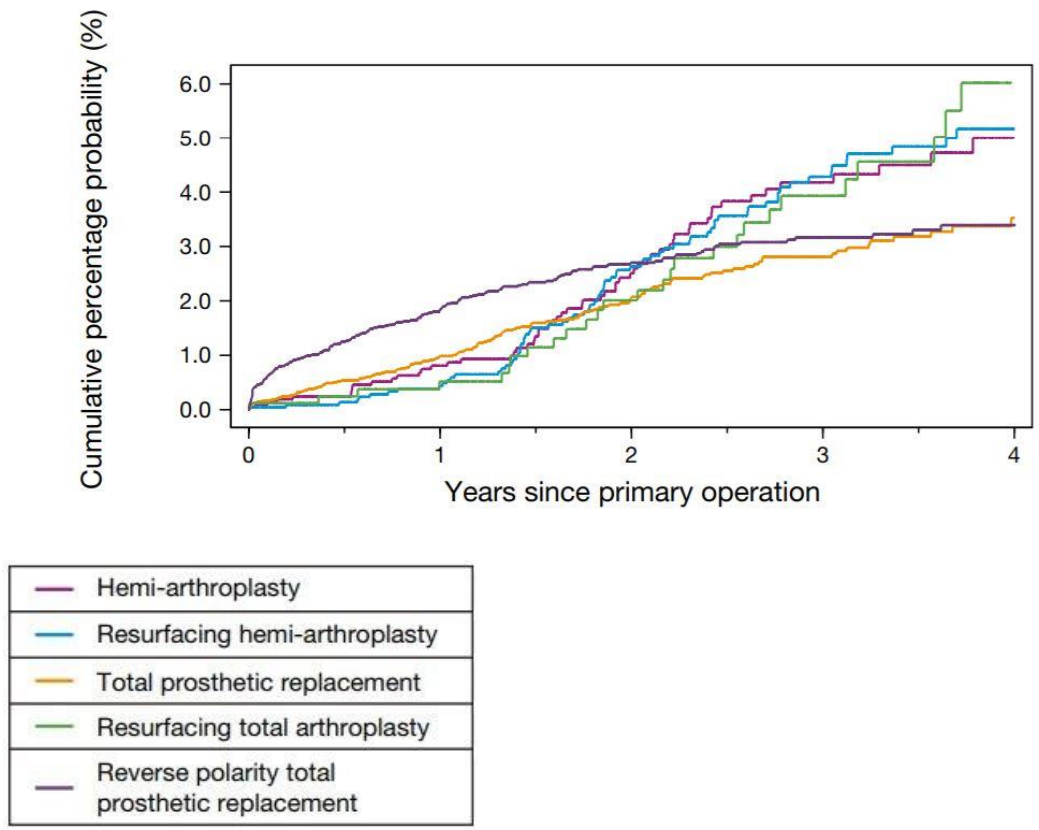


Figure 5. Cumulative percentage of probability of revision in elective cases.[5] Reproduced from http://www.njrcentre.org.uk/njrcentre/Reports,PublicationsandMinutes/Annualreports/tabid/86/Default.aspx.

At 4 years anatomical TSA and reverse replacement provide the lowest cumulative probability of revision. It must be noted that the anatomical systems used are mostly cemented by glenoid type (Figure 6).

Composition	Fixation			Total
	Cemented	Cementless HA coated	Cementless non-HA	
Metal (modular)	3	13	33	49
Metal polyethylene	144	0	233	377
All polyethylene	4521	0	613	5134
Total	4668	13	879	5560

Figure 6. The majority of the trauma and elective cases were treated with cemented glenoid components.[5] Reproduced from http://www.njrcentre.org.uk/njrcentre/Reports,PublicationsandMinutes/Annualreports/tabid/86/Default.aspx.

The UK National Joint Registry does not provide data on glenoid survival alone, nor does it compare survival of cemented versus uncemented glenoid TSAs.

The Australian Orthopaedic Association National Joint Replacement Registry (AOANJRR) in their 2017 Annual Report provided data on 38,265 shoulder replacement procedures up to and including 31 December 2016.[4]

Similarly to the UK register, the AOANJRR shows decreasing popularity of humeral hemiarthroplasty. The decrease is most remarkable in the case of the stemmed humeral hemiarthroplasty, where the annual number of procedures dropped from over 600 cases in 2008 to around 300 cases in 2016. Resurfacing humeral hemiarthroplasty was least popular in 2014 with less than 100 cases a year. For humeral hemiarthroplasties the cumulative revision percentage for all diagnoses combined shows that after year 3 the revision rate of resurfacing hemiarthroplasty is higher than for stemmed hemiarthroplasty. Glenoid erosion or pain are the reasons for 49% of all hemiarthroplasty resurfacing shoulder revisions.

Total shoulder arthroplasty was subdivided into total conventional arthroplasty, total inverse arthroplasty, total mid-head arthroplasty and

total resurfacing arthroplasty groups. The term “total mid-head” replacement stands for systems like Affinis Short Stemmed Total Shoulder Prosthesis (Mathys Ag, Bettlach, Switzerland).

Similar to UK trends the total inverse systems have been gaining popularity over the anatomical or conventional systems (Figure 7).

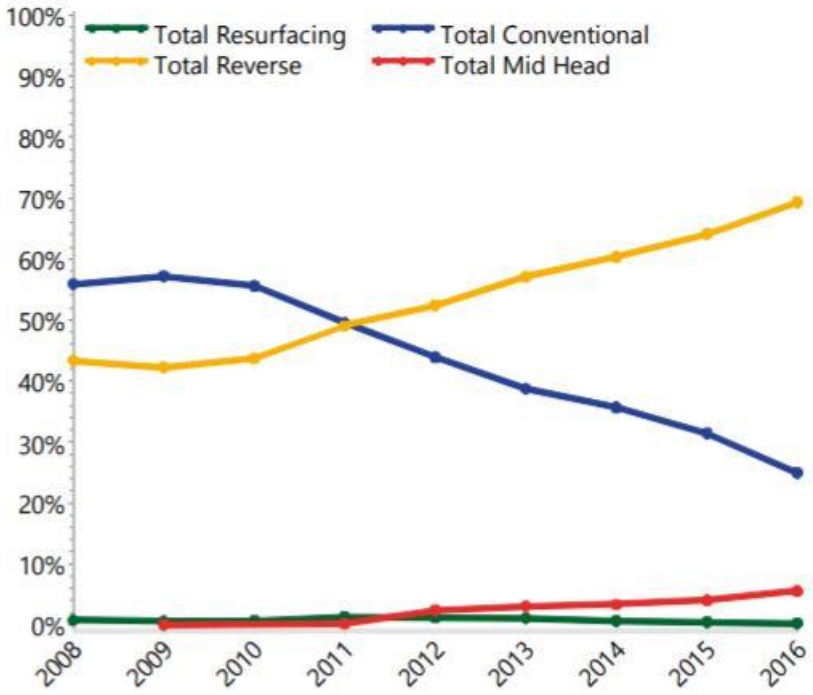


Figure 7. The popularity of total shoulder arthroplasty systems in Australia[32]. Reproduced from http://www.njrcentre.org.uk/njrcentre/Reports,PublicationsandMinutes/Annualreports/tabid/86/Default.aspx.

The AOANJRR provides survival data on anatomical total shoulder arthroplasty depending on the fixation and type of glenoid component, in contrast with the UK NJR (Table 3). Cementless fixation of the glenoid component in anatomical total shoulders had a significantly higher rate of revision than cemented, or hybrids in which the glenoid component was cemented. The 7-year cumulative revision rate for cementless TSA systems in the AOANJRR was 21.4% compared to the Nottingham TSA’s 26.56%.

Glenoid Type	N Revised	N Total	1 Yr	3 Yrs	5 Yrs	7 Yrs	9 Yrs	10 Yrs
Modular Metal Backed	459	2509	7.2 (6.2, 8.3)	15.3 (13.9, 16.9)	20.4 (18.7, 22.3)	23.4 (21.4, 25.5)	26.4 (23.6, 29.4)	
All Polyethylene	255	7634	1.5 (1.2, 1.8)	3.0 (2.6, 3.4)	3.8 (3.3, 4.3)	4.7 (4.1, 5.5)	5.8 (4.8, 6.9)	7.0 (5.3, 9.2)
Non Modular Metal Backed	31	662	2.9 (1.8, 4.6)	5.2 (3.6, 7.5)	5.5 (3.8, 7.9)			
TOTAL	**745**	**10805**						

Table 3. Survival of anatomical glenoid types by fixation, as indicated by revision rates.[4] Reproduced from https://aoanjrr.sahmri.com/annual-reports-2017

Fixation	N Revised	N Total	1 Yr	3 Yrs	5 Yrs	7 Yrs	9 Yrs	10 Yrs
Cemented	1	72	1.6 (0.2, 10.7)	1.6 (0.2, 10.7)	1.6 (0.2, 10.7)	1.6 (0.2, 10.7)		
Cementless	203	5692	2.6 (2.2, 3.1)	3.7 (3.2, 4.3)	4.3 (3.7, 5.0)	5.3 (4.4, 6.3)	7.0 (5.4, 9.2)	
Hybrid (Glenoid Cemented)	1	45	2.3 (0.3, 15.4)	2.3 (0.3, 15.4)				
Hybrid (Humerus Cemented)	44	1365	1.9 (1.2, 2.8)	3.3 (2.4, 4.5)	4.2 (3.1, 5.8)	4.5 (3.3, 6.2)		
TOTAL	**249**	**7174**						

Table 4. Survival of inverse glenoid types by fixation.[32] Reproduced from https://aoanjrr.sahmri.com/annual-reports-2017

If the 7-year revision rate of an anatomical TSA with modular metal back glenoid (23.4%), revision rate of an anatomical TSA with all poly cemented glenoid (4.7%) and the revision rate of inverse joints (5.3%) is compared (Table 4), interesting observations can be made. (AOANJRR does not declare if the latter two figures are statistically different or not. A generalised Wilcoxon test could be constructed but this test requires the data to be pooled and raw AOANJRR data are not available.) A metal back glenoid survives longer if part of an inverse prosthesis than if it is part of an anatomical shoulder prosthesis. Why do the modular uncemented metal back inverse glenoids survive better than the modular uncemented metal back anatomical glenoids? This question underlines why research of the

anatomical metal back glenoid systems is important, as a better understanding could be utilised in inverse metal back glenoid design.

Comparison of data of different joint registries can be challenging and requires caution. Considering anatomical total joint replacement, the UK and AOA registries depict similar indications. The overwhelming majority of anatomical total shoulder arthroplasties was implanted for osteoarthritis. The indications for inverse prostheses at the same time show that in Australia a lot of cases with osteoarthritis were treated with inverse arthroplasty. In the UK, the casemix is dominated by cuff tear arthropathy as the indication (Table 5). In other words, the difference in indication for surgery may have an impact on implant survival and outcome.

The distribution of the most frequent indications for anatomical and inverse prosthesis types

	Osteoarthritis	Cuff tear arthropathy	Trauma sequelae	Inflammatory arthropathy	Avascular necrosis	
Inverse	26.8	54.6	8.7	3.7	1.8	% UK
Inverse	45.5	34	15	2.2	1.1	% Aus
Anatomical	90.3	1.3	2.7	4.1	2.5	% UK
Anatomical	94.2	0.5	0.9	1.8	1.5	% Aus

Table 5. Indications for a certain implant type may differ between countries. Data reproduced from http://www.njrcentre.org.uk/njrcentre/Reports,PublicationsandMinutes/Annualreports/tabid/86/Default.aspx. and https://aoanjrr.sahmri.com/annual-reports-2017

If reasons for revision are compared between the two registries, further differences are revealed. Infection rate and periprosthetic fracture rate are similar, but there is more than two-fold difference between the cuff

insufficiency revision rates (Table 6). Although this is speculative, this difference may be due to the increased use of inverse total shoulder arthroplasty in osteoarthritis in Australia. Differences in instability and aseptic loosening figures are also evident, but further research would be needed to explain the deviance.

Reasons for revision		
	UK	Aus
Infection	5	6.2
Instability	38.8	24.2
Cuff insufficiency	45.3	22.6
Aseptic loosening	10.8	16.5
Periprosthetic fracture	2.9	2.5

Table 6. Most frequent reasons of revision. Notable differences are present. Data reproduced from http://www.njrcentre.org.uk/njrcentre/Reports,PublicationsandMinutes/Annualreports/tabid/86/Default.aspx. and https://aoanjrr.sahmri.com/annual-reports-2017

Careful interpretation when comparing joint registry data from different countries is essential.

2.2.3 The science behind prosthesis loosening – biological factors

The causes of loosening can be either biological or mechanical.[33, 34]

Wear debris is thought to be the major cause of osteolysis and implant failure through loosening.[35, 36] Wear debris is produced at the interfaces of the prosthetic joint. The biological response is dependent on the debris production rate, particle size, shape, charge, material of debris, immunological and genetic characteristics of the host.[33, 37]

2.2.3.1 What triggers osteolysis?

Some authors have suggested that wear particles and implant surfaces may be contaminated by toxins which trigger the immune response,[38-42] though most authors, as described in the following sections, hold the wear particles themselves to be responsible for osteolysis.

2.2.3.2 The micron-size particles

Debris particles in the micrometre range, mostly 0.5-20 microns activate macrophages by phagocytosis or surface contact. Typically polyethylene and polymethyl methacrylate cement produce debris in this size range. The activation of the host immune system manifests in the production of pro-inflammatory cytokines such as IL-1alpha, IL-1beta, TNF, RANKL, PGE2, and others.

The biological response is described in the RANK/RANKL pathway. This pathway regulates osteoclast differentiation. There is evidence that TNF, as a stimulator of osteoclastogenesis also depends on the RANK/RANKL pathway. [33]

Further downstream signalling includes the tyrosine kinase c-src, mitogen-activated protein kinases, and the nuclear factor-κB (NF-κB) cascade. [33]

Some genetic markers have been linked to an increased susceptibility to wear-debris induced osteolysis. TNF-alpha-238A allele, homozygous genotype T/T for RANK 575, and IL6-174G allele are some examples. Protective genetic factors have also been identified, such as IL1RA+2081 which is an Interleukin-1 receptor antagonist that is an osteoprotective immune modulator.[37]

Morphologically, the initial inflammation results in fibrous encapsulation of the implant. Synovial membranes producing synovial fluid may also be formed. Granulomatous tissue is established, with macrophages, fibroblasts, giant cells, neutrophils, and lymphocytes. This matures into

poorly vascularised connective tissue with macrophages and fibroblasts. Gelatinases and other proteases also contribute to periprosthetic osteolysis.[37]

2.2.3.3 The nano-size particles

Anatomical TSA joints with extensive polyethylene wear may develop a metal-on-metal contact interface, and the debris produced could play a role in cellular loosening. Data on the debris produced is available from Metal-on-Metal (MOM) prosthetic joints.

The size of debris particles generated by Metal-on-Metal (MoM) prostheses is typically less than 50 nanometres. It has been generally accepted that these joints generate less debris as far as the total volume of wear products is concerned, though the difficulties in identifying particles smaller than 10 micrometres may have resulted in an underestimation of the number of wear particles.[43-46]

Hip MOM joints have been shown to generate $6.7x10^{12}$ to $2.5x10^{14}$ particles a year, which is 13,500 times more than the number of particles produced by a Metal-on-Polyethylene (MOP) hip. Wear and corrosion of MOM joints can produce free particles, metal-protein complexes, salts and oxides, free ions, and metals entrapped in stores like haemosiderin. The particulate debris contains mostly aluminium (Al III), cobalt (Co II), titanium (Ti V), iron (Fe III), nickel (Ni II) and chromium (Cr III). Corrosion products consist of metal oxides and metal hydroxides that become deposited in the synovial environment. Metal phosphates however accumulate in the extrasynovial environment.[47, 48]

Metallic particles are ingested by macrophages or may be disseminated via lymphatics to the reticuloendothelial system. Metal ions are concentrated in the erythrocytes. Although the kidneys may be able to excrete these metals at a similar rate to their production, circulating cobalt and chromium levels can accumulate to several times the normal level.[49-53] These concentrations are well below the limits identified as dangerous to

health in workers exposed to industrial chemicals, but they may reach higher concentrations in certain tissues and potentially may cause local tissue necrosis.[43, 54-56]

Metal nanoparticles translocate across biological membranes by diffusion or endocytosis. Endocytosis can either be receptor-mediated or by non-specific pinocytosis.[45, 57-59]

The mechanism of cell damage can be cell membrane irregularity and mitochondrial damage, malfunction of intracellular signalling pathways, chromosomal damage and oxidative stress. Co (II) and V (III) are the most cytotoxic, Cr (III) is most mutagenic.[60, 61]

Metal debris initiates a vasculitis-like, type IV delayed hypersensitivity reaction. The axis of this is T helper and B cell activation. IFN gamma blocks osteoblasts, IL4 and IL10 activates resting B-cells. Inflammatory chemotactic factors are also present.[49, 62, 63]

The effect of nanometre range debris is widespread. Local toxicity can cause loosening and pseudotumours.[64] Systemic toxicity can interfere with erythropoiesis as well as decreasing the life expectancy of red blood cells.[65-70] General toxicity can also affect the immune system by altering the lymphocyte response to infection stimuli and can have an adverse effect on bacterial killing capacity of neutrophils.[71-77] In addition, toxins can also be nephrotoxic, hepatotoxic and potentially carcinogenic as well as affecting the nervous, cardiovascular, endocrine and reproductive systems.[43]

Morphologically, the pattern of inflammation in the periprosthetic tissue of loose MOM articulations is significantly different from that of MOP articulations, and is characterized by an unusual lymphocytic perivascular infiltration and plasma cell accumulation.[64]

Ceramic on ceramic bearings produce debris that is similar in size to MOM, but appears to be a lot less biologically active.[43] Tissues from around the ceramic-on-ceramic prostheses demonstrate the presence of particles, as

agglomerates inside cells or in distinct channels in the tissues. Mixed histological pathology is present including infiltration with macrophages and necrosis - necrobiosis, with the presence of neutrophils and lymphocytes. The size of alumina wear debris in one study was in the range 5 nm to 3.2 microns, showing a bimodal distribution, with the larger particle range showing some overlap with the particle size typically generated by UHMWPE implants. This may explain the mixed tissue reaction.[78]

Implant chipping, fracture and audible squeaking are also significant additional problems.[37]

2.2.4 The science behind prosthesis loosening – mechanical factors

Implant positioning is of key importance in most arthroplasty procedures. Soft tissue balance is also thought to play an important role with any joint arthroplasty procedure. Positioning and soft tissue balancing in practice is often a challenge as preoperative anatomy may already be distorted.

2.2.4.1 Preoperative anatomy

Walch classified the osteoarthritic changes of the glenohumeral joint (Figure 8). In Type A the humeral head is centred, A1 and A2 are subgroups with increasing erosion. In Type B the humeral head is subluxed posteriorly. In B1 there is no bony glenoid rim erosion, but in B2 posterior glenoid erosion is present and the glenoid is retroverted. A glenoid retroversion of more than 25 degrees is classified as Type C regardless of erosion.[79]

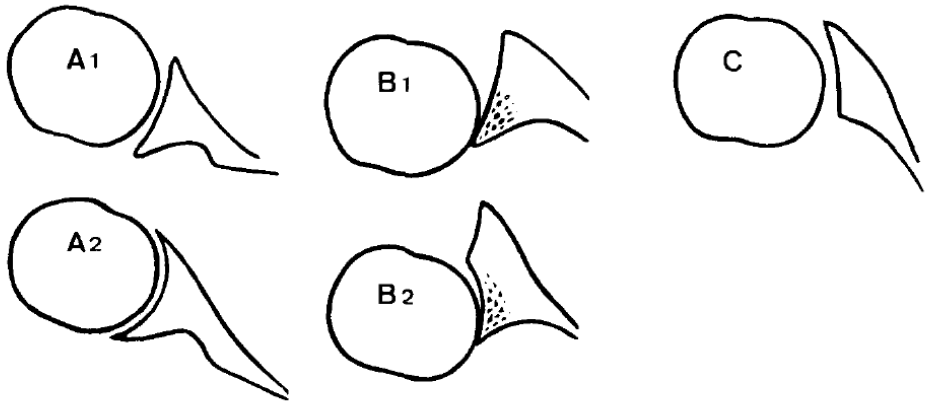


Figure 8. Walch classification of glenohumeral joint osteoarthritis.[79] Reproduced from Walch G, Badet R, Boulahia A, Khoury A. Morphologic study of the glenoid in primary glenohumeral osteoarthritis. J Arthroplasty. 1999 Sep;14(6):756-60.

Changes to the glenoid in cuff tear arthropathy can be classified by the Favard classification (Figure 9). E0 stands for superior humeral head migration without glenoid damage. E1 means concentric glenoid erosion. In E2 only superior glenoid erosion is present, whereas in E3 the erosion extends to the inferior part of the glenoid.[80, 81]

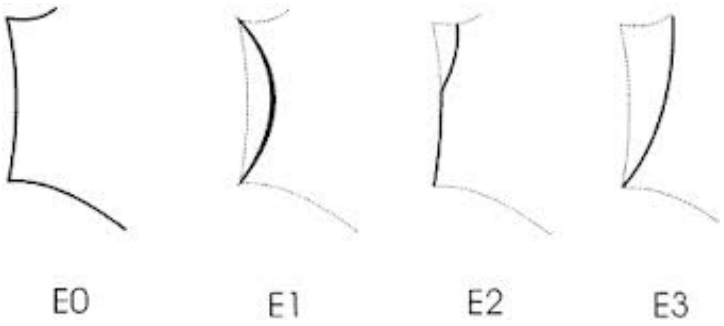


Figure 9. Favard classification for cuff tear arthropathy.[82] Reproduced from Ekelund A, Seebaue L. Advanced Evaluation and Management of Glenohumeral Arthritis in the Cuff-Deficient Shoulder. In: Rockwood C, Matsen F, editors. Rockwood and Matsen's The Shoulder. IV ed. Philadelphia: Saunders; 2009. p. 1247-76.

For dislocation arthropathy of the shoulder the Samilson and Prieto radiological classification is used (Figure 10). In mild arthrosis the size of the inferior humeral or glenoid osteophyte is less than 3mm. In the moderate arthrosis group the size of the glenoid/humeral osteophyte is between 3mm and 7mm. Glenohumeral irregularity is mild. In the severe arthrosis group the size of the glenoid/humeral osteophyte is 8mm or larger, marked narrowing of the glenohumeral joint space is present with sclerosis.[83] Ilg et al. has questioned the reliability of this classification due to poor intra- and inter-observer reliability.[83]

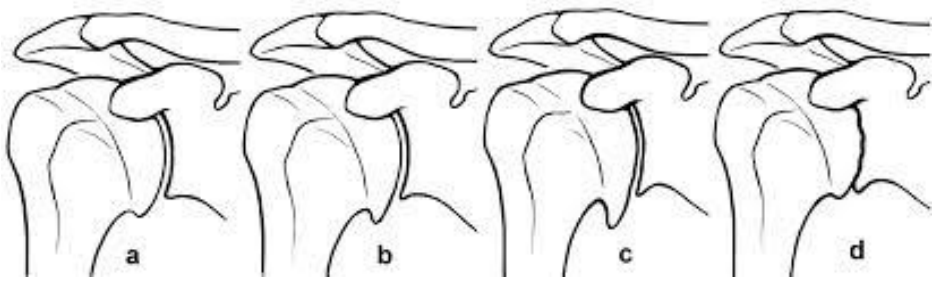


Figure 10. Samilson – Prieto classification for dislocation arthropathy.[84] Reproduced from Buscayret F, Edwards TB, Szabo I, Adeleine P, Coudane H, Walch G. Glenohumeral arthrosis in anterior instability before and after surgical treatment: incidence and contributing factors. Am J Sports Med. 2004 Jul-Aug;32(5):1165-72. Epub 2004/07/21.

The glenoid damage in RA is classified by Levigne and Franceschi as follows (Figure 11). In stage 1 subchondral bone is intact or minimally deformed. In stage 2 the glenoid erosion reaches the base of the coracoid. In stage 3 erosion goes beyond the base of the coracoid.[85]

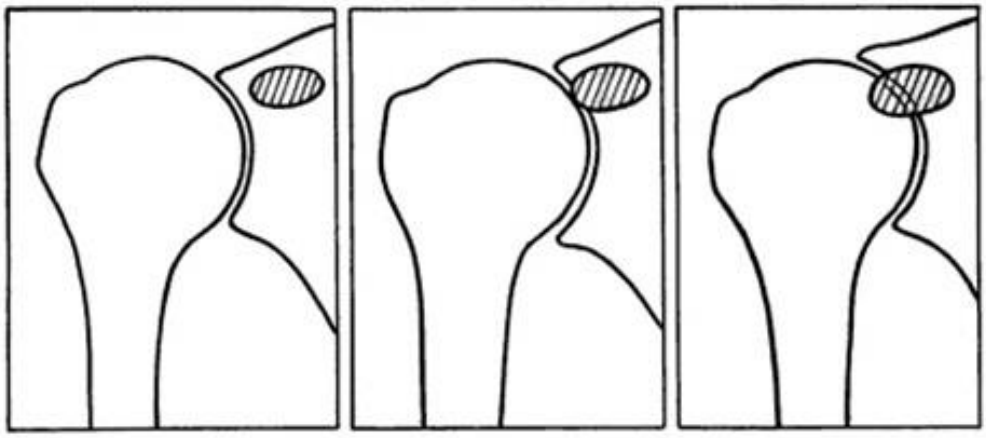


Figure 11. Levigne – Franceschi classification for glenoid erosion in RA.[86]
Badet R, Boulahia A, Walch G. CT scan measurement of the humeral head subluxation in a sagittal plane method and application in primary gleno humeral osteoarthritis without humeral head elevation. Mesure tomodensitometrique de la subluxation humerale antero- posterieure: Proposition d'une methode. Application a l'omarthrose centree. Revue de Chirurgie Orthopedique et Reparatrice de l'Appareil Moteur. 1998;84(6):508-14.

2.2.4.2 Measuring the version of the glenoid

Measuring the retroversion of the glenoid is of major importance.

One recommended method uses axial 2D CT images. The slice corresponding to the base of the coracoid is selected. In this image, the Friedman line is drawn (Figure 12).

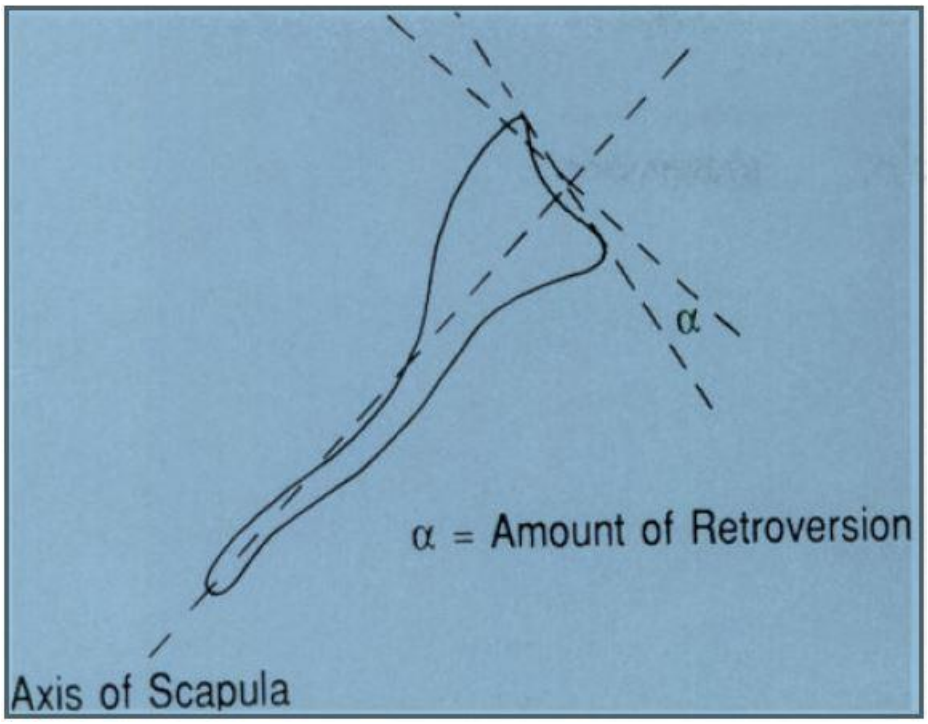


Figure 12. The original figure from the 1992 article by Friedman explaining proposed measurement of glenoid retroversion.[87] The margins of the glenoid (not considering any osteophytes) are joined by a line. The bisection of this line is then joined to the medial margin of the scapula. Scapular retroversion is the angle marked by α. Reproduced from Friedman RJ. Glenohumeral translation after total shoulder arthroplasty. J Shoulder Elbow Surg. 1992 Nov;1(6):312-6

The Friedman line joins the tip of the medial border of the scapula with the midpoint of the glenoid cavity (Figure 13). In case of a Walch Type B glenoid three characteristic reference lines of the glenoid cross section exist (Figure 14). The paleoglenoid is the line of the late, intact glenoid prior to wear as determined by the remaining anterior part of the glenoid. The neoglenoid is the line across the newly eroded, current glenoid. The intermediate glenoid line is drawn from the anterior edge of the glenoid fossa to its posterior edge without considering irregularities secondary to posterior erosion. Retroversion of the glenoid can be calculated from the relationship of the Friedman line and the intermediate glenoid line. This

method is as good as using 3d CT scans, and also works for curved scapulas.[88]

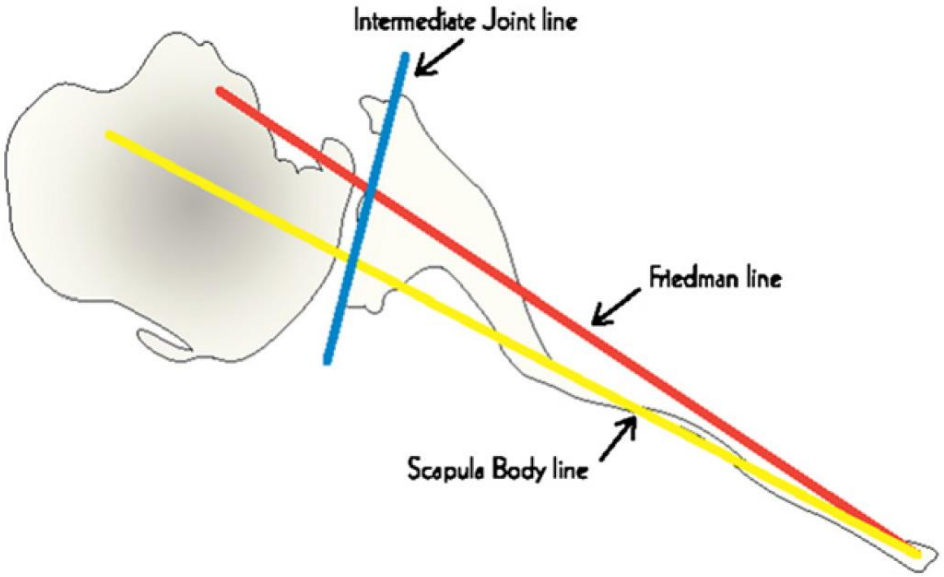


Figure 13. Measurement of glenoid retroversion using the Friedman line.[88] In this example it is obvious that with curvy scapulas the scapular body line and the Friedman line do not coincide. Reproduced from Rouleau DM, Kidder JF, Pons-Villanueva J, Dynamidis S, Defranco M, Walch G. Glenoid version: How to measure it? Validity of different methods in two-dimensional computed tomography scans. Journal of Shoulder and Elbow Surgery. 2010 December;19(8):1230-7.

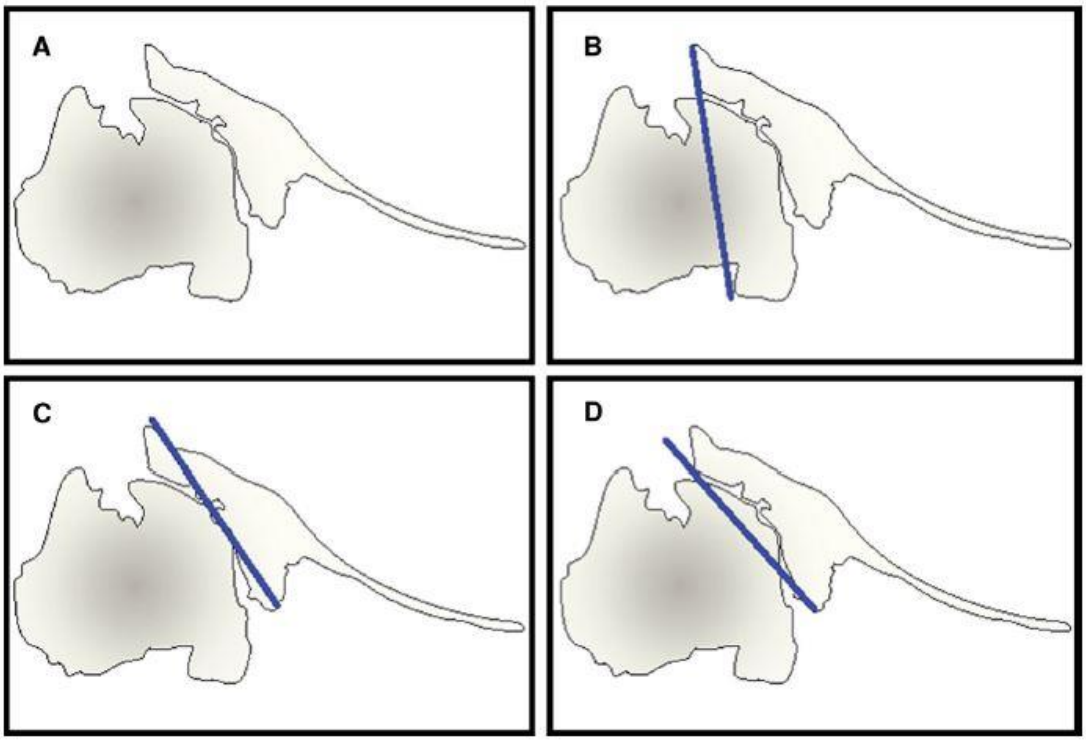


Figure 14. Picture A depicts a glenoid with significant posterior erosion, Walch type B2. Picture B describes the paleoglenoid, the potential plane of the glenoid pre-erosion. Picture D depicts the neoglenoid, which is the secondary socked and is the consequence of erosion. Picture C explains the intermediate glenoid, which is "the line connecting the anterior and posterior margins of the glenoid".[88] Reproduced from Rouleau DM, Kidder JF, Pons-Villanueva J, Dynamidis S, Defranco M, Walch G. Glenoid version: How to measure it? Validity of different methods in two-dimensional computed tomography scans. Journal of Shoulder and Elbow Surgery. 2010 December;19(8):1230-7.

Although the reproducibility of the Friedman line is clear, the authors did not validate this measuring method against in vivo data. It is unclear whether glenoids reconstructed based on the Friedman line improve soft tissue balance better than those reconstructed on the basis of scapular body line.

In practice the scapular body line is more frequently used.

Another proposed method is to use the near-linear lateral border of the scapula as well as the deepest part of the near-linear supraspinous

fossa lines to determine the plane of the scapula. Points around the glenoid rim indicate the glenoid position in 3D.[89]

Ideally the surface of the glenoid would be perpendicular to the resultant force vector of the muscles around the shoulder in any direction within the range of movement. As this cannot happen in a single plane, the shape of the glenoid articular surface must be complex as well. Therefore the optimal position of the glenoid in space as well as the shape of the glenoid articular surface would need to be determined from muscle strength vectors and torques in all possible positions of the shoulder within the range of movement. This would require very complex mathematical simulations. It is questionable if a single optimal version of the glenoid exists, and probably this is why there is no consensus in the literature about the normal glenoid version.

Friedman et al. reported a mean of 2° +/- 5° (range 14° to -12°) anteversion in a group of 63 healthy individuals.[90] In other anatomical studies, normal glenoid version showed a variation of about 20°, with an average retroversion of 1–2°.[91-93]

Ganapathi et al. have designed software to predict the original version of an osteoarthritic glenoid. They were able to predict the original glenoid version within 10°.[94]

The normal glenoid tilt in the coronal plane has been reported to range from –8° to 15.8° (average, 4° to 5°).[95]

2.2.4.3. The glenoid retroversion problem

In glenohumeral osteoarthritis posterior glenoid wear and humeral head posterior subluxation is often present.[96, 97] The non-physiological position of the head can cause soft tissue imbalance. As implantation of the glenoid component in retroversion has an increased failure rate, one should try to

correct the version of the glenoid.[98, 99] Habermeyer et al. described eccentric inferior glenoid wear which is independent of the posterior wear of the glenoid.

Walch described a group of patients (mean age = 40 years) who had static posterior subluxation of the humeral head with posterior glenoid cartilage wear but no glenoid erosion. They had a mean glenoid retroversion of 14.5°. In some patients soft tissue correction was attempted but the posterior subluxation recurred in all of them.[100]

For patients with excessive glenoid retroversion the following treatment options are available:

1) Hemiarthroplasty with or without glenoid reaming (ream and run) – one has to be aware though that the survival and pain relief results with hemiarthroplasty are inferior to total shoulder replacement.

2) Implantation of the glenoid component in retroversion and the humeral component in anteversion – but this is also controversial.[101]

3) Total shoulder replacement with bulk bone grafting and version correction – this method is widely accepted.[102]

4) A custom inset glenoid implant is another option.[103, 104]

5) In cases of a reverse prosthesis one may consider a bony increased offset shoulder arthroplasty, with the bone block compensating for the glenoid defect and/or an offset humeral head.

6) Preferential anterior glenoid reaming – can be a double edge sword as the bone stock of the glenoid is limited, and good quality bone support for the glenoid component is essential.

7) Soft tissue corrections should also be considered when appropriate.

8) Anterior capsulectomy and posterior capsule plication have also been advocated.[98]

2.2.4.4. The problem of surgical orientation on an eroded glenoid

During the implantation of a TSA the glenoid exposure does not provide reliable landmarks, especially if bony erosion is present. Besides orientation, limited bone stock may not allow adequate correction of the eroded glenoid surface. These problems sometimes predispose the perforation of the glenoid vault.

In a study by Gregory et al.[105] implant position has been shown to be determined by the preoperative orientation of the glenoid, in spite of surgeon's effort. With the traditional orientation methods surgery typically did not correct the glenoid version to neutral. Perforation of the glenoid vault by the implant as the consequence of glenoid component mal-positioning also happened.

These are proposed causes of poor clinical outcome.[106-109]

The authors concluded that TSA would benefit from aids to allow accurate seating of the implant on the glenoid.[110]

2.2.4.5. The glenoid component design problem

Different designs of total shoulder arthroplasty glenoid components are available.

In the conforming glenoid design the radius of curvature of the head component is exactly the same as the radius of curvature of the facing glenoid surface. The theoretical advantage of this is that the contact forces are distributed over the entire contact surface, reducing point contact stresses. The disadvantage is that conformed designs do not allow

humeral head translation, thus increasing the stresses across the glenoid baseplate or pegs/bone interface.

With the non-conforming design the radius of curvature of the glenoid is larger than that of the humeral head. This allows a degree of humeral head translation, but eccentric point contact stress occurs within the polyethylene at one location, potentially leading to excessive wear.[98]

Farron et al. prepared a 3D finite element model to determine the optimal glenohumeral conformity mismatch in cemented anatomical total shoulder arthroplasty. They found that a conforming design provides the best load distribution and stability but increases forces acting to loosen the glenoid component. In non-conforming scenarios, if they increased the radius of curvature of the glenoid component to be 10mm larger than the radius of curvature of the head, the contact pressure exceeded the polyethylene yield strength leading to breakage of the polyethylene. With this extent of mismatch glenoid shear stresses become very large resulting in lamination. They concluded that articular conformity was preferable.[111]

Another alternative is the use of a dual radius glenoid component, where a central conforming zone is surrounded by a nonconforming zone. Further studies are needed to assess the usefulness of this theorem.[98]

The problem of polyethylene insert wear is significant. Wear products are likely to cause osteolysis and aseptic loosening. If the humeral head component fully erodes the polyethylene liner and reaches the metal glenoid back in non-cemented designs, it will cause metallosis and also may cause delayed hypersensitivity reactions similar to metal-on-metal prostheses, in addition to the polyethylene debris. Wear can weaken the polyethylene causing loss of structural integrity, and fracture. In uncemented designs the polyethylene insert may disengage from the metal back.

2.2.4.6. Basics of biomechanics of the anatomical total shoulder arthroplasty

Materials under non-simple tension non-uniaxial stress experiments exhibit resistance values that are much larger than the ones observed during simple tension experiments. To describe the phenomenon, the concept of the full stress tensor was developed.[112]

If an infinitesimal or elemental cube is in equilibrium and stationary, the state of stress can be described by a stress tensor.[113] The tensor will have stress elements normal or perpendicular to the cube's faces called normal stress vectors and will have elements parallel to the cube's surface called shear stress vectors. For mathematical description, a matrix representation of the stress state is possible and is widely used. To describe the same state of equilibrium, many different coordinate systems can be used, and some may be more meaningful than others. It is possible to choose a coordinate system position and orientation for each elemental cube in equilibrium where all the shear stress vector components add up to zero and it is possible to describe the equilibrium by stress vectors perpendicular to the faces of the cube. These perpendicular elements are called principal stress vectors.[113] The maximum shear stress or maximum principal shear stress can also be interpreted and determined in the above context. It is equal to one-half the difference between the largest and smallest principal stresses and acts on the plane that bisects the angle between the directions of the largest and smallest principal stresses, i.e. the plane of the maximum shear stress is oriented 45 degrees from the principal stress planes.[113]

The von Mises stress criterion for yielding is widely used in engineering for metals and other ductile materials.[112] It states that yielding will occur in a body if the components of stress acting on it are greater than the criterion:

$$\frac{1}{6}[(\tau_{11}-\tau_{22})^2+(\tau_{22}-\tau_{33})^2+(\tau_{33}-\tau_{11})^2+6(\tau_{12}^2+\tau_{23}^2+\tau_{13}^2)]=k^2$$

τ is the stress tensor, k can be determined experimentally using uniaxial stress.[112] In this latter case:

$$\frac{\tau_y^2}{3} = k^2$$

If τ_y reaches the simple tension elastic limit, S_y:

$$\frac{S_y^2}{3} = k^2$$

Substituting this into the first expression:

$$\frac{1}{6}[(\tau_{11} - \tau_{22})^2 + (\tau_{22} - \tau_{33})^2 + (\tau_{33} - \tau_{11})^2 + 6(\tau_{12}^2 + \tau_{23}^2 + \tau_{13}^2)] = \frac{S_y^2}{3}$$

Or in a simplified form:

$$\sqrt{\frac{(\tau_{11} - \tau_{22})^2 + (\tau_{22} - \tau_{33})^2 + (\tau_{33} - \tau_{11})^2 + 6(\tau_{12}^2 + \tau_{23}^2 + \tau_{13}^2)}{2}} = S_y$$

The von Mises stress (τ_v) is defined as:

$$\tau_v^2 = 3k^2$$

The material is expected to yield if the von Mises stress is greater than the simple tension yield limit stress.[112]

The distortion-energy theory for ductile materials states that yielding occurs when the distortion strain energy per unit volume reaches or exceeds the distortion strain energy per unit volume for yield in simple tension or compression of the same material.[112]

Neer pioneered in stressing the importance of mimicking the original shoulder anatomy as closely as possible. The centre of rotation in a replaced shoulder is no exception.[20, 24] If the artificial head (and the centre of rotation) is too high, the resultant vectors of subscapularis and infraspinatus may fall below the centre of rotation of the humeral head, and from abductors they may get converted to adductors. This results in the overuse of the supraspinatus in elevation and abduction which can

expedite rotator cuff pathologies and tear. Passive structures may also suffer superior head placement, such as the inferior capsule which may become too tight and limit abduction.[108]
If the prosthetic head is implanted too low, the greater tuberosity may impinge under the coracoacromial arch.[108]
Head placement ignoring the anatomical posterior offset of the humeral head moves the centre of rotation anteriorly, altering the lever arms of the internal and external rotators. The result is weakened internal rotation.[92]

As for glenoid mal-positioning, a mal-positioned glenoid can change the length of the motor units around the shoulder causing imbalance. Other than eccentric wear of the glenoid implant, focal overload of the implant-host interface may evolve. One of the first finite element models to investigate the potential effect of eccentric glenoid loading on the von Mises stress distribution of the glenoid-host interface was by Stone from the Cofield group in 1999.[114] They built a two planes model and found that even relatively minor alterations in the loading direction significantly changed the load distribution and maximum stress in the bony glenoid. Iannotti et al showed that retroversion of the glenoid by 20 degrees causes a moderate increase in the peak strains at most locations, with a maximum increase of 32%. Although none of the strain values they observed exceeded the yield strain, they proposed that the component would fail due to loosening. They used cadaveric and finite element models.[108] Lift-off of the glenoid back was also more pronounced in case of retroverted implantation by 20 degrees. The authors concluded that mal-positioning of both the humeral and glenoid components would adversely affect range of motion, kinematics, and stability.[108]
According to the Hopkins finite element model, glenoid mal-positioning directions were ranked based on increasing risk of cement failure: centrally aligned, anteverted, retroverted, inferiorly inclined and superiorly inclined.[115] The authors concluded that accurate glenoid positioning was important.

The effect of glenoid mal-positioning was also studied by Farron et al.[97] They built a more complex model which included the proximal part of the humerus, the whole of the scapula, supraspinatus, subscapularis and infraspinatus, and a numerically implanted anatomical total shoulder replacement. The humeral component was “implanted” to match original anatomy. The glenoid was a keeled, flat back cemented all polyethylene implant with a simulated cement layer. There was a 10mm mismatch between the humeral and glenoid radii of curvature. The tests included 0 degrees glenoid version, and 5-10-15-20 degrees retroversion. External and internal rotation of the humerus were simulated using active muscle force by the above muscles. Glenoid retroversion influenced the position of glenohumeral point contact, as it migrated posteriorly with increasing retroversion, both in external and internal rotation. As expected, peaks of stress also increased posteriorly, parallel to this. The glenoid retroversion increased the peaks of cement stress to 326% at 20 degrees of retroversion. Without retroversion, the glenoid was symmetrically loaded. With increasing angles of retroversion, peaks of stress developed mainly in the posterior part of the cement mantel. As micromotion at the bone - cement interface was allowed by the model, a significant increase of micromotion was observed with increasing retroversion (mean increase of 669%, peak of 706%). Without retroversion, micromotion was reported to happen all around the bone - cement interface. At 20 degrees of retroversion peaks of tangential micromotion (slipping) were observed at the anterior side of the keel and perpendicular micromotion (debonding) was typical under the anterior back of the glenoid. One would also expect micromovement posterior to the keel, as the “rocking horse” mechanism would necessitate that, but there are no data reported in this paper to suggest this either in external, or in internal rotation.[97] The significant biomechanical alterations above 10 degrees of glenoid retroversion predispose the glenoid for loosening.

Contact forces in the glenohumeral joint are large, from 1.3 to 2.4 times body weight in computer models (930-1720 N).[116] Bergmann et al. created and implanted an instrumented shoulder implant with telemetric data

transmission to measure six components of joint contact forces and moments. During the first 7 postoperative months, the contact force remained below 100 percent body weight for most activities of daily living. Certain forceful manoeuvres later after implantation resulted in forces around 130-188 percent body weight. This means that contact forces in the glenohumeral joint are high.[117, 118]

Force vector directions relative to the humerus are not greatly influenced by the type of exercise, the arm position or the external resistance (Figure 15).[117]

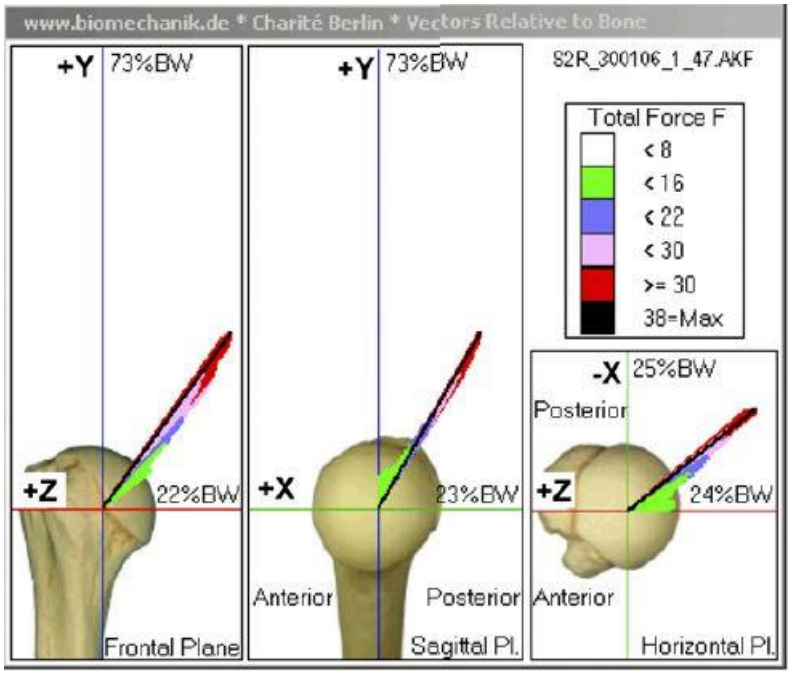


Figure 15. The direction of the force vector in the glenohumeral joint remains relatively uniform during different activities.[117] Figure reproduced from Bergmann G, Graichen F, Bender A, Kääb M, Rohlmann A, Westerhoff P. In vivo glenohumeral contact forces - measurements in the first patient 7 months postoperatively. J Biomech. 2007;40(10):2139-49.

Anatomical total prostheses where the radius of curvature of the head is smaller than that of the socket are designed to allow translational movement of the head. There is no consensus in the literature about how much play is ideal. Anglin calculated with a head travel of 90% of subluxation distance for stability testing.[119]

2.2.4.7. Degrees of freedom in shoulder movement

The shoulder has 6 degrees of freedom, with rotation about 3 axes and translation along 3 spatial axes.[120]
Many experimental models are simplifications of the biomechanical complexity.
A constrained ball and socket prosthetic joint is able rotate and bend along two axes, hence the degrees of freedom are reduced to three.

2.2.4.8. Spatial description of shoulder movement

The use of Euler angles is an accepted method for describing spatial movements of one bone in relation to another. In the shoulder, movements of the humerus can be described if a coordinate system is attached to the midpoint of the glenoid surface and another to the humeral head. Angles of movement of the humerus can be recorded this way. Due to the nature of the spatial movement, the sequence of each movement is also important determining the new position of the humerus. This method has only 3 degrees of freedom, hence it is not capable of describing the entire complexity of the shoulder movements including translation[120].
The Helical Axis Motion model is capable of describing rotation and translation, but the way this model describes spatial position is different from how clinicians describe shoulder movement and is thus difficult to interpret. The Helical Axis Motion model for this reason is not very popular.

2.2.4.9. Muscoloskeletal shoulder models

Musculoskeletal shoulder models allow non-invasive prediction of parameters that are difficult or impossible to measure.

Many of the available models are based on inverse dynamics approach. This approach uses observational data (joint kinematics) as input and attempts to calculate the biomechanics leading to this.
Muscle dynamics models are based on neural-excitation dynamics, muscle activation dynamics as well as muscle force–velocity and force–length relationships predicting movement. This latter group is called forward simulations.
Another option is to combine forward simulations of muscle dynamics models with the outputs of inverse dynamics simulations.[121]
Inverse dynamic models are very sensitive to their input data. Some artefacts such as skin movement may result in poor quality data input. Repeat measurements or other means of kinematic data optimization are generally useful.
Precise localisation of joint centres is essential in any model, as even minor errors are amplified when calculating moments and lever arms. Errors in joint centres, rotations and segment lengths accumulate as the kinetic chain lengthens.
Anthropometric parameters and individual variations in anatomy also affect the accuracy of a model.
Muscles are usually represented as frictionless tight strings. For muscles that follow bony contours adding virtual muscle origins gives a more realistic scenario than calculations using the straight line of action between the origin and the insertion of the muscle.[121]
Many recent publications focus on finite element analysis of different arthroplasty designs. Mostly these results are not validated against real world cyclic tests.[122, 123] Real world cyclic tests on the other hand are very time consuming and lack the numbers.[124]

Validating these models against in vivo data is important but difficult. Implantable measuring devices are useful but interfere with the original anatomy.

2.2.4.10. Glenoid component damage patterns in vivo

Braman et el described wear patterns in retrieved cemented all polyethylene glenoid implants, using a laser scanning technique. They reviewed anatomical prostheses in which the radius of curvature of the glenoid was 3mm larger than that of the humeral head. They found diffuse wear and rim wear. One wear pattern resulted in the humeral head component creating a new indentation matching its curvature. Another pattern of diffuse wear was pitting, where a wide range of radii of curvature was found, most likely a consequence of abrasive wear. Rim wear had two typical appearances. In the first subgroup the glenoid developed a biconcave shape suggesting subluxation of the head. In the second subgroup the rim wear had no characteristic radius possibly suggesting repeated movement of the head across the rim of the glenoid. In all the cases, wear led to decreased stability as characterized by the balance stability angle (the maximal angle that the net humeral joint reaction force can make with the glenoid centre line before the humeral head would dislocate).[125]

Scarlat et al made similar observations.[126] Rim erosion was found in 34 cases out of 43, surface irregularity in 39 out of 43 cases. Fracture of the implant happened in 13 cases, excessive central wear was also commonly seen. In this study clinical history was only available for 19 cases. The average survival time for these latter cases was only 2.5 years. The authors conclude that the degree of damage seen in the explants were sufficient to compromise smoothness and stability of the joint. The paper includes photographs of the explants, but the authors do not draw far-reaching conclusions other than that none of the retrieved glenoid components was reported to have the same surface and shape as when new. Wear rate is not quantified either.

2.2.4.11. Failure patterns of cemented all polyethylene glenoid components

Walch et al. described typical loosening patterns of all polyethylene keeled cemented glenoid components in anatomical total shoulder arthroplasties. They found definite radiographic evidence of glenoid loosening in 166 shoulders (32%), This was characterized by radiolucency of $\geqslant$2 mm over the entire bone - cement interface in thirty shoulders and by a migration of the glenoid component (shift or subsidence) in 136 shoulders. The failed glenoids had three typical patterns of failure. Superior tilting (10%), subsidence (7.9%), and posterior tilting in thirty-three shoulders (6.4%). Superior tilting of the glenoid was associated with three risk factors: low positioning of the glenoid component, superior tilt of the glenoid component on the immediate postoperative coronal plane radiographs, and superior subluxation of the humeral head ($p < 0.05$ for all). Subsidence was a result of excessive reaming of the glenoid surface on implantation. Posterior tilting of the glenoid component was associated with preoperative posterior subluxation (i.e., a Walch type-B glenoid) and with excessive reaming ($p < 0.01$ for both). They stressed the importance of preserving subchondral bone when implanting the glenoid.[127]

An interesting attempt to overcome the problems with metal-backed glenoids is an uncemented “soft-metal-backed” glenoid component. This is a polyethylene glenoid component with a titanium mesh on the back side facing the bony glenoid and titanium pegs. The rationale is that the titanium mesh has stiffness closer to bone, and at least in models, this provides better fixation. This design also allows moulding of the polyethylene into the porous titanium mesh, avoiding a metal-polyethylene interface problem. Fucentese et al. reported a high incidence of glenoid implant fractures in this group of prostheses.[128]

2.2.5 Bone grafting in shoulder replacement

Using structural block bone grafts for reconstruction of deficient glenoids in primary and revision surgery is a well-accepted practice. Some papers, however, state that structural bone grafts do not incorporate very well. Bonnevialle et al studied results of revision of shoulder replacements in a retrospective multicentre study. They used cemented all polyethylene glenoid components for revision. In 10 cases due to a defect in the bony glenoid, they used structural bone grafts. In 7 cases the graft was an iliac crest autograft, 2 allografts and one central cancellous bonegraft. Grafts were stabilized with screws in 5 cases. Among the 10 cases of glenoid bone graft, there was a complete resorption of the graft in 4 cases and a partial resorption in 6. At last follow-up, the glenoid component was loose in 6 cases (60%) and further surgery had been performed in 3 cases.[129]

Enneking et al. studied 73 human long-bone allografts, retrieved from 2 to 156 months. These grafts were very different from the grafts used for grafting the glenoid but they give us a valuable insight into the healing of allografts. Union at the cortical - cortical junctions occurred slowly (approximately twelve months) by host-derived external callus that bridged the junction and filled the gap between the cortices. The bone in the gap did not undergo stress-oriented remodelling even after many years, and, when the union was intentionally disrupted, failure occurred at the cement line that marked the allograft - host junction. Repair of the necrotic graft matrix was both external and internal. External repair consisted of the apposition of a thin seam of host bone on the outer surface of the graft, coating about 40% of the surface at one year and 80% at two years. Internal repair was confined to the ends and the periphery of the cortices and penetrated so slowly that only 15% to 20% of the graft was repaired by five years, after which deeper repair seldom occurred. Graft fractures in specimens retrieved soon after fracture showed only necrotic bone adjacent to the fracture site, whereas those retrieved after fracture-healing showed a marked increase in internal repair of the bone about the

fracture site.[130] The results reported by Steinmann et al. were significantly better.[131]

2.2.6 Ream and Run

The "ream-and-run" technique aims to avoid problems of glenoid loosening. The humeral head is replaced but the glenoid is only reamed to a shape similar to the shape of the humeral head to get rid of the often seen biconcave surface, and this is followed by careful soft tissue balancing. The rationale behind this is that once the head is re-centred, the contact surface of the glenoid regenerates and eventually becomes covered by a fibrocartilaginous layer. Matsen et al. used this technique successfully on highly selected patients.[132] Hemiarthroplasty without re-centring the replaced humeral head gives disappointing results.[133, 134]

Interposition arthroplasty for the shoulder is not a new concept. The interposed material can be anterior capsule, fascia lata, tendo-Achilles graft or lateral meniscus allograft. Promising results have been published with lateral meniscus allografts in young, active patients.[135-138]

There are numerous reported problems with hemiarthroplasty. Glenoid wear seems to be progressive. Parsons et al. reported an average rate of 2mm over a mean follow up of 42 months, and the functional score average was only 60% of age- and gender-adjusted healthy subjects.[139, 140]

2.2.7 Humeral component loosening

Humeral component loosening is rarely an indication for revision. Cil et al. analysed patient data with humeral component loosening as outcome. Over the course of 20 years 1,423 patients underwent 1,584 primary Neer and Cofield shoulder arthroplasties. Estimates of survivorship free of revision or removal of the humeral component for any reason were 94.8% (95% confidence interval [CI], 93.6-96.0) at 5 years, 92.0% (95% CI, 90.4-93.6) at 10 years, 86.7% (95% CI, 84.2-89.4) at 15 years, and 82.8% (95% CI, 78.5-

87.5) at 20 years. Younger age, male gender, replacement due to posttraumatic arthritis, an uncemented component, and use of a metal-backed glenoid component increased the likelihood of humeral component failure.[141] The AOANJRR data can be misleading, as when a total shoulder system has failed, revision surgery will very frequently get rid of a well-fixed stem to address system incompatibility issues.

2.2.8 Tribological considerations and nomenclature

Wear by definition is loss of material in the form of debris from the implant surface.[142]

Wear has three classical mechanisms: adhesion, abrasion and fatigue. Other means of surface damage are also possible (scratches, lamination, etc.) but these usually do not result in loss of material from the implant surface. Throughout this work, the effect of true wear and other means of damage together is referred to as “damage”, whereas “wear” is the consequence of adhesion, abrasion and fatigue.[143]

Wear modes, the production of debris in an artificial joint, can be classified into four groups (Figure 16).

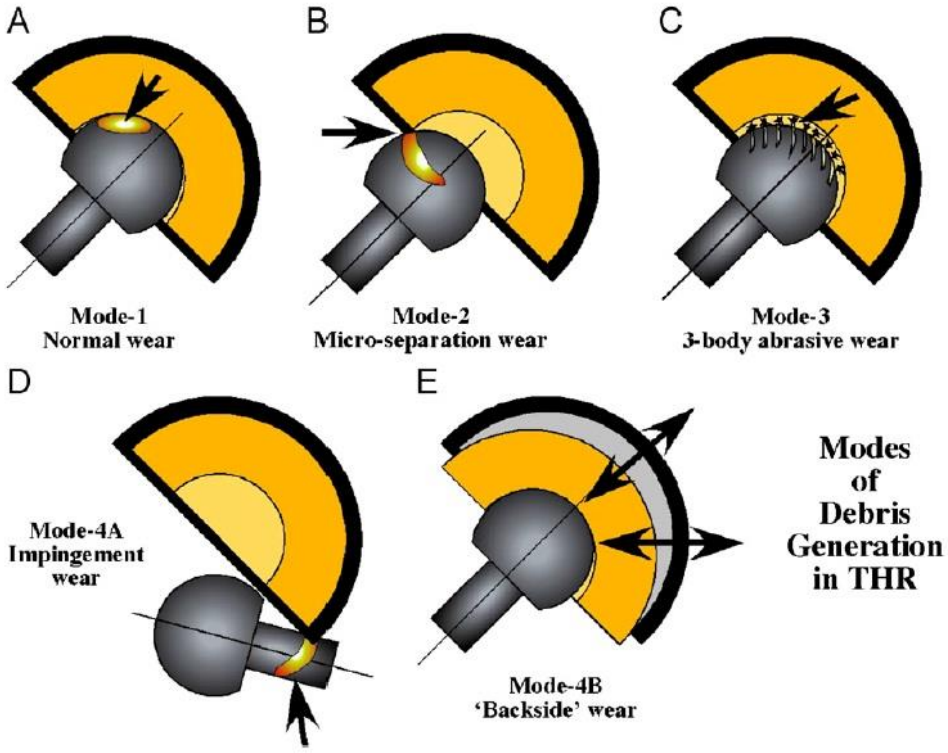


Figure 16. The four modes of artificial joint wear.[143] Reproduced from McKellop HA. The lexicon of polyethylene wear in artificial joints. Biomaterials. 2007 Dec;28(34):5049-57.

In Mode 1 wear occurs at the intended bearing surface. In Mode 2 one intended bearing surface causes wear on a non-intended bearing surface. An example is when the humeral head wears completely through the polyethylene glenoid liner and touches the metal baseplate. Mode 3 means abrasive third body particle wear. Mode 4 is when two non-intended bearing surfaces are in contact under load. One example of this is scapular notching seen in conjunction with reverse shoulder replacement.[144]

Adhesive wear can be minimised by the use of a lubricant (such as the synovial fluid).[145] Abrasive wear can be minimised by optimal polishing of the bearing surfaces. This also reduces the potential of the surface to capture third body particles. Fatigue wear can be addressed by a design that minimises contact stress, and by making the implant materials tough and crack resistant.[143, 144]

Wear debris is the material removed from the surfaces by wear. In conjunction with polyethylene liners this may mean particles ranging from several mm down to nanometre range.[143]

2.2.9. Assessment of polyethylene wear in anatomical total shoulder arthroplasty

Current methods include computer modelling, in vitro wear tests and in vivo wear rate measurements.

2.2.9.1. Current wear laws and computer modelling of polyethylene wear

Finite element models are often used to model complex biomechanical scenarios. When used to model intended bearing surface polyethylene wear in total shoulder arthroplasty, mathematical rules or laws are necessary to describe the expected wear.

Archard's law is the basis for the earliest algorithms to predict polyethylene wear[146].

$$\delta^{AL} = kw \times p \times s$$

Kw is the wear factor (bearing coupled dependent), p is contact pressure and s is the sliding distance. This formula describes a linear wear depth and assumes that the movement between the contact surfaces is linear.

The so called second generation law is the evolution of Archard's law. The second generation law tries to take into account the experimental findings that multi-directional motion produces a higher wear rate. It introduces the concept of cross-shear. This concept is based on the assumption that polymer chains preferentially align in the direction of the dominant frictional work, in other words the principal molecular orientation is the direction of the highest friction. The principal molecular orientation hence can also be defined as the orientation that minimizes the amount of

transverse frictional work. Cross shear ratio is transverse frictional work divided by total frictional work[147].

$$w=\sum_{i=1}^{n} k(CSR)\cdot\sigma_i\cdot\left|\vec{u}_i\right|$$

In the formula w is the local wear depth per duty cycle, k is the local wear coefficient, CSR is cross-shear ratio, *σi* and *ui* are the local contact pressure and sliding distance vector for increment *i* to n.

In volumetric wear, the interpretation of the above is:

$$\mathrm{VW}=\sum_{p=1}^{n_p}\delta^p A^p$$

where n_P is the number of nodes of the surface domain, δ_P is the linear wear of node P, and A^P is the contact area associated with node P.[148] This is the integration of linear wear over the surface domain.

In a computer-simulated wear study by Quental et al. the volumetric wear rate for an anatomical glenoid was 7.9-9.21mm^3 /year, depending on the degree of joint conformity. They found no difference between the wear rate of metal back and all polyethylene cemented components. Their result must be evaluated with caution. The authors used shoulder kinematic data from only one, 25 years old healthy male. Although the simulated movements included abduction, flexion and rotation, all these movements were unloaded. No plastic deformation was observed on the simulated liners which is unrealistic. Due to these facts this study can be expected to underestimate in vivo wear rate.

An earlier study by Ribeiro et al.[149] simulated wear only in abduction in their computer model, and the biomechanical scenario is probably even less realistic.

Overall, computer simulation of wear has a large potential as it is less time consuming than in vitro test and more controlled regarding parameters than in vivo wear assessment.

2.2.9.2. In vitro wear tests

In vitro tests are performed using mechanical wear simulators mimicking in vivo shoulder kinematics. Other than ad- abduction, flexion-extension and rotational movements, translation of the ball in the socket is possible in the shoulder, unlike the hip joint for example. This complexity is hard to reproduce, and many studies use simplified joint kinematics. One example is the paper by Haggart[150] (Neer award 2017) where only flexion-extension and abduction-adduction was simulated, and not simultaneously. The latter can be a significant problem, as shown later in this chapter.

Other studies, such as the recent study of Braun et al.[151] strive for a more realistic modelling of wear in anatomical shoulder replacement. Other than abduction-adduction and rotational movements, translational movements were also simulated in a servohydraulic machine. The experimental setup included a freely programmable virtual soft tissue model, to allow simulation of a rotator cuff defect. The system tested had 8mm mismatch between the glenoid and humeral radius, and the glenoid component was UHMWPE.

The basic setup of the experiment was glenohumeral rotation mimicking abduction-adduction, superior-inferior translation in a force-controlled manner. These movements, unlike the aforementioned Haggart experiment, were simultaneous. Initially an intact rotator cuff was simulated. The measurements showed a low polyethylene wear rate in the magnitude of 0.1mg/10^6 cycles. When anteversion-retroversion rotation of +-5 degrees was added, the wear rate rose to 46mg/10^6 cycles. With the anteversion-retroversion rotation of +-10 degrees, the wear rate went up to 58.9mg/10^6 cycles.

In the above, intact rotator cuff scenario, the superior-inferior movement translation of the humeral head was 3.93 ± 0.52 mm, as determined by the complex soft tissue simulation. Simulation of wear was also done using a rotator cuff deficient model. With the insufficient rotator cuff simulation, the translational movement increased to 5.33 ± 0.23 mm. It must be noted that Tempelaere et al. found larger superior-inferior translation in cuff-deficient shoulders using 3D real time MRI[152]. In a normal, native shoulder the superior-inferior translation was 3.4mm, in a cuff-deficient native shoulder 6.4mm. The wear tests with the insufficient rotator cuff showed further increase in the wear rate of the glenoid polyethylene, to 79.7mg/10^6 cycles. Considering a density of 0.97g/cm^3, this translates to 77.3mm^3 in volumetric wear.

The size and number of debris particles was also higher when anteversion-retroversion movement was introduced.

The authors explained the findings with cross-shear effect. Although this conclusion is not directly supported by their data, they speculate that the unidirectional motion with the combination of superior-inferior translation and GH rotation could align the polyethylene molecular chains, leading to strain-hardening of the wear surface. This could explain the low wear rate in this group. The introduction of anteversion-retroversion movement increased cross shear and increased wear rate as well. This theory is in keeping with the current concept of polyethylene wear in computer simulations.

Mueller et al.[153] using a very similar experimental scenario concluded that ceramic-on-polyethylene joints produced significantly less polyethylene wear than metal-on-polyethylene (45.99mg/10^6 cycles vs 62.75mg/10^6 cycles, respectively). They concluded that wear speed also depends on the material of the artificial joint.

2.2.9.3. In vivo volumetric wear rate in anatomical total shoulder arthroplasty

Searching Pubmed using terms “in vivo” “wear” and “glenoid” gave 8 hits, none of which was relevant from polyethylene anatomical glenoid wear rate. Search terms “in vivo” and “wear” and “shoulder arthroplasty” returned 9 hits, none relevant. Search terms “glenoid wear” and “shoulder arthroplasty” gave 174 hits, and again none was relevant. Few papers reported on alterations of glenoid bearing surface describing the modes of wear, described location of wear, radius of wear, presence or absence of edge damage, deformation but none reported on volumetric wear rate.[116, 154, 155]

Searches in other databases and review of reference lists of reviewed papers identified one study in the subject, that of Swieszkowski et al.[156] The study reports on 6 explanted glenoid components, 1 of which was a metal back while all the others were all-polyethylene. The mean in vivo time was 10 years with a range of 7 to 14 years. A laser scanner was used for the tests. Ironically the only metal back component, which showed the highest linear penetration per year, was excluded from their volumetric analysis as the liner had been so badly damaged that it could not be assessed. Out of the 5 all-polyethylene cases patient data were not available for 2 cases, so eventually volumetric wear rate was presented for only 3 cases. The figures were 6.95mm^3/year, 30.39mm^3/year and 27.02mm^3/year.

Comparison of results of in vivo and in vitro, or even computer simulated tests would require the average number of cycles per year. Some data on shoulder activities is present,[157-160] but no joint load has been recorded synchronously. For the sake of simplicity I will assume 10^6 cycles per year, which is in the magnitude of cycles proposed by Cole et al.[160]

Due to the very small number of in vivo wear cases, comparison of in vitro wear simulation and in vivo wear figures should be done with great caution.

Using a larger ex vivo glenoid cohort would be more meaningful, and this is what is going to be attempted later in this work.

To conclude this chapter, computed wear simulation has a great potential but more complex models are needed. The current models either focus on fatigue, loosening and force transmission at the bone - glenoid implant interface, or on the wear simulation between the artificial humeral head and the glenoid component. A more realistic model would incorporate both. Other elements, such as computer modelling of osteolysis and the consecutive component migration would also need to be considered, as the latter significantly changes kinematics and biomechanics. Until this is achieved, computer models can be expected to underestimate glenoid polyethylene load – although this conclusion is highly speculative.

Current, up to date in vitro glenoid wear models are very complex, but still there is no complex model that considers polyethylene wear at the glenohumeral interface and biomechanical changes due to glenoid position changes secondary to loosening.

In vivo wear analysis provides the most realistic wear figures but data analysis is extremely difficult due to impossible control or unavailable record of biomechanics, kinematics and shoulder activity.

2.2.9.4. The biomechanics of the glenoid liner – bony glenoid interface

2.2.9.4.1. Computer simulated models

Joint load transfer

Joint load transfer in conjunction with the glenoid component and the bony glenoid is of fundamental importance. In a recent study by Patel et al. a finite element model of the shoulder was built.[161] The authors assessed load transfer in a native shoulder as well as in a cemented all-polyethylene glenoid component scenario and a metal back glenoid scenario. No rotator cuff-deficient scenario was simulated, but instead, a posterior eccentric

loading simulation was done. The methodology of the paper can be criticised because the posterior loading scenario did not simulate a retroverted glenoid. The results can still be interpreted as an anatomically rebuilt glenoid post surgery. Although the study included a low loading (14MPa) and a high loading (3 times the low loading scenario) analysis, these were static at a simulated 60 degrees abduction, without the complex movements in a shoulder joint. Also, the biomechanics of the shoulder girdle muscles and dynamic translation were not considered. The study used a commercially available glenoid component for the simulations, but only one, 3 pegged design. The metal back glenoid simulations were done such that the 1mm cement mantle was given metallic properties which did not reflect the bulkier nature of a real life metal back glenoid component.

In a native shoulder joint the majority of stress was distributed in the cancellous bone at the centre of the glenoid. The cortical layer of the glenoid vault at the more proximal, narrower section of the glenoid vault concentrated these forces (Figure 17). In the posterior loading scenario of the native glenoid the posterior half of the cancellous glenoid was loaded and conveyed more force to the posterior cortical section of the vault.

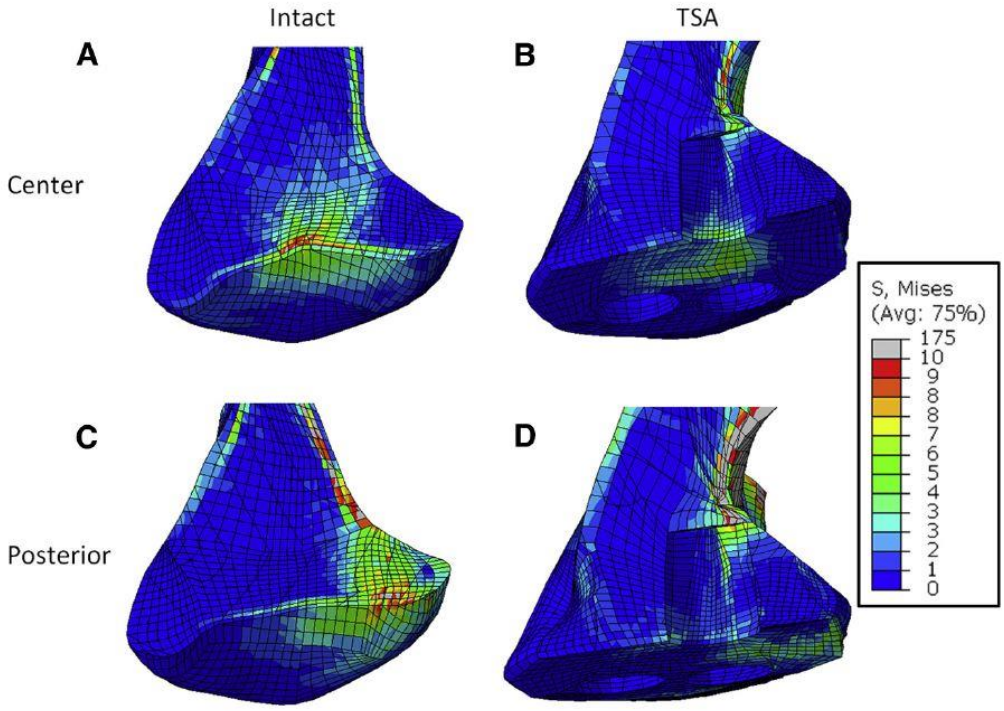


Figure 17. Cross sectional images of computer simulated glenoids in superior view. A and C are native, B and D are replaced glenoids. A and B represent central, normal loading (not high loading) scenarios, C and D are normal, posterior loaded. The magnitude of Von Mises stress is colour coded in MPa.[161] Reproduced from Patel RJ, Wright TM, Gao Y. Load transfer after cemented total shoulder arthroplasty. J Shoulder Elbow Surg. 2014 Oct;23(10):1553-62. Epub 2014/04/18.

In the case of a cemented glenoid and central loading, greater than 67 percent of the applied load was still carried by the cancellous bone between the pegs, cement carried between 13% and 24%, polyethylene pegs carried between 3% and 11% of the load. In the case of a cemented polyethylene insert, less load affected the cancellous bone and the polyethylene implant and cement transferred the difference directly onto the cortical section of the glenoid vault, proximal to the ends of the pegs. This indicated a degree of stress shielding.

In case of eccentric loading, the loading distributions among the bone, cement, and implant remained relatively consistent, although some minor differences were observed.

Compressive load and tensile stresses were observed during eccentric loading of the polyethylene implants (Figure 18 and Figure 19).

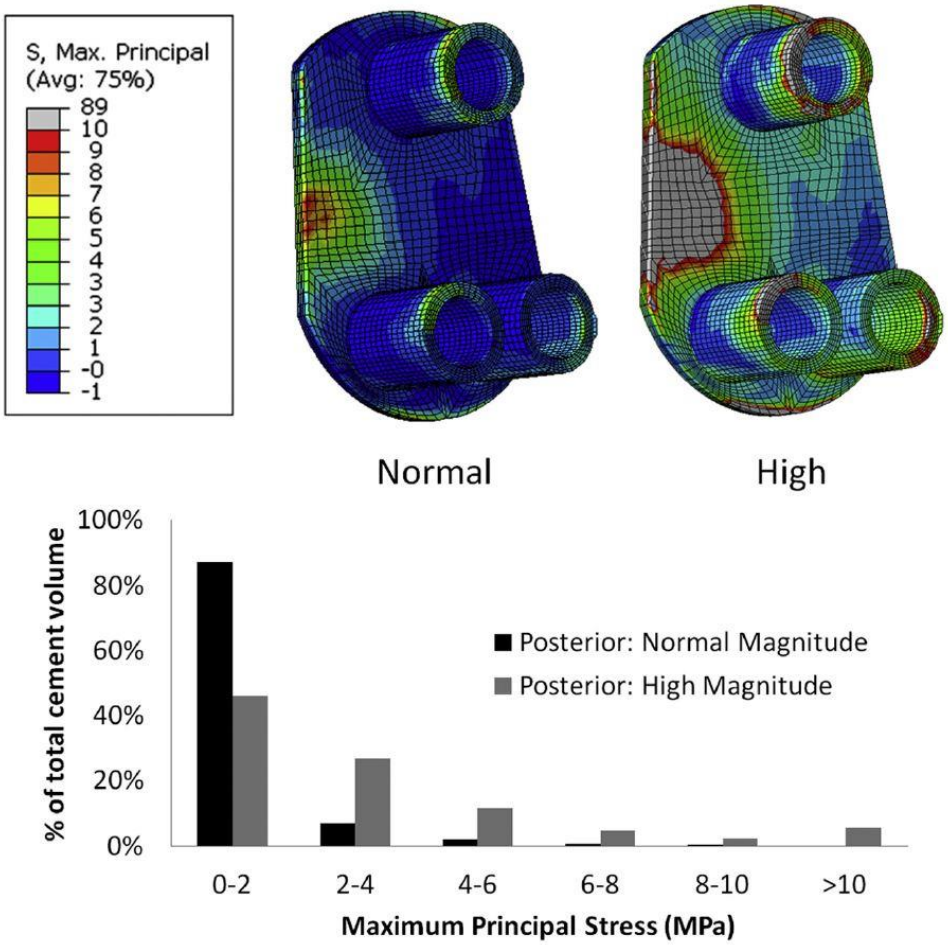


Figure 18. Cement layer maximum principal stress distribution in eccentric posterior loading, for high and normal loading. Although high stress in excess of 10MPa was observed over the posterior margin of the cement layer, the extent and magnitude of tensile stress was almost negligible. Reproduced from Patel RJ, Wright TM, Gao Y. Load transfer after cemented total shoulder arthroplasty. J Shoulder Elbow Surg. 2014 Oct;23(10):1553-62. Epub 2014/04/18.

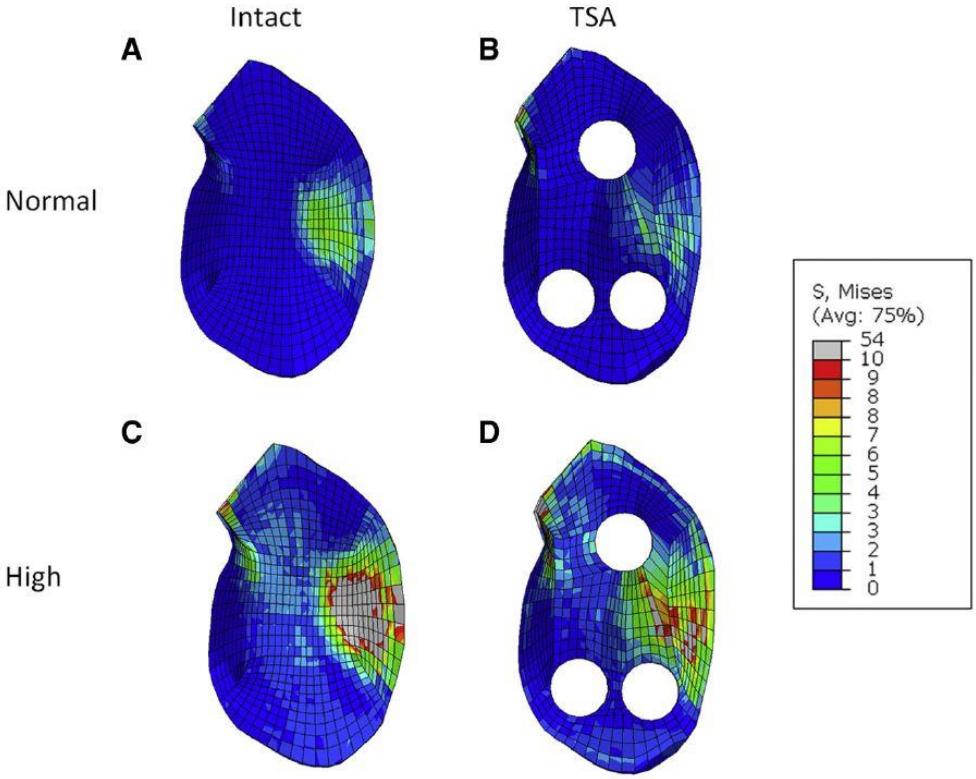


Figure 19. Bone layer von Mises stress distribution in eccentric posterior loading with normal and high load, in a native and replaced glenoid. Reproduced from Patel RJ, Wright TM, Gao Y. Load transfer after cemented total shoulder arthroplasty. J Shoulder Elbow Surg. 2014 Oct;23(10):1553-62. Epub 2014/04/18.

In case of a metal back glenoid stress shielding was more pronounced than in a cemented implant. The joint load carried by the bone was as low as 42%, with the metal backing carrying as much as 57% (Figure 20).

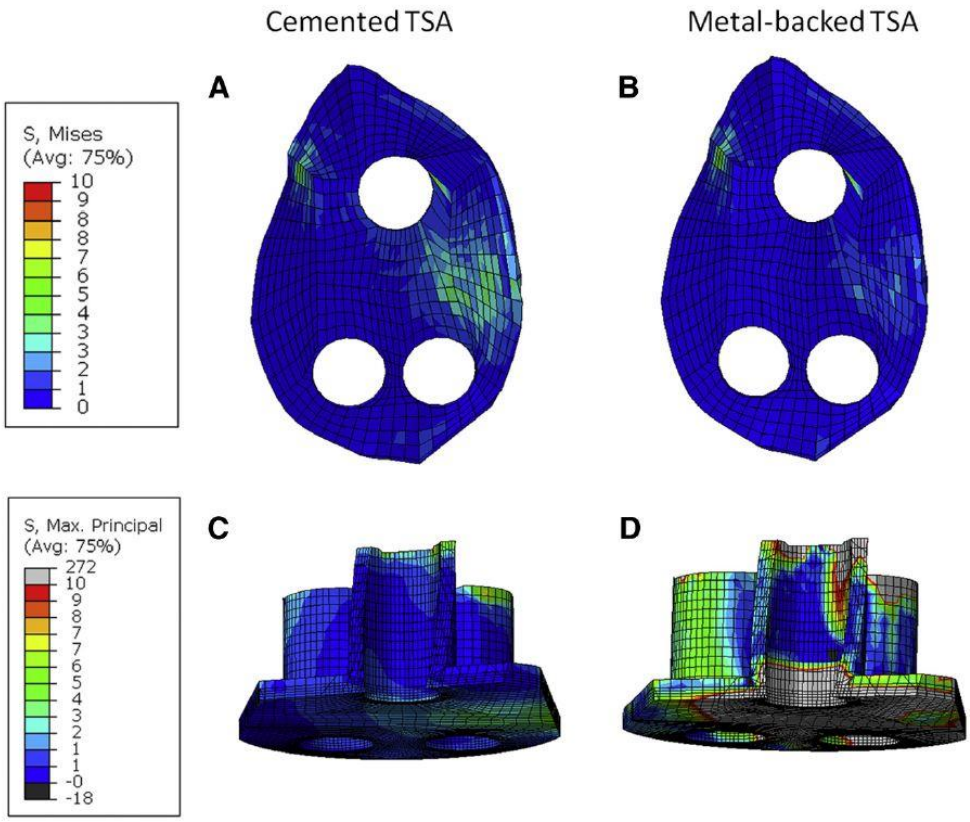


Figure 20. Von Mises stress distribution in cemented and metal-back glenoid. A and B are the glenoid bone layers, C is the cement mantle in the all-polyethylene replacement, D is the metal back. Normal eccentric loading. The metal component conveys more stress than the corresponding cement layer, with more stress shielding.[161] Reproduced from Patel RJ, Wright TM, Gao Y. Load transfer after cemented total shoulder arthroplasty. J Shoulder Elbow Surg. 2014 Oct;23(10):1553-62. Epub 2014/04/18.

Geraldes and al.[123] built a computer model based on finite element analysis and tested 1376 different glenoid designs, in about 25 hours. This highlights the importance of creating validated computer models as this volume of data in in vitro experiments would require a lot of time. The variants tested differed in thickness, number, position and thickness of pegs, presence or lack of a central peg, keeled or pegged design, etc. The variants tested are summarised in Figure 21.

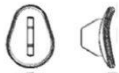
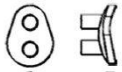
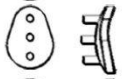
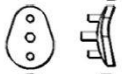
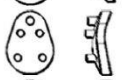
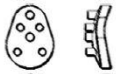
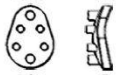
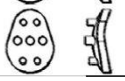
	Fixation Type	Reference Geometry	Number Features	Central Peg	Fixation Width or Diameter (mm)	Fixation Length (mm)	Component Thickness (mm)	Total Number of Geometries
1	Keel		1	No	3, 4, 5, 6	15, 17.5, 20	4, 5, 6, 7	48
2	2Peg		2	No	7, 8, 9	7, 10, 13	4, 5, 6, 7	36
3	3Peg		3	Yes	4, 4.5	5, 6, 7	4, 5, 6, 7	24
4	3PegC		3	Yes	4, 5, 6	5, 7, 9, 11	4, 5, 6, 7	48
5	5Peg		5	No	3.5, 4, 4.5, 5	3.5[b], 4, 4.5, 5	4, 5, 6, 7	28
6	5PegC		6	Yes	3.5, 4	3.5[b], 4, 4.5, 5	4, 5, 6, 7	24
7	6Peg		6	No	3.5, 4, 4.5, 5[a]	3.5[b], 4[c], 4.5, 5	4, 5, 6, 7	40
8	6PegC		7	Yes	3.5, 4, 4.5, 5	3.5[b], 4, 4.5, 5	4, 5, 6, 7	28
9	6PegA		6	No	3.5, 4, 4.5, 5[a]	3.5[b], 4[c], 4.5, 5	4, 5, 6, 7	40
10	6PegAC		7	Yes	3.5, 4, 4.5, 5	3.5[b], 4, 4.5, 5	4, 5, 6, 7	28

Figure 21. Summary of the glenoid designs tested by Geraldes et al. using finite element analysis.[123] Reproduced from Geraldes DM, Hansen U, Amis AA. Parametric analysis of glenoid implant design and fixation type. J Orthop Res. 2017 Apr;35(4):775-84. Epub 2016/06/20.

They concluded that peripheral fixation features were better than central from the point of view of stability. Larger number of smaller and shorter peripheral pegs also resulted in better bone preservation and smaller likelihood of vault perforation. Central pegs, however, decreased the degree of central displacement (sinking of the centre of the implant into the glenoid vault on loading). Central pegs however, as proven by Patel et al.[161] result in stress shielding. As expected, a thicker implant also resulted in less central displacement for load. 6PegA, 5Peg, and 6PegAC versions, however, did not do well in edge loading scenarios (superior, inferior and posterior), with 6PegAC and 6PegA exceeding their yield strength. Thicker implants, due to increased stiffness, produced more simulated movement

of the unloaded side in eccentric loading scenarios, meaning more tensile forces. Thicker implants may overstuff the replaced joint while thinner implants may result in decreased wear resistance. Keel, 2Peg, 3Peg models, that is, the ones with thicker central fixations produced the lowest stresses under edge loading, especially for the superior and inferior loading.

Unfortunately, the magnitude of tensile load on the unloaded side of the glenoid implant in eccentric loaded scenarios was not specified in the paper, nor was the magnitude of displacement ("lifting off").

The paper did not simulate a metal back glenoid.

2.2.9.4.2. In vitro biomechanical tests of the glenoid implant – bone interface

In vitro mechanical tests tend not to measure forces in and around the implant - bone interfaces, but attempt to recreate and model implant failure through fatigue or other means of material failure.

Junaid et al.[162] investigated the mechanism of failure of cemented all-polyethylene implants. Instead of using factory standard implants, they used a "2D" custom implant (Figure 22) to simulate the rocking horse effect.

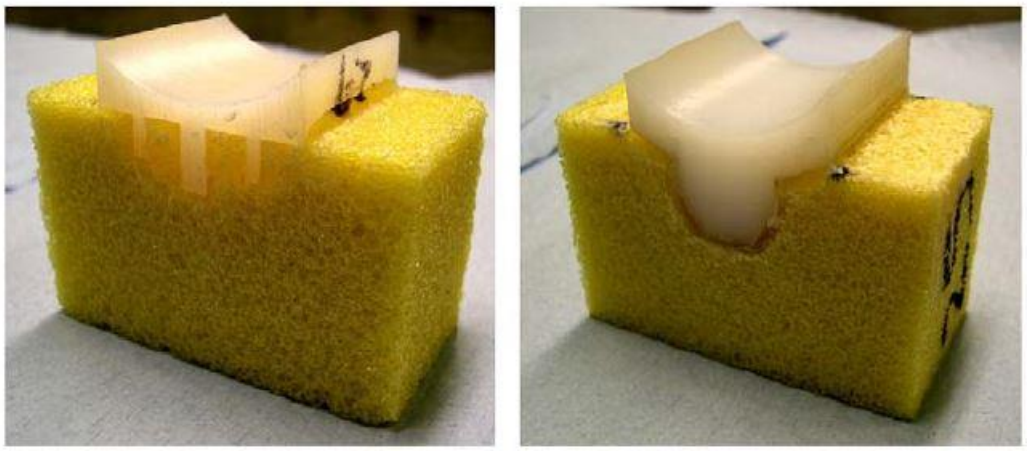


Figure 22. The 2D implant to simulate the rocking horse effect.[162] Reproduced from Junaid S, Gupta S, Sanghavi S, Anglin C, Emery R, Amis A. Failure mechanism of the all-polyethylene glenoid implant. Journal of Biomechanics. 2010;43(4):714-9.

A compressive force of 1800N was applied with a matching 2D head (Figure 23). The head was moved upwards from the centre of the glenoid to reach 83% average subluxation load, in repeated cycles. It was concluded that failure happened at the cement - implant interface and the initial separation of the implant started at the inferior edge of the component. Further propagation of the crack was different depending on glenoid implant type, as depicted in Figure 23.

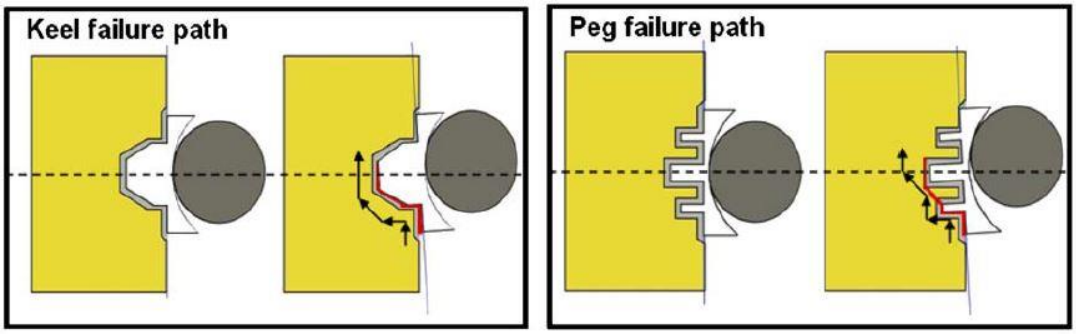


Figure 23. Propagation of crack depending on pegged or keeled glenoid design[162]. Reproduced from Junaid S, Gupta S, Sanghavi S, Anglin C, Emery R, Amis A. Failure mechanism of the all-polyethylene glenoid implant. Journal of Biomechanics. 2010 10/05/accepted;43(4):714-9.

Progressive superior bone crushing was also observed although the study used forces that appeared reasonable based on literature data. Although this is speculative, it is easy to interpret the above phenomenon the following way. Fatigue compression fracture occurs superiorly and the implant starts to pivot around the fixed central part. This movement lifts the low end of the glenoid off the cement bed.

It is unclear though, or at least not proven by the above paper, whether the lower end implant - cement bed separation would have happened without the superior bone crushing, therefore the above experiment proves only the existence of the rocking horse phenomenon in the presence of bone crushing. Taking further the conclusion of the paper, to improve implant survival, stronger bone or lower forces would be needed to avoid rocking horse failure.

Another interesting result was that the cyclic tests were also repeated using more conforming prosthetic designs (Figure 24). Although the numbers were small, except in the case of the curved backed pegged implant, the conforming pair of the same glenoid design withstood more cycles than the less conforming one. This seems to contradict real life experience, but this phenomenon was not explained by the authors.

	 Flat-back peg	 Flat-back keel	 Curve-back keel	 Curve-back peg
Less conforming (5 mm radial mismatch)	8275 (7 0 6), $n=4$	9764 (5 2 5), $n=4$	10,519 (8 5 8), $n=4$	13,150 (7 6 3), $n=4$
Conforming (1 mm radial mismatch)	13,969, $n=1$	12,297, $n=1$	14,905, $n=1$	12,100, $n=1$

Figure 24. The number of cycles survived by implant types[162]. Reproduced Junaid S, Gupta S, Sanghavi S, Anglin C, Emery R, Amis A. Failure mechanism of the all-polyethylene glenoid implant. Journal of Biomechanics. 2010 10/05/accepted;43(4):714-9.

One potential explanation could be better load distribution by the more conforming implant and slower fatigue of bone. Furthermore, this study as well as other studies[119, 162, 163] uses two elements of mechanical testing: compression and up - down movements, and there are no tests to show what repeat compression alone could do regarding glenoid loosening. This idea will be further discussed in the discussion chapter of the vacuum tests (Chapter 4.4).

A slightly different approach was taken by Gregory et Al.[163] to assess the rocking horse mechanism and cemented glenoid component loosening. A real life keeled glenoid component was cemented into either cadaveric glenoid or bone substitute. A compressive force of 750N was used between the glenoid and an artificial humeral head and the head was moved from the centre of the glenoid upwards to 90% subluxation load, to simulate the rocking horse mechanism. The experimental setup is depicted in Figure 25.

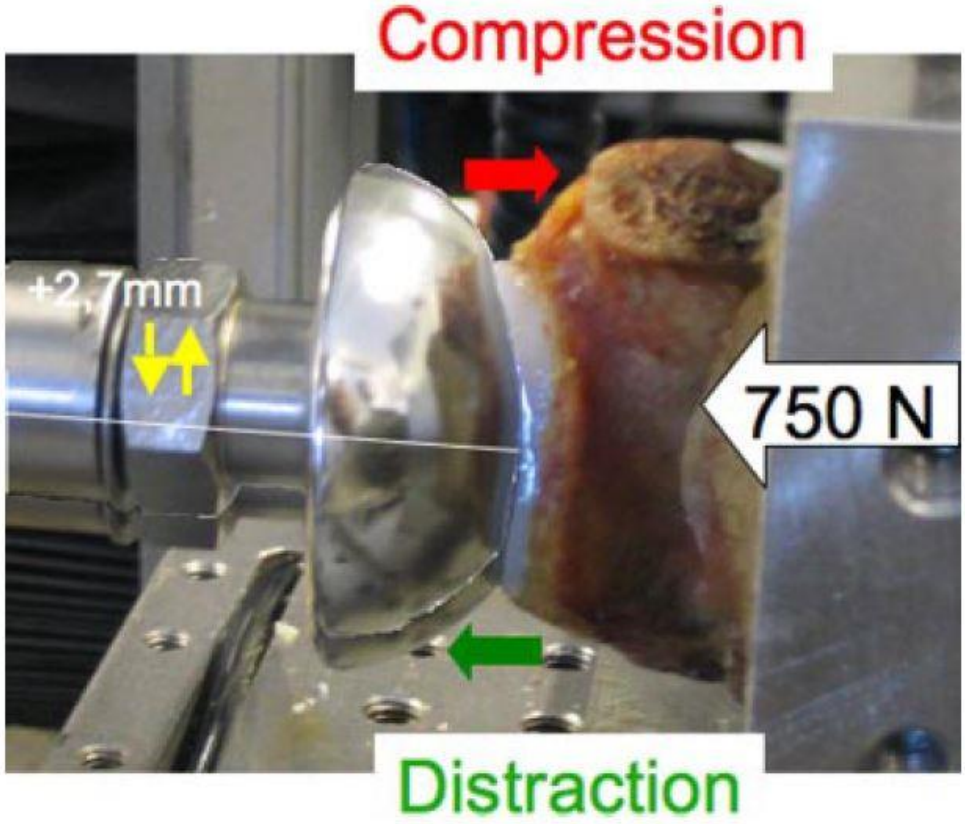


Figure 25. The experimental setup to simulate the rocking horse mechanism by Gregory et Al.[163] Reproduced from Gregory T, Hansen U, Taillieu F, Baring T, Brassart N, Mutchler C, et al. Glenoid loosening after total shoulder arthroplasty: an in vitro CT-scan study. J Orthop Res. 2009 Dec;27(12):1589-95.

In order to make the signs of component fixation failure visible, CT scanning as well as direct observations with microscopy were made. The implant – cement - bone interface was divided into zones as shown in Figure 26.

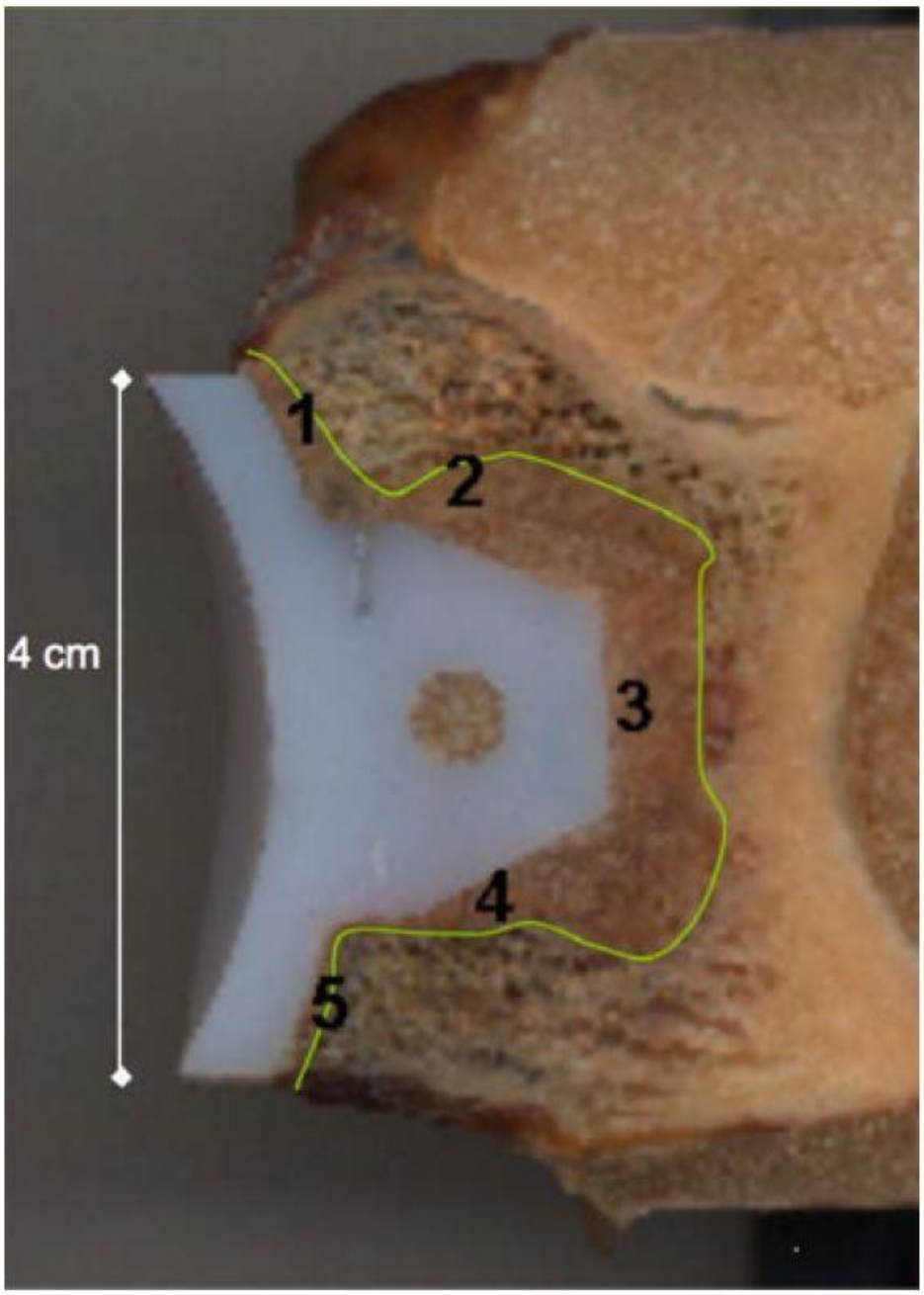


Figure 26. Zones of glenoid fixation failure[163]. Reproduced from Gregory T, Hansen U, Taillieu F, Baring T, Brassart N, Mutchler C, et al. Glenoid loosening after total shoulder arthroplasty: an in vitro CT-scan study. J Orthop Res. 2009 Dec;27(12):1589-95.

Micro CT scan results were validated against cracks observed using microscopy, and good agreement was observed in zones 1 and 5.

Cracks started to occur simultaneously in zones 1 and 5 after 10000 cycles. In zone 1, all specimens showed a crack involving the whole length of the zone after 70000 cycles. In zone 5, 2 cadaveric specimens did not show a crack affecting the full length of the zone. Cracks were initiating at the edge of the implant progressing towards the keel. Debonding always happened at the cement - implant interface. The authors also state that the middle, keel region remained partially intact and that the cracks in zone 1 developed independently from the crack in zone 5. Cement creep or bone yielding was undetected by this study.

Again, this study provides indirect evidence of the rocking horse mechanism as the main mode of failure. The effect of compression alone is not assessed.

Studies assessing the same phenomenon in metal back glenoids are not available.

2.2.9.4.3. In vivo observations of glenoid component loosening

The original concept of the rocking horse mechanism was proposed by Franklin et al. in 1988[164]. Although there is no doubt about this study's impact and relevance, its methodology would not be considered sufficiently robust nowadays.

The study included 3 groups of patients. There were 7 cases with radiological signs of extensive glenoid osteolysis or a migrating glenoid; one case out of these 7 had a dislocated glenoid component. All cases in this group had unreconstructable cuff deficiencies at the time of surgery. Another group of 7 cases were cuff deficient shoulders without evidence of glenoid loosening. The last group of 16 cases had intact glenoid components radiologically and intact rotator cuffs at the time of surgery.

The authors created a radiolucency score to describe the degree of osteolysis around the glenoid component, which had no validation. This is not surprising as the relevance of radiolucent lines around the glenoid was

a subject of debate at the time. The lucency scores for each patient were recorded. The authors introduced the concept of "glenohumeral centre-to-centre distance" to describe the cranial migration of the humeral head in relation to the glenoid centre. The methodology of the measurement in the paper does not mention any attempt to standardise the radiographs, or demonstrate that standardisation was not necessary. Then a correlation analysis was done to prove that more superior migration of the head led to more extensive osteolysis. The statistical metric they used was "r^2", and the value they acquired was 0.25, which indicates a correlation coefficient of 0.5. One possible interpretation of "r^2" is that it describes the percentage of points that fall on a linear regression line. Either way, this statistic does not prove causality.

Another important question is the problem of glenoid loosening. Glenohumeral centre-to-centre measurements may not be very reliable in the light of a migrating glenoid, especially if the reference used is the immediate postoperative radiograph, where the glenoid is well fixed. So although the second group of patients with a deficient cuff but without a radiologically lose glenoid had lower glenohumeral centre-to-centre values and lower osteolysis scores, the validity of this statistical analysis is debatable.

The introduction of the rocking horse concept is speculative in the paper and is not backed up by any scientific data. The paper did not suggest that the rocking horse mechanism was the only mean of glenoid loosening.

As the theory of the rocking horse mechanism is very logical, its validity has not been questioned.

The very frustrating question of radiolucent lines around the cemented all polyethylene glenoid implant was clarified by Gregory et al[163]. It has been proven that evolving radiolucent lines are in fact signs of failure and debonding at an interface. Gregory also suggested a CT scan protocol for the in vivo detection of radiolucent lines, with the full description of methodology in his PhD thesis.[165]

Gregory's findings have been verified by Streit et al. in an in vivo study using tantalum bead-marked cemented glenoid components and radiostereometry.[166] Radiolucencies were mostly found around components that showed high levels of rotational motion, although some well-fixed components also showed surprisingly high mobility relative to the bony glenoid. The significance of the latter is unknown.

3.0 Hypotheses and aims

3.1 Hypothesis 1.

Vacuum forces between the artificial head and the polyethylene glenoid liner play an important role in the disassembly of the polyethylene glenoid insert from the metal glenoid baseplate, in the Nottingham TSR system.

3.2 Hypothesis 2.

Central wear of the polyethylene glenoid liner is slower than eccentric.

4.0 Hypothesis 1. Vacuum forces between the artificial head and the polyethylene glenoid liner play an important role in the disassembly of the polyethylene glenoid insert from the metal glenoid baseplate, in the Nottingham TSR system.

4.1 Introduction

In this section a novel mechanism for disassembly is proposed. Describing this mechanism is important from the point of view of future prosthesis design.

There are no publications to suggest that vacuum forces exist between artificial shoulder components. Rosenberg et al. reported that disassemblies were the second most frequent cause of failure in the Nottingham TSR system.[3]

The Australian Orthopaedic Association National Joint Replacement Registry in their 2015 report publish a component disassembly rate of 4.5% in total shoulder arthroplasty,[2] in spite of decades of surgical experience and research into the subject. Even contemporary designs seem to suffer this problem.[167] In the Nottingham Total Shoulder Database 32 dissociations were recorded in 464 primary and revision arthroplasty cases (6.89%), with the glenoid implant dissociation ranging from 2 months to over 7 years postoperatively.

Although this is a recognised complication described by several authors,[21, 129, 168-170] very little has been published to explain the underlying possible mechanisms in metal back glenoids.[171, 172]

The “rocking horse” mechanism is currently the accepted model for glenoid component loosening for all-polyethylene cemented glenoid components, described by Franklin[164]. Franklin based his idea on the fact that the amount of superior migration of the humeral component was closely correlated with the degree of glenoid loosening. This assumption was made on 7 cases with non-functional rotator cuff. The study proves only that superior migration of the head leads to glenoid loosening, and although the

“rocking-horse” mechanism is proposed as an explanation, the paper gives no direct evidence for it. The “rocking horse” is also not claimed to be the only mechanical mechanism for loosening.

Anglin set up a test method[119] for cemented all-polyethylene implants which, to date, forms the base of mechanical test standards by ASTM. Although Franklin[164] was suggesting that a superiorly displaced humeral head was levering the glenoid out of its position, Anglin used superior and inferior movement of the artificial head in the glenoid socket. This method first produces compression at one end of the glenoid and distraction at the other, and then vice versa, but ignores anteroposterior eccentric loading. In spite of the otherwise thorough methodology the study does not assess the effect of repetitive, cyclic compression on its own, raising questions about the validity of the paper’s conclusions.

The Lazarus glenoid component loosening scoring system seems to contradict the rocking horse mechanism. The observations were made on 289 cases with radiological follow up. Radiolucency in the grading system diagrams starts from the cranial end of the glenoid and the distal peg preserves contact till the late stages of loosening. What the scoring system suggests is collapse of support cranially precedes the loosening distally. This resembles the findings of Junaid[173], in the sense that distal glenoid failure was preceded by superior bone crush.

Patel et al. in a finite element analysis verify the presence of compressive and tensile stresses in the cement layer of a glenoid component in an eccentric loading scenario.[161]

Although nobody has questioned the rocking horse mechanism as a potential mean of glenoid loosening, there is no evidence to suggest its exclusivity.

The Nottingham metal back glenoid component has an interface between the polyethylene liner and the metal back. One obvious explanation of glenoid liner dissociation from the baseplate is the rocking horse mechanism.

It is not unreasonable to speculate that there could be mechanisms other than the rocking horse that play role in glenoid dissociation.

An obvious further explanation for the glenoid component disassembly would be surgical error: improper assembly of the components. In our experience surgical error resulting in faulty assembly of the glenoid component can lead to early disassembly of the glenoid components, but usually within days after surgery. The temporal distribution of our disassembly cases, with all instances occurring more than 2 months post-surgery, does not support surgical error being the cause in our cases.

Ideally the component disassembly rate in a metal back glenoid system should be close to 0%. The high disassembly rate observed could mean that an important biomechanical element is generally overlooked during design.

The idea that vacuum forces play an important role in stabilising a native shoulder joint is an accepted concept.[174-176] The space between the head of the humerus and the glenoid contains synovial fluid, and as long as no gas is allowed to enter the joint capsule, significant vacuum forces resist any attempt to move the humeral head away from the glenoid.[176]

If the same mechanism were to exist in an anatomical artificial shoulder joint, these forces could – amongst other effects - fatigue load the glenoid liner causing its disassembly from the metal glenoid baseplate.

The hypothesis is that vacuum forces in an artificial shoulder replacement do exist, and these forces are capable of uncoupling the plastic glenoid liner from the metal baseplate.

Movements such as pulling oneself up in bed, pulling on door handles, playing tennis, or carrying bags should be capable of creating an element of force with its axis perpendicular to the plane of the metal glenoid baseplate. If these forces are not fully neutralised by the muscles of the shoulder girdle, vacuum forces similar to what has been observed in a native shoulder joint can appear. Whilst such forces may not be large enough to result in disassembly after a single cycle, many cycles at a lower load may lead to disassembly. The average competitive swimmer swims approximately 60 000 to 80 000 m per week. With a typical count of 8 to 10

strokes per 25m lap, each shoulder performs 30 000 rotations each week.[177] A professional tennis player would carry out around 1000 serves per tournament.[178] It is therefore quite reasonable to propose a fatigue failure mechanism for glenoid component disassembly.

Current ASTM standards necessitate only two tests for metal back - polyethylene modular components (Figure 27 and Figure 28). These are inferior-superior and anterior-posterior locking tests. In the standard there are no cyclic prise out tests perpendicular to the glenoid plane.

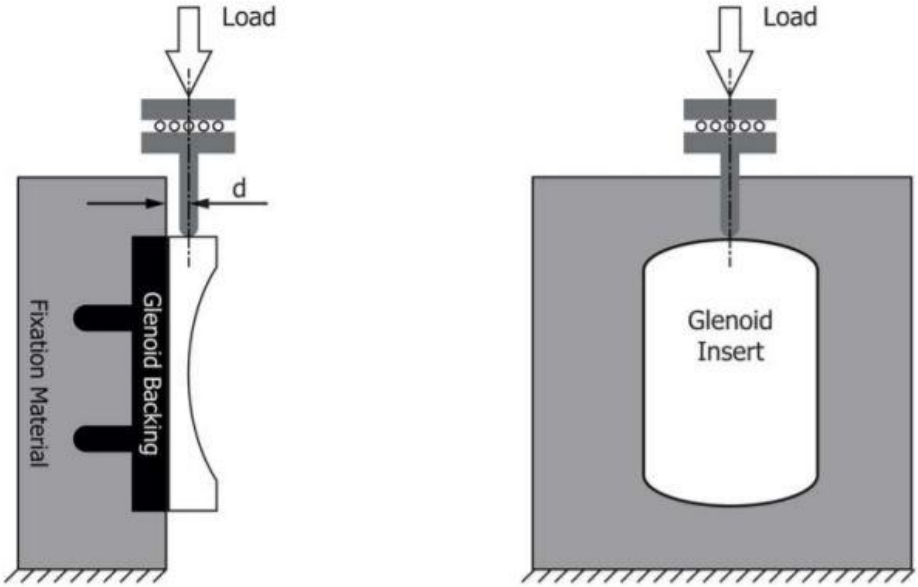


Figure 27. ASTM superior-inferior test method on modular glenoids. Reproduced from ASTM standard.

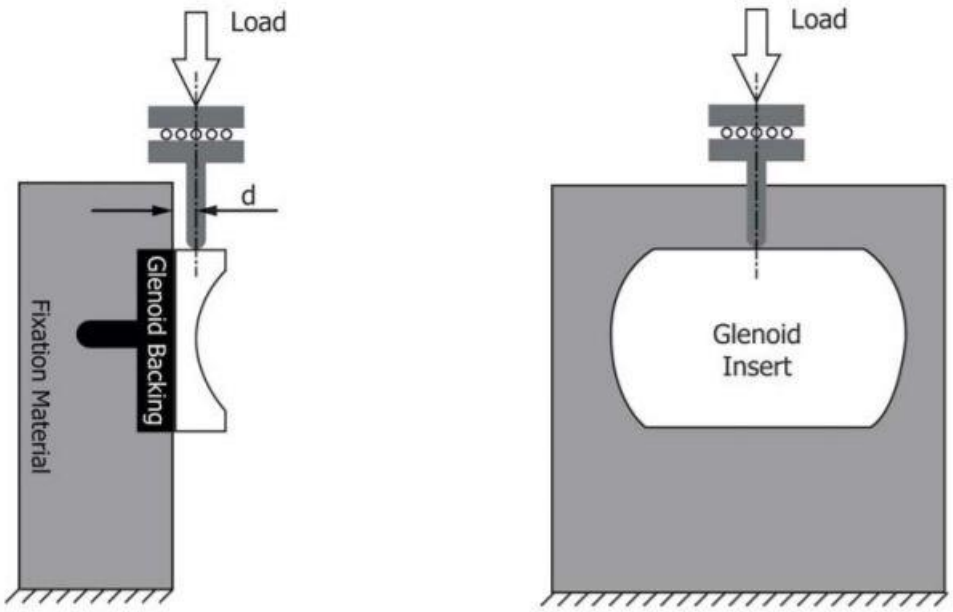


Figure 28. ASTM anterior-posterior test method for modular glenoids. Reproduced from ASTM standard.

The vacuum forces developed between the head and glenoid component were measured *in vitro*. Fatigue tests were also carried out to assess the strength of the clip-on mechanism between the metal glenoid baseplate and the glenoid liner, to test if, in vitro, the vacuum forces would be capable of causing component dissociation.

This study should influence the clinician's implant choice for total shoulder arthroplasty.

4.2 Materials and methods

4.2.1 Tests to measure the actual vacuum forces

An in vitro experimental setup was designed and built to detect vacuum forces. Total shoulder arthroplasty components surrounded by synovial fluid were distracted from each other, and the forces required were measured.

A new Nottingham metal glenoid baseplate, polyethylene glenoid liner and a humeral head was provided by the manufacturer (Biomet UK Ltd, Swindon, UK). The components were assembled and mounted on an Instron 3367 tensile test machine using purpose-made jigs, within an environmental chamber keeping the temperature constant at 37 °C (Figure 29).

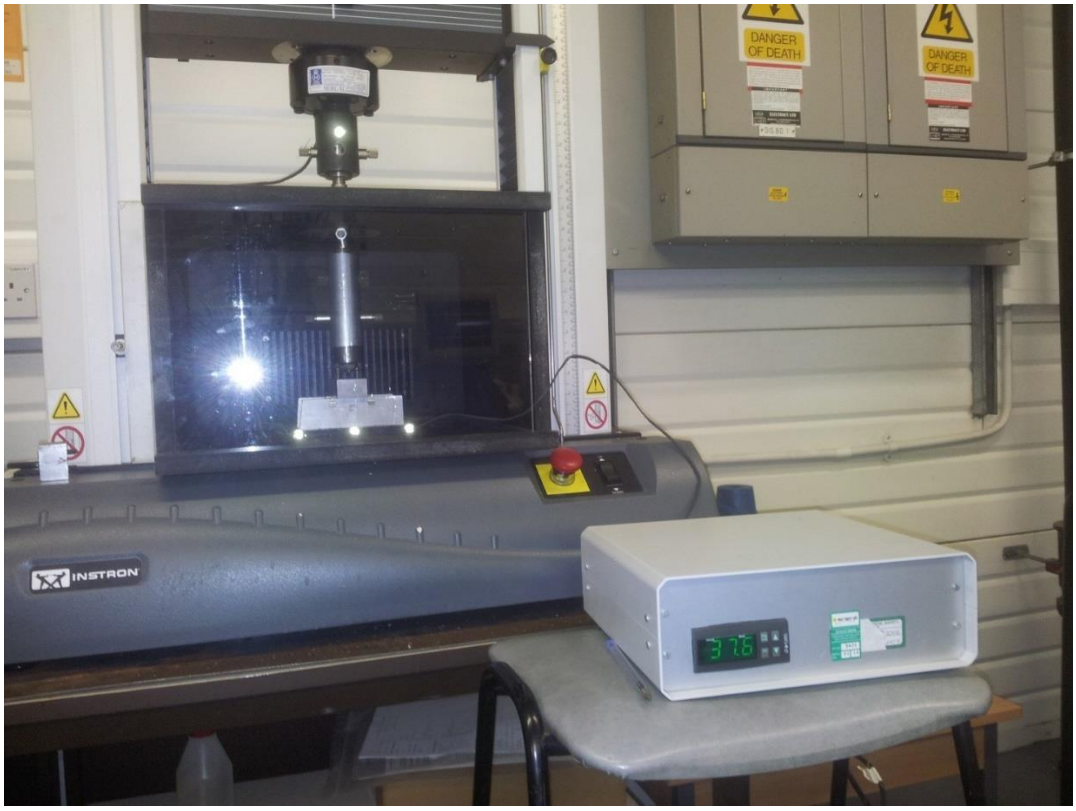


Figure 29. The experimental setup (Part 1)

Bovine synovial fluid (courtesy of School of Veterinary Medicine and Science, Nottingham, UK) was used to surround and lubricate the artificial joint components; this fluid was retained by a commercially available latex condom simulating the joint capsule (Figure 30 and Figure 31). The synovial fluid and space within the joint capsule was free of air bubbles. The radius of curvature of the glenoid liner was the same as that of the humeral head prosthesis, as had been designed and confirmed during the manufacturing process.



Figure 30. The experimental setup (Part 2).

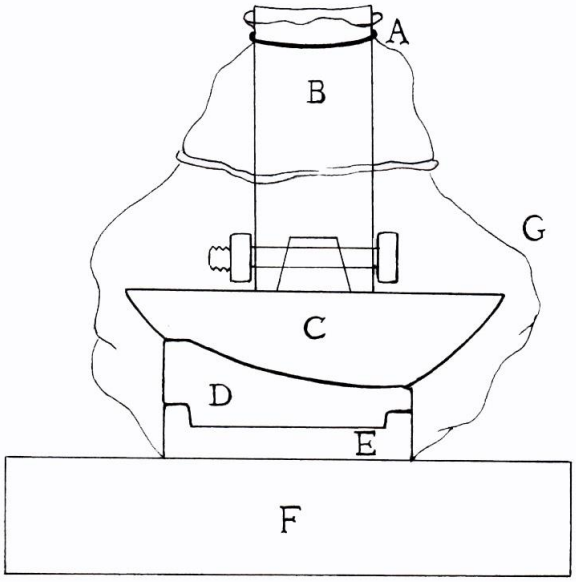


Figure 31. The experimental setup. The metal glenoid baseplate (E) is secured solidly on a fixed metal block (F). The plastic glenoid insert (D) is clipped into the baseplate as per manufacturer's instructions. The prosthetic humeral head (C) is attached to the pulling arm of the Instron machine (B). The shoulder arthroplasty components are surrounded by bovine synovial fluid constrained by a latex condom (G) with an air and water-tight seal (A). During the experiment the humeral head (C) is moved away from the plastic liner (D), and the forces are measured.

Initially the joint was loaded with a small compressive force (10N) to ensure that the components were brought fully into contact. The components were then distracted at 30 mm s^{-1} along an axis perpendicular to the plane of the baseplate. The forces generated by the distraction were measured.

To act as a control, the experiment was repeated without synovial fluid in the joint capsule, five times. Air was therefore free to enter the joint space and expand on distraction. This was to evaluate tensile forces due to the elasticity of the condom.

4.2.2 Cyclic tests to measure the disassembly or disassociation forces required

An in vitro experimental setup was designed and built to detect if the vacuum forces measured in the in vitro tests were capable of causing early disassociation of the glenoid components. This may be particularly interesting as the ASTM standards do not require cyclic tests perpendicular to the plane of the glenoid.

A new, unused Nottingham metal glenoid baseplate (provided by the manufacturer) was mounted on an Instron 3367 machine. For each test, a new plastic liner (provided by the manufacturer) was clipped on. The plastic liner was cyclically loaded along an axis perpendicular to the metal baseplate through the existing screw holes on the back of the metal baseplate (Figure 32 and Figure 33).

The tests were conducted with peak cyclic loads of 40, 60, 80N and 300N on a new set of implants each time. The push rods were pushed at the rate of 5.34 N/s to achieve the desired maximum load (40N, 60N, 80N, 300N), and then the rods were withdrawn at 5.34 N/s to 0N load. Between each push there was a pause of 2s. The pause was chosen to be sufficiently long for visual inspection of the implant. The endpoint of the test was the complete disassembly of the liner from the baseplate. These forces had been chosen to simulate the magnitude of the forces observed in native shoulders in cadaveric tests, from 68N to 225N, 146N mean.[179] The number of cycles to failure for each load were recorded. The experiment for each peak force was completed once.

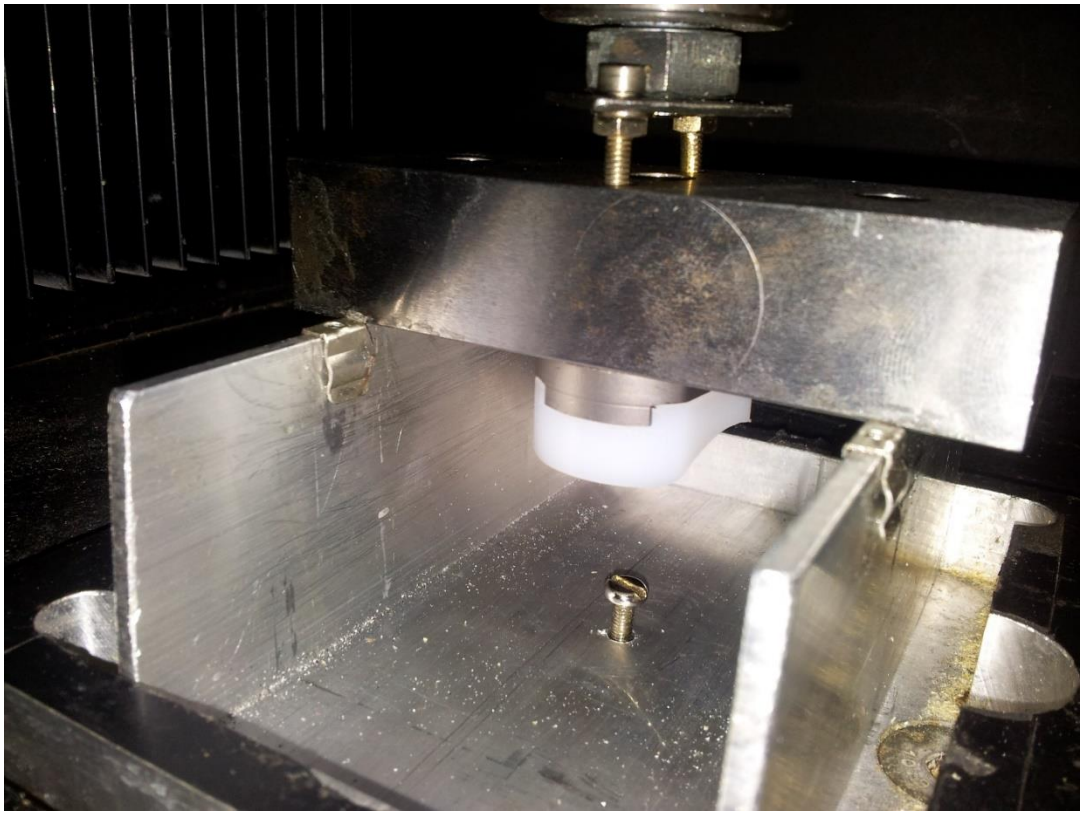


Figure 32. The pushout tests.

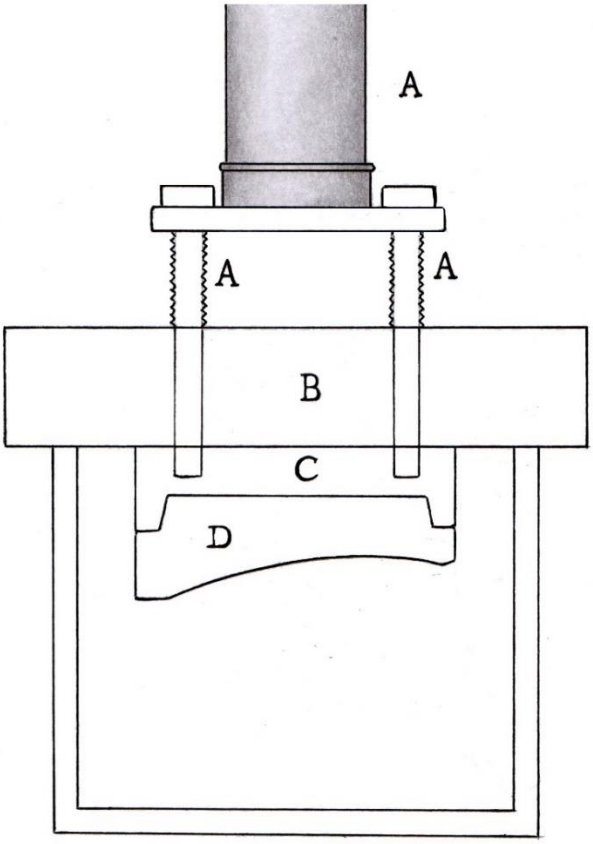


Figure 33. A metal glenoid baseplate (C) is mounted on a fixed metal block (B). A glenoid liner is clipped onto the baseplate as per manufacturer's instructions. Two pushing rods (A) are mounted onto the pushing arm of the Instron machine (A). Both the metal mounting block (B) and the metal baseplate (C) have two holes through them, to accommodate the pushrods (A). During the experiment the two pushrods (A) push against the back surface of the plastic liner (D) trying to prise the liner out from the glenoid baseplate (C).

4.3 Results

4.3.1 Measurement of the vacuum forces

Examples of experimental and control vacuum force experiments are shown in Figures 34 and 35. The peak force in the experimental tests with synovial fluid was found to be 50.4±3.8N (mean ± SD) at 9mm of distraction. It can also be seen that there were tensile forces present in the control test due to the elasticity of the latex 'joint capsule'. The mean value of these forces was found to be 10.20±0.01N (mean ± SD) at 9mm of distraction. This value must be subtracted from the values with synovial fluid present to give the forces due to vacuum effects. Therefore, this experiment indicates that the magnitude of the forces generated by vacuum effects was 40.2±3.8N.

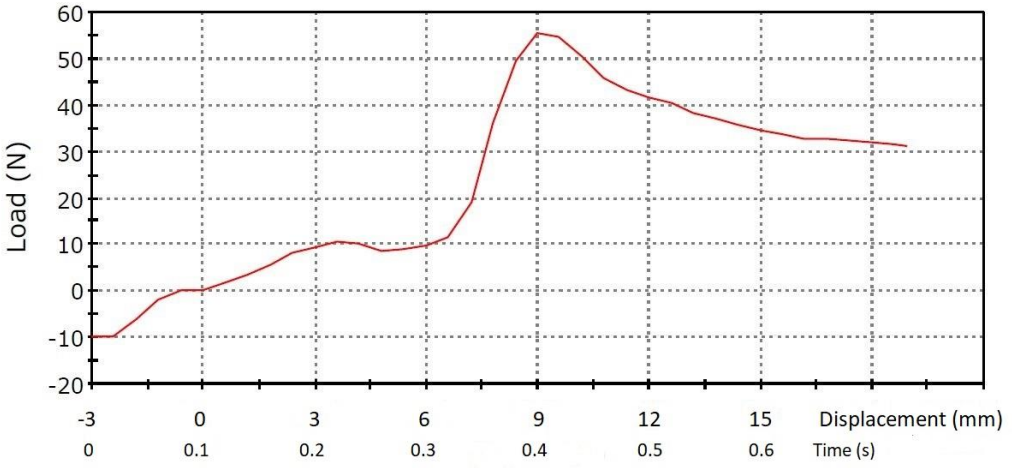


Figure 34. Typical example of vacuum force experiments showing a peak force of 55N between the head and the glenoid liner.

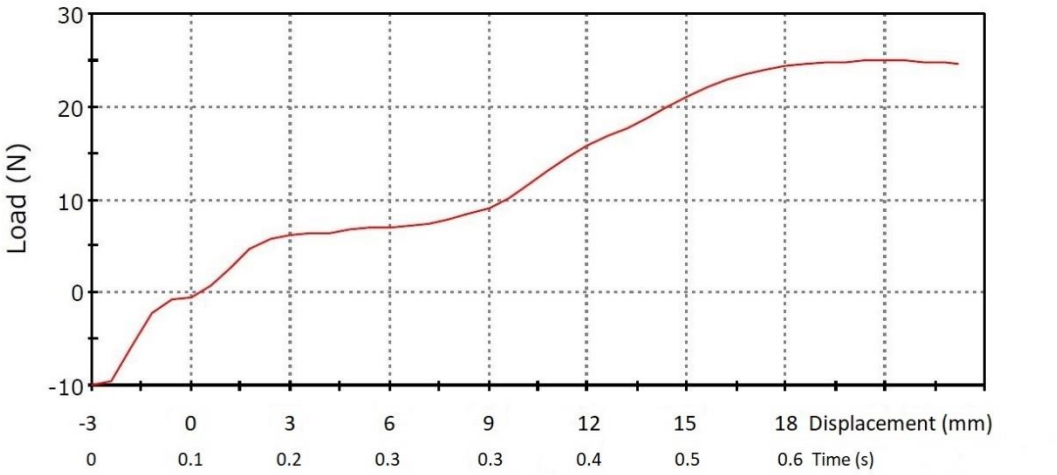


Figure 35. Control for the vacuum test experiment, with no synovial fluid present in the “joint capsule”.

4.3.2 The push-out tests

The SN-curve (Stress v No of Cycles) for push-out failure load for the plastic liner is shown in Figure 36. The SN-Curve in general is a plot of the magnitude of an alternating stress versus the number of cycles to failure for a given material. In this case it is used to demonstrate cumulative damage to the clip-on mechanism of the liner. Using the logarithmic curve fit indicated in the figure, failure at 12500 cycles is predicted for the vacuum forces that we observed in the actual vacuum forces measurements.

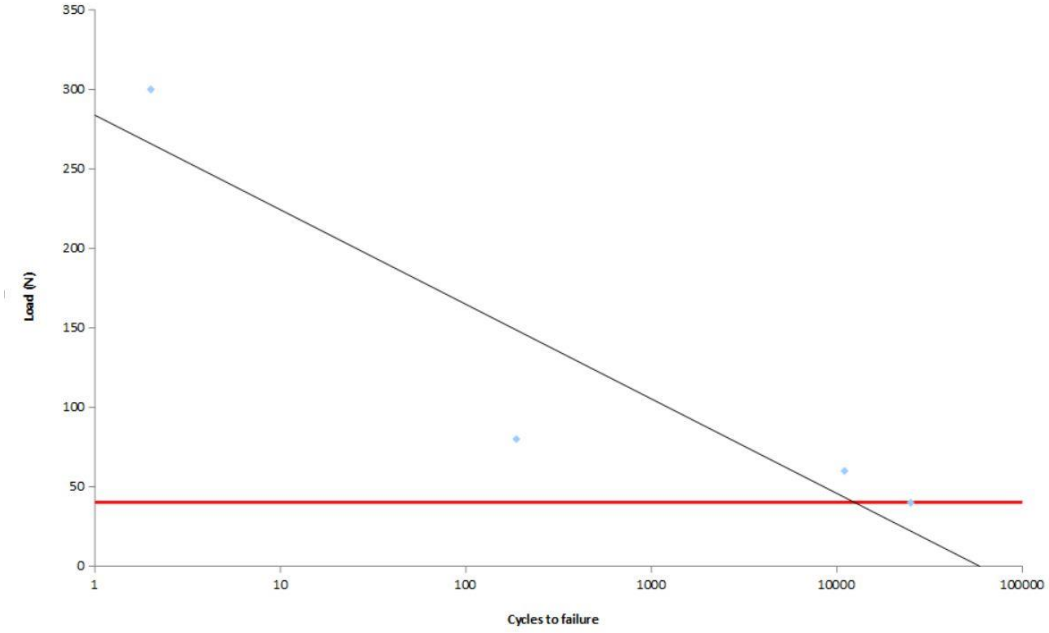


Figure 36. SN curve for pushout failure load (R^2 0.38).

With 40N cyclic force the glenoid liner completely disassembled after 25,000 cycles. Similarly, with 60N the disassembly happened after 11,000 cycles. As for the 80N test, disassembly happened after 187 pushes. With 300N, disassembly took 2 pushes.

Recorded data showed that there was a gradual migration of the glenoid insert as cyclic pushes continued. Figure 37 shows this process. This example was taken from the 40N tests. As the cycles continued, the 40N endpoint was reached after longer and longer pushes of the test arm. The diagram (Figure 37) depicts about 0.2mm of displacement by the glenoid insert relative to its original position flat on the glenoid baseplate.

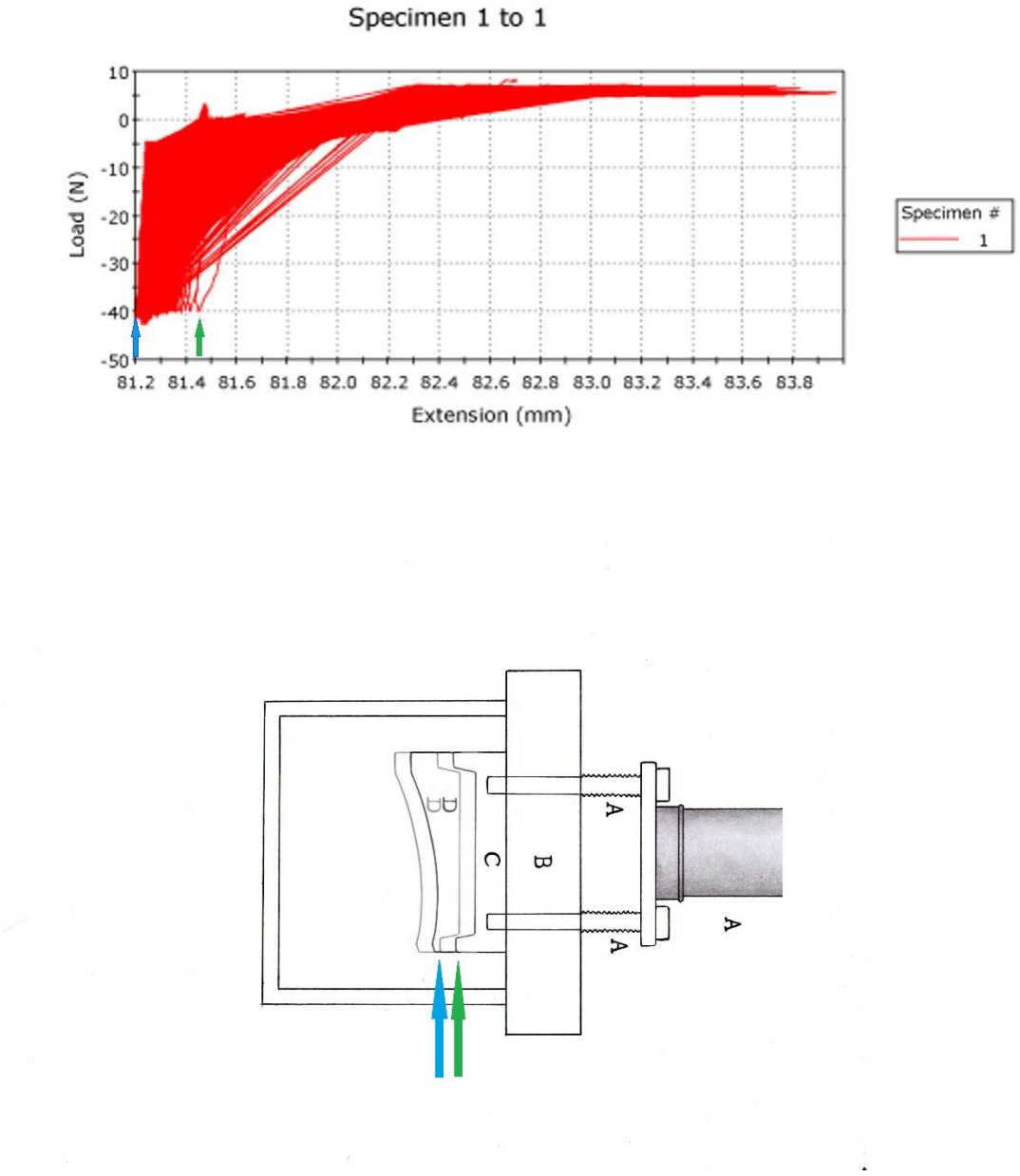


Figure 37. The initial phase of the 40N test, plotted by the test machine software. The red lines indicate the superimposed hysteresis curves during a cumulative damage test. The green arrow indicates the first push, the blue arrow indicates that the pushrods travelled more than 0.2mm more at the last push. That is, during the depicted cycles the glenoid liner was pushed out from the baseplate by more than 0.2mm. This is also depicted in the schematic diagram, showing the migration of the polyethylene glenoid liner “D” from the metal baseplate “C” due to fatigue loading with pushrods “A”.

4.4 Discussion

The role of vacuum forces within the anatomical total shoulder replacement system is poorly understood. The Nottingham TSA system had a high rate of the polyethylene liner uncoupling from the metal glenoid baseplate, in spite of tests by the manufacturer, more rigorous than the ASTM standards.

Regarding the experimental setup several theoretical considerations were made.

In the in vitro experiments the major in vivo elements were attempted to be recreated. The experimental setup consisted of total shoulder arthroplasty components, bovine synovial fluid and a latex condom as joint capsule.

In the initial phase of the experiment, as seen in Figure 34, relatively little force resists the artificial joint distraction (0 to 0.3s). This resistance is possibly derived from the flow of the viscous synovial fluid.

Human synovial fluid is a non-Newtonian fluid as with increasing shear rate viscosity shows a non-linear behaviour, with non-linear decrease in viscosity. Synovial fluid exhibits high viscosity at low shear rates and frequencies, and acts like a quasi-Newtonian fluid (Figure 38). At higher shear rates and frequencies, such as in sports, the viscosity of synovial fluid decreases. This thinning contributes to the formation of a fluid film on the articular surfaces and helps lubrication.[180]

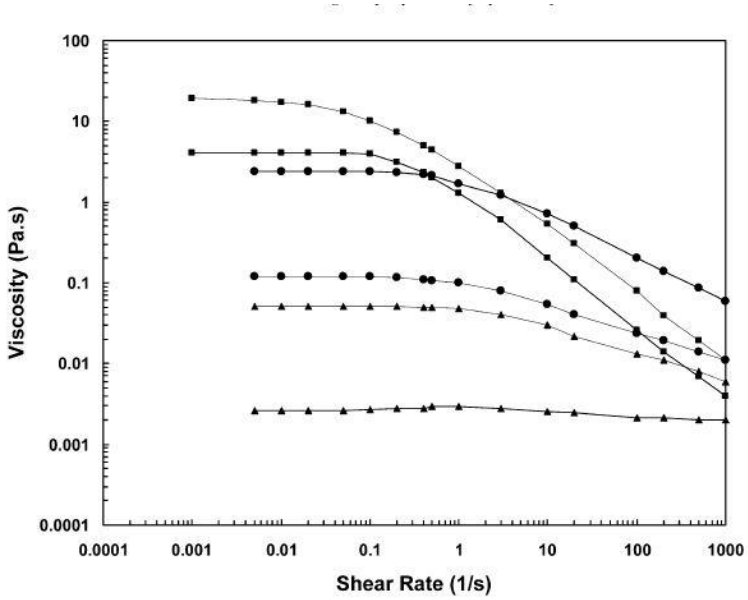


Figure 38. The relationship between shear rate and the viscosity of synovial fluid. Squares represent the upper and lower border of healthy synovial fluid viscosity changes with increasing shear rate. Circles indicate osteoarthritic synovial fluid, triangles rheumatoid synovial fluid viscosity changes versus shear rate. At low shear rates the viscosity remains almost linear, but at higher rates strong shear thinning can be observed. Joint pathologies significantly alter physical and chemical properties of synovial fluid. Reproduced from Schurz J, Ribitsch V. Rheology of synovial fluid. Biorheology. 1987;24(4):385-99.[181]

To complicate things further, synovial fluid exhibits a shear history dependence of viscosity.[182] This means that previously applied shear will affect the response of synovial fluid unless sufficient time is allowed for the hyaluronic acid (HA) molecules to relax.

Extensional flow refers to a type of flow deformation that involves the elongation, or stretching, of a fluid. When subjected to strong extensional flows, synovial fluid undergoes extension thickening and exhibiting sometimes orders of magnitude increases in the measured extensional viscosities.[183]

The viscoelastic properties of synovial fluid have been largely attributed to hyaluronic acid. Hyaluronic acid is a linear polymer, and its concentration

and molecular weight significantly affects the properties of synovial fluid. Protein complexes also influence the behaviour of hyaluronic acid. Over decades of research, the role of proteins such as albumin, γ -globulins, fibrinogen, and proteoglycan 4 (PRG4 or lubricin) has been investigated.[184-186] However, their exact role is still debated.[184]

Other than fluid flow, the phenomenon of fluid adhesion was also considered. Adhesion is the tendency of dissimilar particles of the synovial fluid and the joint replacement component surfaces to cling to one another. In the case of synovial fluid, adhesion is complicated by the hyaluronic acid, protein and phospholipid content. There is no agreement in the literature about the exact mechanism of synovial joint lubrication, and there is even less consensus about synovial lubrication of artificial joints, indicating the complexity of the problem.[187] It is clear though that proteins tend to adhere to polyethylene significantly altering fluid adhesion to polyethylene surfaces.[188]

It is not unrealistic, although it is a considerable simplification of the problem, to assume fluid adhesion only between the components of a total shoulder arthroplasty system in vivo. In the case of the Nottingham TSA, which is a conforming design, the area of fluid adhesion may be big enough to be considered.

The conclusion from the above considerations is that it would be a very complex task to try to model or calculate fluid flow in the initial phase of the TSA component distraction experiment, and such modelling would exceed the scope of this work.

Following the initial phase of the distraction curve, forces resisting the distraction of the components start to build up (Figure 34, 0.3s to 0.4s). It is likely that the space between the artificial head and the glenoid component is sealed off by the condom. The fluid flow is cut off, and therefore the distraction force increases rapidly.

It is possible to calculate the maximum vacuum force (actually the force of atmospheric pressure acting on the contact area) using simple geometry. The surface area of the glenoid liner in contact with the humeral head is 7.47cm^2; the vapour pressure of water is 6.27 KPa at 37°C; considering an atmospheric pressure of 10^5 Pa the vacuum forces should approximate 70N in a perfect seal:

$(10^5 Pa - 6.27x10^3 Pa) \times 7.47x10^{-4} m^2 = 70.02N$

This calculated force is larger than those observed in the experiments reported here. The factors that would act to reduce this theoretical force are release of dissolved gas, evaporation of water vapour, fluid flow due to imperfect seal and deformation of the condom.

The processes by which bubbles containing a vacuum or gas form is often referred to as cavitation. In practice hard (a vacuum) and soft (gas) cavitation may be distinguished.

For hard cavitation in water, degassing the fluid is essential. If we consider two glass surfaces with a thin fluid film between them and assume that the molecules of water adhere strongly to the surfaces, and move the surfaces away from each other at such speed that due to inertia (or a seal) no fluid inflow is possible into the space between the components, the cohesion between the water molecules or the implant surface and the water molecules may break and cavitation may happen. Cavitation bubbles are short lived and collapse in a violent explosion with photoemission. Other than the light emission, the collapse of the bubble produces a very characteristic sound – these are the most reliable ways to identify hard cavitation.

Soft cavitation occurs in non-degassed fluids. Cavitational bubbles contain undissolved gas, and these bubbles tend not to be quite as violent in nature. Although only marginally related to potential cavitation in the shoulder joint, a recent paper suggested that the cause of knuckle cracking could well be soft cavitation with a partially collapsing cavitation bubble, leaving a stable bubble behind in the joint.[189]

The occurrence of cavitation is a stochastic phenomenon, cavitation pressure by definition is the pressure where cavitation happens with 50% chance.

Cavitation may incept on small solid particles, and this phenomenon is called tribonucleation-mediated cavity inception. In a replaced shoulder, solid debris is likely to be present and this can provide nucleation points.

In these experiments no hard cavitation was visualized, although visual inspection is not a reliable method to monitor cavitation.

The third section of the distraction curve (Figure 34, 0.4s onwards) is the part following the peak force resisting distraction, in spite of increasing tensile forces from the condom. It is assumed that the synovial fluid continues to degas decreasing the resisting force. Besides, as the gap between the head and the glenoid liner increases, the fluid column within the condom deforms, and eventually the condom would rupture.

The distraction speed was chosen to be 30mm/s as this corresponds to the rate of deformation that may be expected in vigorous activity such as sports. At this speed no stable, visible bubbles were created (suggesting no hard cavitation) but was quick enough to form a seal.

The vacuum experimental setup could have been accomplished using different distraction speed.

In the case of a very high distraction rate one may expect fluid adhesion and potentially cavitation to dominate. The forces acting between the head and the socket, mediated by the fluid could be much larger than eventually measured in this experiment.

In case of medium rate of distraction synovial fluid is able to flow into the space between the components of the TSA. The forces are determined by the viscoelastic properties of synovial fluid, shear flow and extensional flow, amongst other factors. The speed of distraction however, is large enough for the inflowing fluid to bring the joint capsule (condom) in

contact with the circumference of the implant contact area, to form a seal. As the seal is formed, fluid flow into the space between the TSA components is stopped. The limited expansion ability of the fluid creates a pulling force between the head and the glenoid liner.

Habermeyer et al.[174] stated that the glenoid labrum acts like a seal around the fluid in the cavity between the humeral head and the glenoid, in a cadaveric non-replaced shoulder. They proved that if attempts were made to move the ball of the shoulder joint away from the socket, vacuum forces would counteract the motion. If the labrum is damaged and can no longer act as a seal between the ball and the socket, the resisting forces are much lower. Their measurements showed larger, but comparable forces to the measurements reported here (67.6 to 224.6N 95% CI).[174] A similar phenomenon was observed with the latex condom representing the joint capsule in this experiment. As attempts were made to move the artificial humeral head away from the polyethylene glenoid liner, the condom was sucked in (in other words pushed in by atmospheric pressure) to form a seal around the edges of the liner and then the forces started to increase (Figure 34). This also means that the magnitude of the force measured may be dependent on the properties of the material that provides the seal around the joint components, which could be considerably higher than those produced by the condom alone.

In case of a very slow rate of distraction the joint capsule does not form a seal and the distraction of the head is hindered only by the viscosity of the synovial fluid.

In any scenario, enough time needs to be left for the synovial fluid to cancel the shear memory effect. Previous experimental data states 100s as necessary to cancel the shear memory effect, hence at least 5 minute gaps were held between the experimental runs.[181]

It would be well beyond the scope of this work to try to determine the distraction speed for the 3 different acceleration scenarios mathematically or experimentally. The very fast distraction speed scenario would be very

interesting, but the Instron machine is not capable of initiating a prompt large scale acceleration. Besides, the medium speed scenario is probably more likely to happen in real life.

We demonstrated that a force of approximately 40N caused disassembly of the polyethylene liner from the metal glenoid baseplate following 12,500 - 25,000 cycles. As the glenoid component used in these tests is no longer in production, the number of implants available was limited; the SN curve is therefore necessarily rather sparse. However, there is a clear and steep decrease in dissociation load with number of cycles. The test performed with a peak force of 40N resulted in component disassembly after 25,000 cycles, whilst the log curve fitted to all data points predicted a failure at 12,500 cycles. There are no normative standards for assessing glenoid disassembly in tension. However, to place the number of cycles to failure into context, comparison may be made to other similar tests:

- ASTM F2028: Standard Test Methods for Dynamic Evaluation of Glenoid Loosening or Disassociation, describes a protocol where the glenoid assembly is tested in compression and shear for 100,000 cycles. [190]
- Wirth et al. describe a shoulder prosthesis wear protocol to 5,000,000 cycles. [191]
- Kohut et al. describe a similar wear protocol to 500,000 cycles. [192]

Disassembly was observed here at numbers of cycles a factor of 10-100 times smaller than these protocols.

In the pushout test setup, the “two points” contact of the pushout rods is not realistic. One alternative solution could be gluing the artificial head component into the polyethylene glenoid liner, and pulling the head to fatigue load the clip-on mechanism between the metal baseplate and the plastic liner. Gluing the liner and the head together would have two important problems. The metal humeral head is very rigid, and would make the liner very rigid, making the experimental setup unrealistic again. Besides, the solvent in the glue may interact with the chemical and

physical properties of the liner. Whichever way applied, forces in the magnitude of 40N should not be able to uncouple the liner from the baseplate even with cyclic application.

Until real time recording of movements and forces within a TSA while conducting real world activities becomes a reality one cannot be sure if the artificial head has a significant travel in the direction perpendicular to the glenoid.

4.5 Conclusions

The in vitro tests verified two important conclusions:

- Vacuum forces of 40N could be observed between the head and socket components of a total shoulder replacement system.
- Disassembly of the Nottingham TSR System occurred after only 12,500 – 25,000 cycles under tensile loading equivalent to the magnitude of such vacuum forces.

The current ASTM standards may be criticised as no cumulative damage tests are necessitated by it for the metal glenoid back – polyethylene liner interface.

It is recommended that preclinical evaluation of TSR Systems should include a disassembly test where a tensile force of 40 – 80 N is applied for 100,000 – 5,000,000 cycles.

5.0 Hypothesis 2. Central wear of the polyethylene glenoid liner is slower than eccentric.

5.1 Introduction

The polyethylene debris produced by the artificial joint is thought to be an important activator of the immune system and through that, to cause loosening (please refer to Section 2.2.3). The speed of production of debris may be related to contact surface area, or more precisely, point contact stress (please refer to 2.2.9).

If this is the case, eccentric wear should be quicker than central, producing more wear products per unit of time.

This is important as it helps to evaluate if non-highly crosslinked polyethylene is the optimal material for the bearing, and also underlines the importance of soft tissue balancing during surgery.

For accurate measurement of polyethylene wear, a white light scanner was used, and this is a novel method.

The aim is also to give absolute wear rate figures that can be compared to generally better-performing prosthetic joints.

Complex wear patterns as well as implant material creep may lead to defects in the implants that are difficult to characterise. The shape, the depth, the volume of the defect as well as the deformation and the characteristics of the worn bearing surface are potentially important. Several techniques have been used to quantify dimensional changes of worn implants. Stylus-based measurements are based on physical contact with the implant,[193] and can lead to surface scratching and other damage. The fluid-displacement method is suggested to be the most accurate way to determine the volume of material worn away from the implant,[194] but it does not give any information about the location of the wear. Microcomputed tomography has also been shown to be an accurate way to investigate worn implants.[195-197]

A simple method for 3D scanning of ex vivo implants, using coherence scanning interferometry is proposed. Also known as white light scanners, these machines provide a method of acquiring 3D images of objects without contact, ionising radiation or extensive surface preparation. A series of fringe patterns are projected onto the object and a high resolution camera is used to capture images of the fringe patterns. Light waves collected by the high resolution camera will undergo constructive or destructive interference and this superposition principle is used to calculate changes in surface topography across the object. Scanners can be configured for varying measurement volumes. As a guideline, feature accuracy is approximately 1/20000 of the body diagonal of the measurement volume.[198]

Using a 3D white light scanner 32 explanted polyethylene glenoid liners were examined, from 32 consecutive revision arthroplasty operations. These were all Nottingham total shoulder system UHMW polyethylene glenoid bearings, anatomical by design, explanted at various stages after implantation (Table 7). The polyethylene used for these components is not highly cross-linked since, at the time of design, the use of highly cross-linked polyethylene was not widespread. The Nottingham system is a conforming design, and from this aspect it may be considered an atypical prosthesis.

The aim was to observe any typical wear and plastic deformation patterns as well as to describe the amount of polyethylene worn away during the implant's lifetime. Polyethylene wear has often been suspected of causing osteolysis and implant failure.[199-203]

Determining an average wear rate therefore could be useful, more so because the life expectancy of a total shoulder replacement appears to be shorter than that of a hip or knee total prosthesis even with highly crosslinked polyethylene bearings.[2] One possible explanation could be faster wear in the shoulder implants, with more polyethylene particles, but so far no accurate in vivo wear rates have been published in conjunction with metal back total shoulder arthroplasty, though some in vitro data are

available.[204, 205] The nature (size, shape and cross-linking density) may also be different. Scanning electron microscopy was also performed to characterise the wear of the polyethylene glenoid liner.

In this chapter a simple method is proposed for wear analysis of implants, and wear patterns of an anatomical polyethylene glenoid liner are described, as well as wear rate for the glenoid liner and worn surface properties based on scanning electron microscopic images.

5.2 Materials and methods

The glenoid liners (or bearings) were explanted from 32 consecutive revision shoulder arthroplasty cases and included glenoid liners removed for any reason. The explanted arthroplasty components were carefully washed following explantation using surgical hand scrubs to decontaminate them and kept away from sunlight in plastic bags – except for one component which was sterilised in an autoclave. Implant survival times and reasons for revision are shown in Table 7.

Case No	**Implant survival in months**	**Reason for exclusion**	**Reason for revision**
Case 1	209.3	Included	Worn polyethylene liner
Case 2	53.8	Included	Poor function and pain
Case 3	11	Included	Dislocation
Case 4	6.4	Included	Recurrent posterior dislocation post tsa
Case 5	49.7	Included	Loose, malpositioned glenoid component
Case 6	126.6	Included	Not known
Case 7	18.6	5mm liner	Glenoid liner disassembly
Case 8	121.2	Included	Worn polyethylene liner
Case 9	52	Included	Not known
Case 10	67.5	Included	Not known

Case 11	79.1	Included	Glenoid liner disassembly
Case 12	191.7	Included	Not known
Case 13	66.2	4mm liner	Glenoid loosening
Case 14	111.8	Included	Worn polyethylene liner
Case 15	120.9	4mm liner	Not known
Case 16	26.8	Deformed d/t autoclave	Subluxed tsa previous Erb palsy
Case 17	111.9	Included	Not known
Case 18	43.4	4mm liner	Glenoid loosening
Case 19	18.7	Included	Glenoid loosening
Case 20	35.9	Included	Glenoid liner disassembly
Case 21	45.77	Included	Cuff deficiency and pain
Case 22	43.1	Included	Cuff deficiency and disassembly
Case 23	97.67	Included	Cuff deficiency and overstuffed joint
Case 24	37.47	Included	Loose glenoid
Case 25	N/A	Improperly labelled	
Case 26	86.67	Included	Septic loosening
Case 27	66.47	Included	Painful tsa, subsidence of humeral stem
Case 28	61.43	Included	Loose glenoid

Case 29	N/A	Improperly labelled	
Case 30	60.83	Included	Glenoid liner disassembly
Case 31	N/A	Improperly labelled	
Case 32	94.07	Included	Not known

Table 7. Survival times of explants

All explanted glenoid liners were Nottingham Total Shoulder Arthroplasty System components. New, unused polyethylene glenoid liners for reference use were kindly provided by the manufacturer.

3D scanning of the explanted glenoid liners took place at the Faculty of Engineering, University of Nottingham, using a Phase Vision Quartz DBE 800 scanner. The machine was calibrated according to German VDI/VDE 2634 standard[206] (2002). To enhance the scan quality, commercially available developer spray (Ardrox 9D1B, Chemetall, Frankfurt am Main, Germany) on both control and explanted liner surfaces was used, as per standard methodology.

The wear volume was calculated using a reference 3D image of an unused liner which was then compared to that of worn liner.

The weight of the five new, unused size 3 reference liners were measured using Precisa XT220A analytical scales (Precisa Gravimetrics AG, Dietikon, Switzerland). The one closest to the mean weight was selected.

The above size 3 polyethylene glenoid liner was scanned 5 times. The mean volume was calculated and the image that was closest to the calculated average was used as the reference surface.

The manufacturing accuracy was within the accuracy of the measuring method, as shown by the finding that the unworn parts of the explanted liners compared well with the reference liner manufactured many years later, during the 3D image analysis.

Thirty-two explanted glenoid liners were scanned using the white light scanner. Most of these explants were Size 3 in thickness. One size 5 explant and three size 4 explants were excluded from the volume analysis as no unused sizes 4 and 5 glenoid liners were available to be scanned as a reference. One case, although scanned, was excluded from the analysis because it was autoclave-sterilised after explantation, and it sustained a deformity that would have made data interpretation difficult. Three explants were not labelled properly on explantation and were unidentifiable. Three further implants were identified with the help of manufacturer implant despatch data. This left 24 explants to analyse.

During the scans a three-dimensional representation of the glenoid liner surface was created. The images of worn liners were registered to the reference image, using computer software (Geomagic, Rock Hill, USA). For accurate registration a reference (unworn) plane was needed and the base surface of the glenoid liner, that is, the surface in contact with the metal glenoid baseplate, was used. This had two advantages:

1. Upon removal of the plastic liner from the metal glenoid baseplate, during surgical explanation, the protruding elements on the base of the plastic liner were often damaged. Setting the plane of reference on the flat under-surface of the liner excluded this factor from the analysis.
2. While some liners sustained deformity during their time implanted, the base of the implants remained flat.

The disadvantage of this approach is that the wear from the metal baseplate-plastic liner interface was excluded from our analysis. Also, it was not possible to remove a liner from the metal baseplate without causing damage to the clip-on elements of the liner, therefore analysis of these stabilizing structures was not undertaken.

The volume analysis was done by Geomagic software. The time the explants spent in vivo were calculated from the Nottingham Total Shoulder replacement database, and wear rates were calculated using Excel.

Wear rates were then statistically analysed in both the central wear and the non-central wear group, using descriptive and comparison statistics from SPSS (IBM Analytics, Armonk, USA). A possible significant difference between the wear rate in the central wear group and the non-central wear group was of particular interest.

Visual analysis of the scanned images revealed two major wear patterns. In central wear cases there was no biconcavity of the worn surface, and the worn surface was roughly in the intended ball and socket interface area. In non-central wear cases there was either biconcavity present, or clear signs of the artificial head slipping in and out of the socket frequently. To understand these wear patterns more fully, the surfaces were imaged using scanning electron microscopy. A Hitachi S-2600N Variable Pressure Scanning Electron Microscope (VPSEM) was used. This machine could image uncoated biological samples. For this reason no sample preparation was necessary.

Using the same 24 explanted liners and the five unworn, unused reference liners the volumetric measurements were validated against implant weight loss. Elements of the clip-on mechanism were removed from the back of the polyethylene liners. Each implant, including the five reference liners were measured five times using Precisa XT220A analytical scales (Precisa Gravimetrics AG, Dietikon, Switzerland). Mean weight loss for each liner was calculated and expressed as percentage of the mean reference weight. This was compared to the percentage of volume loss, using a Bland-Altman plot.

5.3 Results

The mean volume of the reference (new, unworn, Size 3) glenoid liners from 5 measurements of the same liner was 4557± 48 mm^3 (mean ±SD). The standard deviation is 1.05% of the liner volume, and this verifies that the setup gives reproducible results.

During volume analysis, the 3D scan images of the worn liners were registered to the 3D scan image of the reference liner. The unworn circumferential area of the worn liners compared well with the same area of the reference glenoid liner in all cases, except for the liner sterilised by autoclave – hence the exclusion of the latter from the analysis. Hence it was concluded that variations in dimensions due to manufacturing tolerances were below the measurement resolution of this method.

Seventeen explanted glenoid liners were visually grouped as having central wear, and seven cases were grouped as having non-central wear. Average wear rates for each group were calculated.

The central wear group had a polyethylene wear rate of 115 ± 55mm^3/year (mean ± SD). The wear figures were following a normal distribution (Shapiro-Wilk test, p=0.97).

In the non-central group, with all seven cases the Shapiro-Wilk test showed a sample with a non-normal distribution (p=0.008). This was found to be the consequence of two outliers which had very rapid wear rate secondary to large fragments of polyethylene breaking off from the edge of the glenoid liners (Figure 41 and Figure 42). As this is a different mechanism of material loss, these two cases were excluded from the non-central wear group. The remaining five cases showed a normal distribution (p=0.723), and a wear rate of 112 ± 42 mm^3/year (mean ± SD). Without the two outliers, the wear rate of the central wear rate group was not significantly different from the non-central wear group (t-test, p=0.426). The two outliers showed a wear rate of 550 mm^3/year and 540 mm^3/year.

Group	Wear rate
Central wear (n=17)	115 ± 55mm^3/year (mean ± SD)
Non-central wear (n=5)	112 ± 42 mm^3/year (mean ± SD)
Rapid edge wear (n=2)	550 mm^3/year and 540 mm^3/year

Table 8. Wear rates in the central, non-central and edge wear groups

Typical merged images from the central wear group and non-central wear group are shown in Figure 39 and Figure 40, respectively.

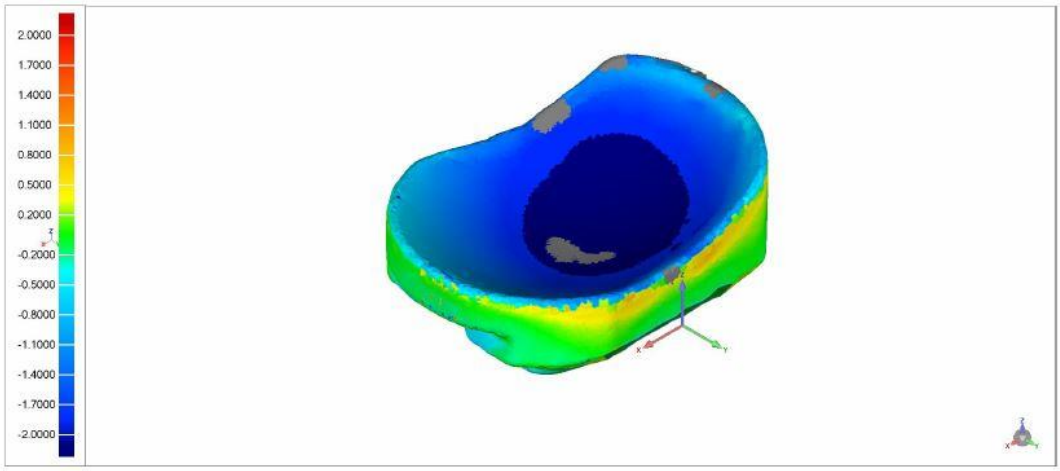


Figure 39. Central wear. Wear is colour-coded, cold colours indicating material loss, warm colours material being more prominent than the control. Green indicates no material loss. Note that the edge of the contact surface with the head is deformed. The scale and the colour coding was created by the computer software. The scale is in mm, the deepest blue indicating over 2mm of material loss. The darkest red indicates over 2mm of material excess. Explanted from left shoulder, the right side of the picture is the cranial end of the implant.

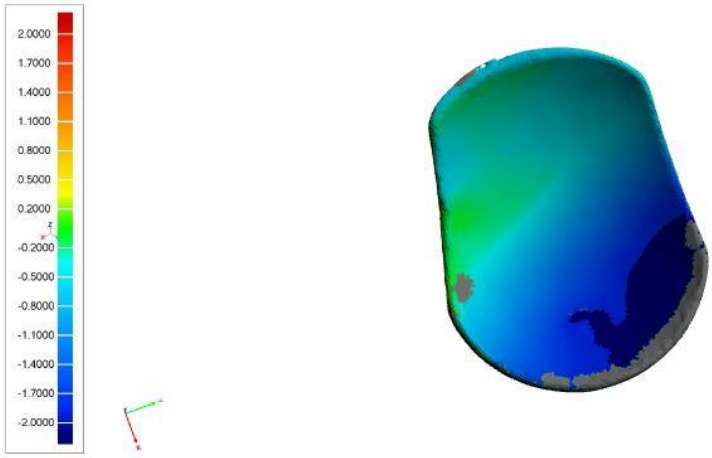


Figure 40. Non-central wear. The head was assumed to initially have caused a degree of central wear and then it gradually migrated posteroinferiorly. Explanted from left shoulder. The top of the image is the cranial end of the implant. (Scale in mm, deepest blue indicates over 2mm of material loss, darkest red indicates over 2mm material excess)

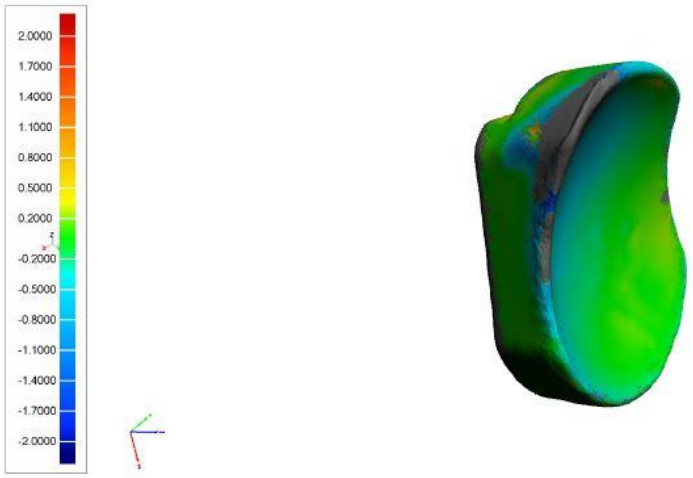


Figure 41. Implant revised due to dislocation, with little wear and a large piece of the rim missing (Case 3). The pattern of wear and the clinical data also suggests an element of anterior-superior escape. (Scale in mm). Explanted from left side. The top of the image is cranial end of the implant.

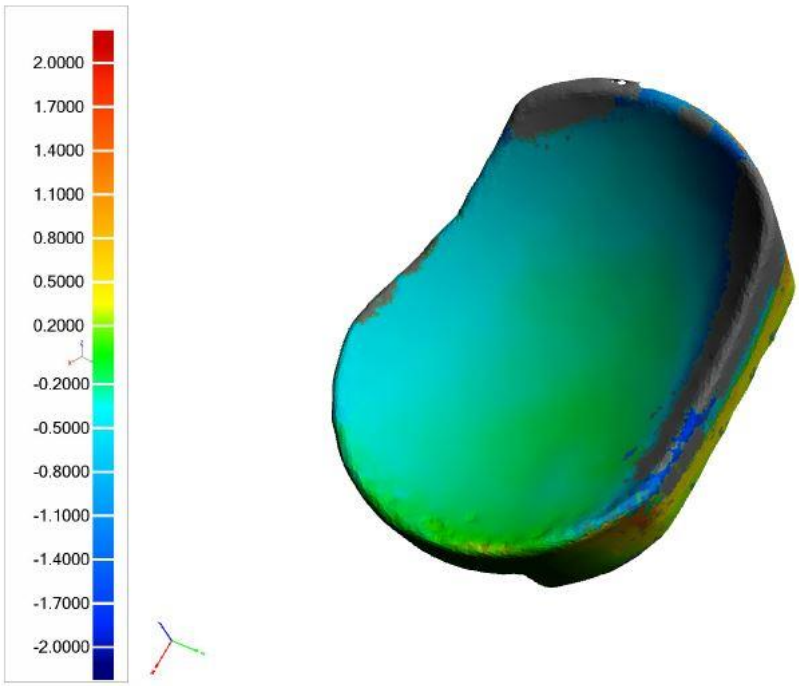


Figure 42. Implant with rapid edge wear revised due to recurrent posterior dislocation (Case 4). Explanted from left side. The top of the image is the cranial end of the implant.

The two outlier cases had rapid edge wear mainly secondary to abnormal prosthetic head movement in the socket.

The patient referred to as Case 3 had rheumatoid arthritis. Following the implantation of TSA the humeral head gradually developed an anterior-superior escape. The patient eventually suffered bilateral traumatic lower limb amputations, and the shoulder was revised due to dislocation.

The patient referred to as Case 4 developed recurrent posterior dislocations following TSA.

The Bland-Altman plot in Figure 43 shows good agreement between white light scanning and weight measurements for the assessment of glenoid wear, with the mean difference not being statistically significant from 0 ($p=0.441$). Figure 44 verifies the practical experience that material loss in highly worn liners is slightly underestimated by white light scanning. This is probably because the edges of the highly worn implants are thin and more

translucent in spite of the developer spray, and less of these areas are picked up by the scanner. Figure 44 shows a gradient 1 relationship between the two measurements (solid blue line). The weight of the reference liners was 3.7978 ± 0.015g (mean ± SD) which means that the liners with little wear have a manufacturing inaccuracy comparable to the weight loss. This explains the scatter of the data in the low wear region of Figure 44.

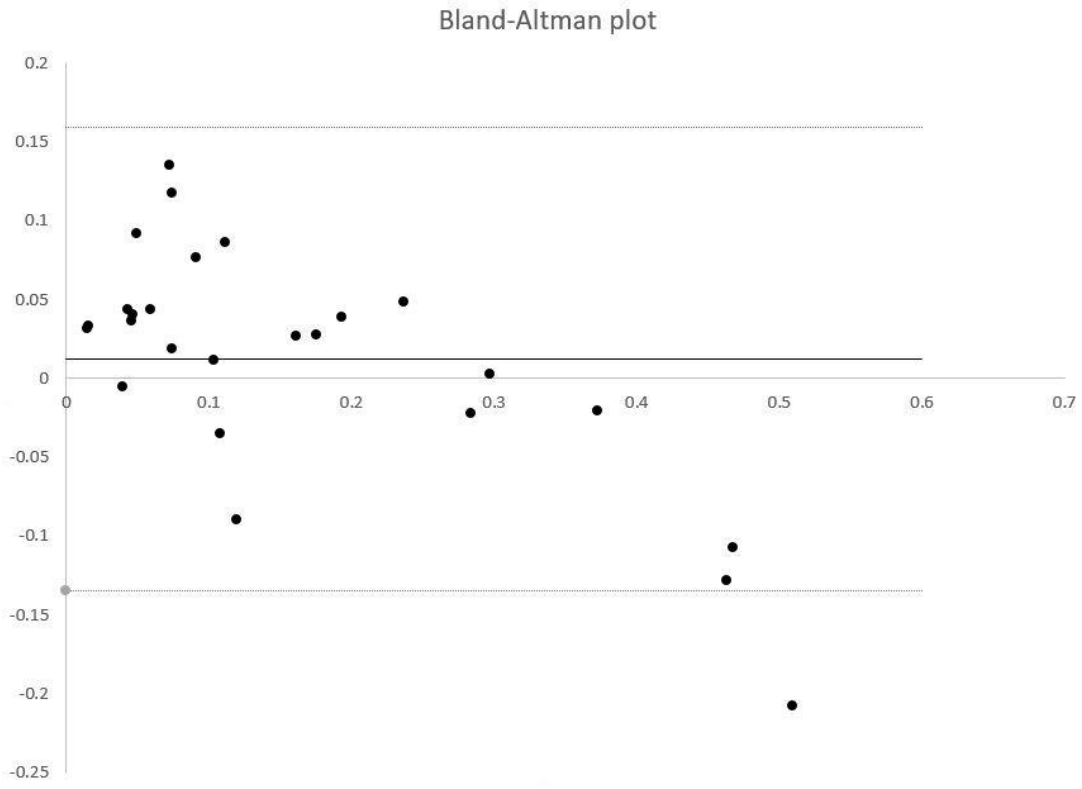


Figure 43. Bland-Altman plot depicting correlation between wear quantification using coherence scanning interferometry and weight measurement.

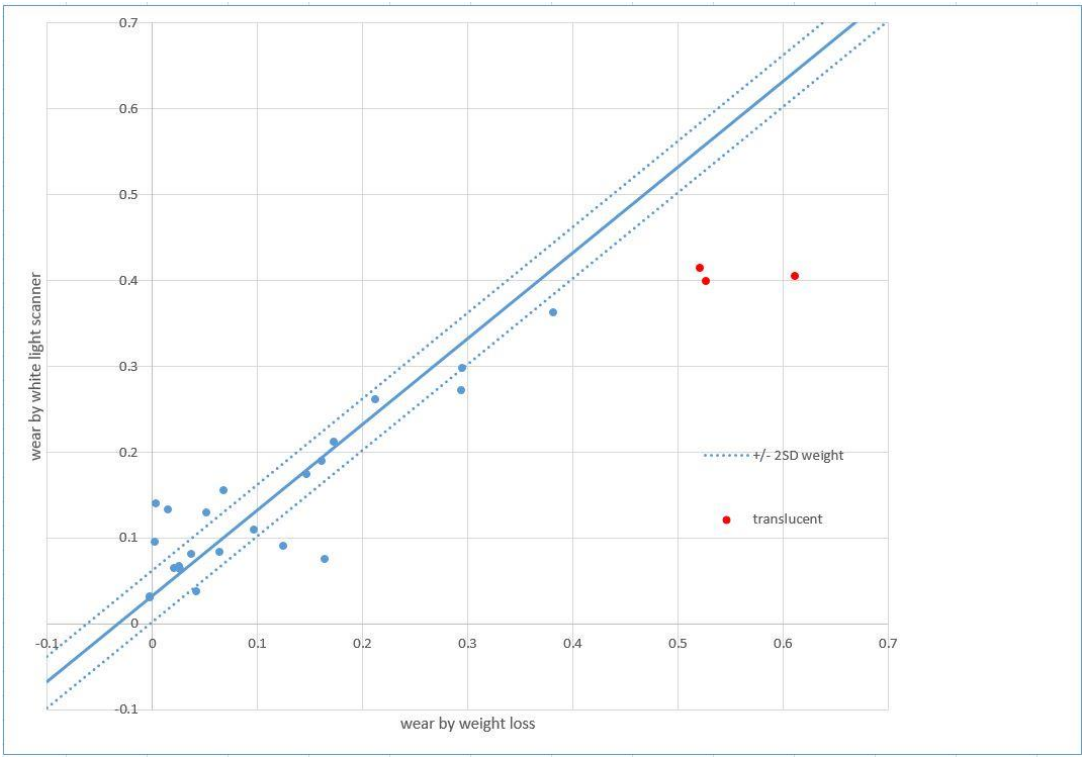


Figure 44. White light scanning slightly underestimates the wear in the case of highly worn polyethylene liners, compared to weight measurements.

One explanted liner was examined with scanning electron microscopy to assess the contact surface between the polyethylene glenoid liner and the metal humeral head.

The images showed that the polyethylene was coming off in tiny laminar flakes which indicates fatigue wear as the main wear mechanism (Figure 45, Figure 46, Figure 47, Figure 48). The “crater” observed in Figure 47 suggests formation of polyethylene flakes larger than the typical 0.5-20 µm polyethylene debris,[33] offering one potential explanation to faster wear.

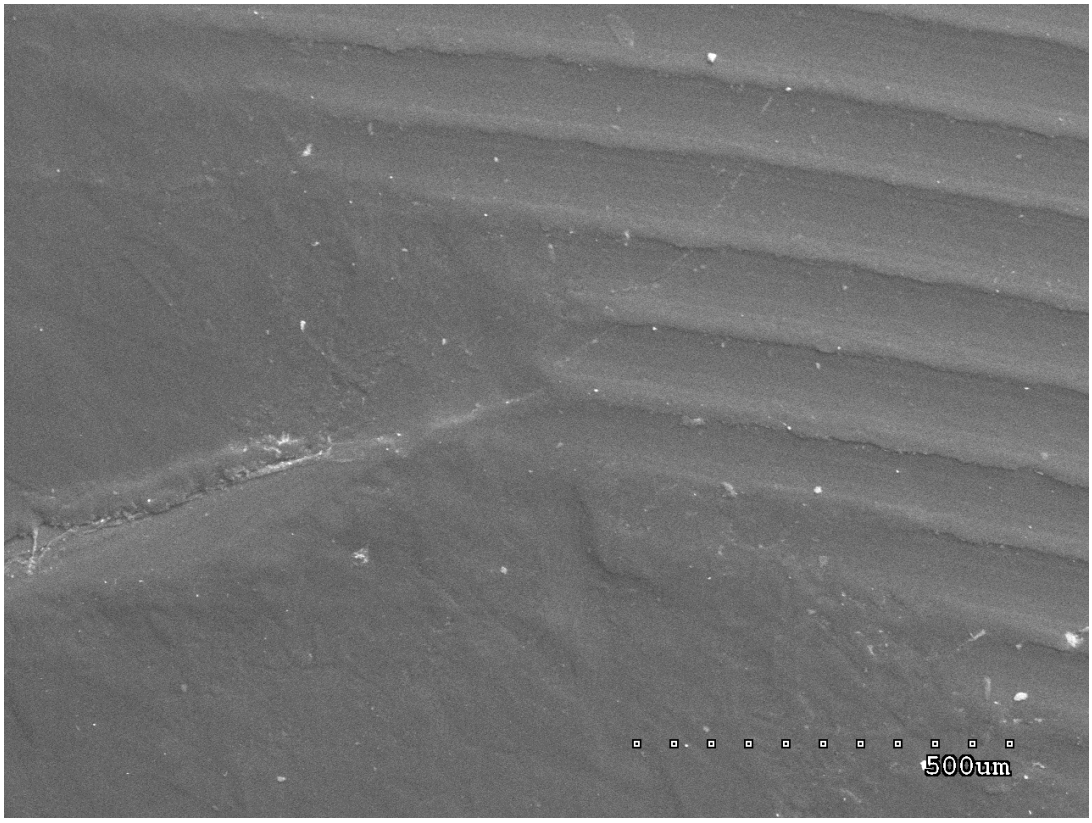


Figure 45. Scanning electron microscopic image of the implant seen in Figure 40. Magnification is shown by the scale bar. On the right hand side one can see the lightly worn surface with machining marks still visible. The left side of the image shows an area with more wear, and a scratch of the surface created during implant removal.



Figure 46. Image of the worn surface. Magnification is shown by the scale bar. Larger grooves are present most likely created by larger scale movements of the humeral head. The area at the bottom of the picture, left of the scale will be further magnified in Figure 47.

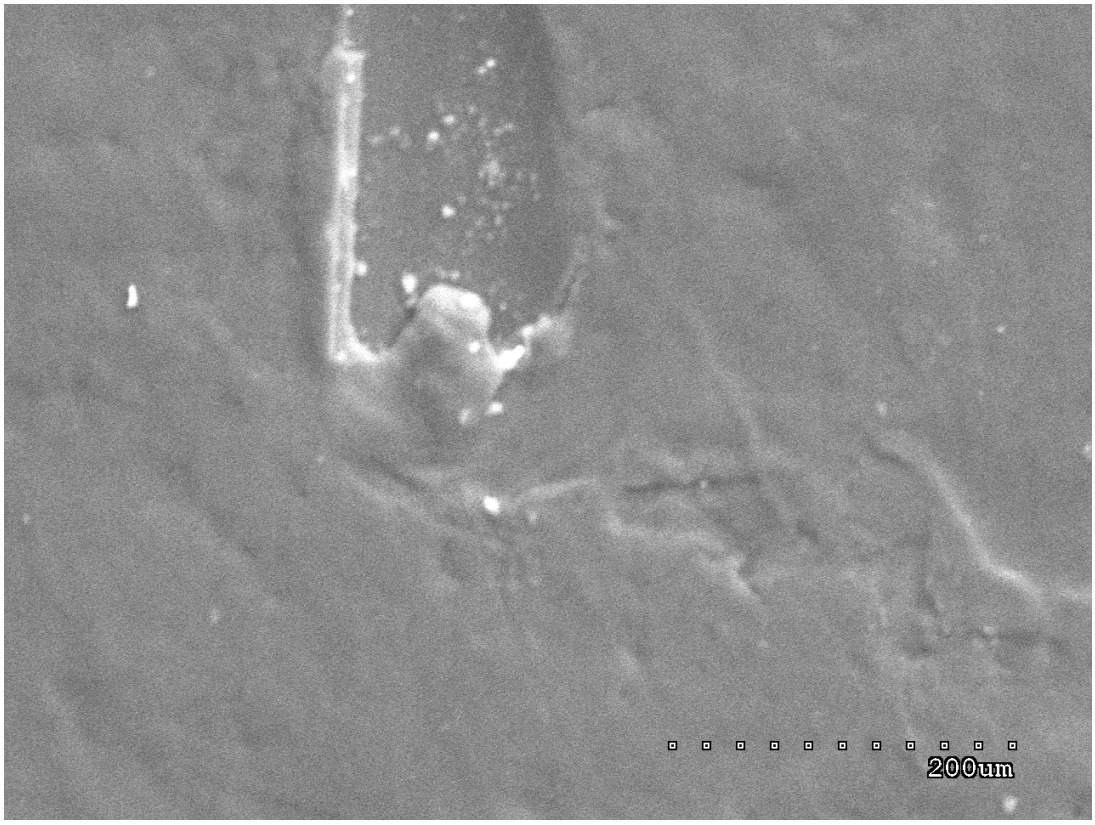


Figure 47. One can observe the irregularities of the surface. In the top centre half of the picture the polyethylene came off in a flake. The white dots are charging artefacts. The bottom right corner of this picture is further magnified in Figure 48. Magnification is shown by the scale bar.

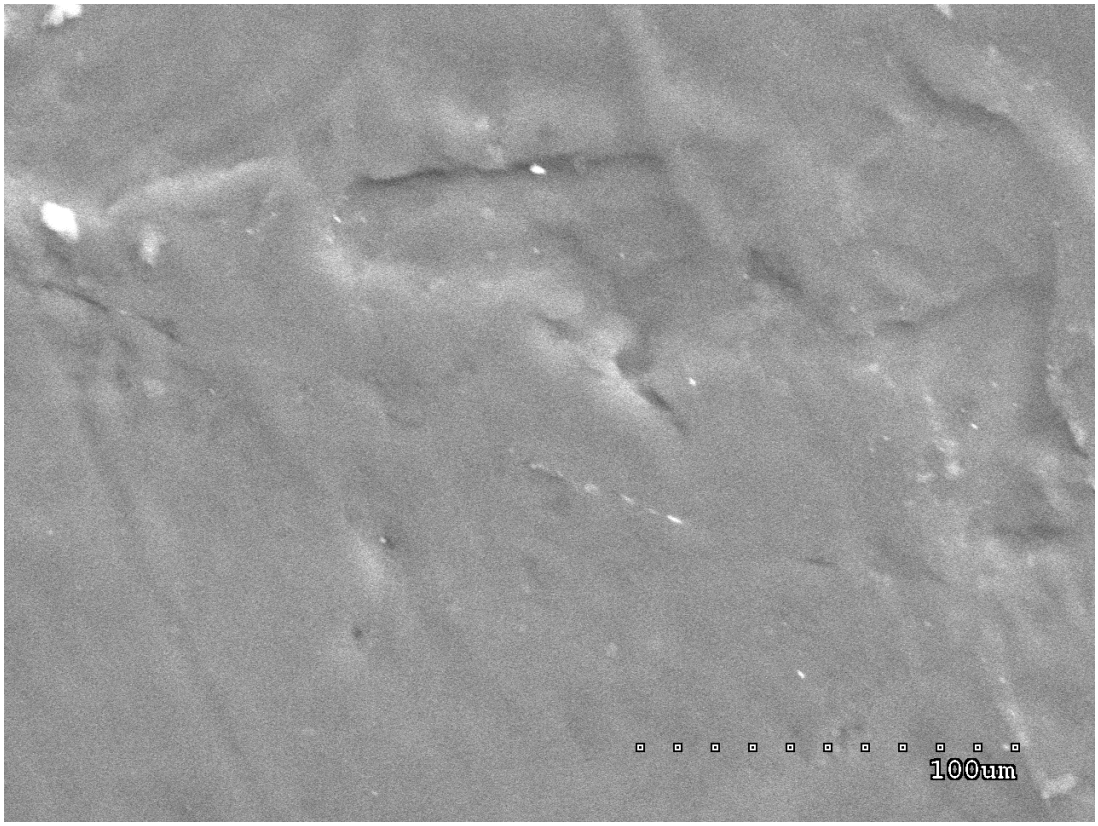


Figure 48. Uneven surface with cracks. Further pieces of polyethylene debris could be expected from this area. Magnification is shown by the scale bar.

5.4 Discussion

Swieszkowski et al. reported an in vivo volumetric wear rate of 6.9 to 30.4 mm^3/year measured by laser scanning. These were all polyethylene glenoid components, though (n=3), whereas the Nottingham TSA system has a metal back glenoid component;[207] yet these figures indicate an almost three-fold wear speed difference.

Depending on prosthesis design and material, the volumetric wear rate in a metal on polyethylene total hip replacement system is about 9-47 mm^3 per year,[208-211] and in-air gamma sterilised HMWPE acetabular liners from total hip replacements the volumetric wear rate is about 38-47mm^3 per year.[210]

The results show that the wear rate of the polyethylene glenoid liner in an anatomical total shoulder arthroplasty system is more than twice the

acetabular polyethylene wear in a total hip arthroplasty system, both based on non-highly crosslinked polyethylene components.

Wear rate in an artificial shoulder joint with no edge wear was shown to be statistically indistinguishable whether the artificial head remained in its intended position centred in the socket or whether it took up a non-central position. This could have been due to the small sample size, or because the very fast wear masked more subtle differences. The wear rate of a polyethylene glenoid liner in a shoulder replacement with a degree of instability is, as expected, much quicker than in a non-dislocating shoulder replacement (Table 8).

More rapid polyethylene wear in a total shoulder replacement in vivo can lead to a higher level of wear debris, and hence causing loosening quicker than in a metal on polyethylene hip replacement. This could explain inferior shoulder arthroplasty survival times. The reason for quicker polyethylene wear, however, is uncertain. One could speculate that faster wear is the consequence of different biomechanics of the shoulder. Visual analysis of the glenoid liner suggests that it loses its conformity with the head during its lifetime. The artificial humeral head apparently has a rather large play in the socket, causing predominantly fatigue wear. This was also evident in the scanning electron microscopy surface scans. In Figures 45-48 the polyethylene particles can be seen to come off the surface in flakes, along surface microcracks. This could be the consequence of a thicker plasticity-induced damage layer at the bearing surface of the non-highly crosslinked implant and subsurface fatigue. Besides flakes, scratches were also observed indicating third body wear.

Another observation made was significant polyethylene plastic deformation (Figure 47), mostly around the edges in contact with the artificial head.

Overall, non-highly crosslinked HMWPE does not appear to be the optimal raw material for glenoid liner production.

If the HMWPE glenoid liner wears quicker than an acetabular liner of the same material, one may ask if the highly crosslinked polyethylene glenoid

liner also wears quicker than the equivalent acetabular implant. This question requires further research.

For the volume analysis 3D images from a white light scanner were used.

The accuracy of both the weight loss and white light measurements are limited by the manufacturing tolerances of liner since we are able to compare only the explanted devices with new controls rather than the actual weight or volume lost from an individual liner. Liner mass measurements for this reason also have a degree of uncertainty. Given the standard deviation of 0.015g for the mass of new liners, we would expect 95% of devices to fit within the range ±0.031g of the mean value (assuming a t distribution). This range is marked on Figure 44 to give a baseline confidence when interpreting the results. The white light and weight loss results show a discrepancy at high wear volumes, of order 25%. We think this is because the edges of the highly worn implants are thin and more translucent in spite of the developer spray. Care should therefore be taken when interpreting volumetric wear results from white light scanning for wear of more than 0.4g (1800mm^3).

Alternative measuring techniques would involve coordinate measuring machines (CMM). This method gives precise spatial data of three-dimensional objects. CMM is a very useful method where a relatively small number of points are required to describe the object, and, in general, is more accurate than white light scanning. However, when complex surfaces need to be characterised, the point cloud representation of the surface by a white light scanner is more helpful. CMMs are typically equipped with a mechanical probe, but they can also be fitted with an optical probe lens, amongst others, but the principle is the same. In the case of the explanted glenoid components the complex surface wear was better represented by the white light scanner than with a CMM machine. The use of a white light scanner could have been combined with a CMM to obtain a large number of data points across the entire surface, to increase the accuracy of certain features such as part width or thickness at a small number of specific

points. This would have been particularly difficult in our case as each part was a unique shape.

µCT scanners outperform white light scanners with objects where the shape of the object causes visibility issues. Holes and complex geometry shapes as well as mid-substance defects are better represented by µCT scanners. This method involves radiation and is also very expensive. In this case there were no visibility issues with the glenoid implants making micro CT analysis unnecessary. Compared to white light scanners, laser scanners can be used in a wider range of lighting conditions. However, single colour laser scanners can create a speckle effect due to the crossing of the light beams, often mistaken for the surface during analysis, and this 'noise' significantly reduces the accuracy of the method. White light scanners are typically up to 10 times more accurate than laser scanners. However, they have their own disadvantages. The system is sensitive to background light, and transparent or translucent materials and reflecting surfaces may be difficult to scan optically. Scanning must take place in a controlled environment with the same lighting conditions for each scan and avoidance of vibrations. This problem is overcome by coating the object to be scanned with a fine developer spray paint before a white light scanner is used. In this study a surface developer spray was used to enhance the scan quality. The accuracy of white light scanners ranges from 50µm to 150µm, less accurate than a CMM (1-50µm) but far more versatile. In this study the largest benefit of using a white light scanner was the high point cloud density, resulting in a higher resolution 3D model once the point cloud is reconstructed using the accompanying software. Without the point cloud data much information on the deformation and surface wear would have been lost.

The shortcomings of the work include the small sample size that was used. As no difference was seen in the polyethylene wear rate between the central and non-central wear group, the two groups together allowed reliable wear data to be generated and analysed.

5.5 Conclusions

The wear rate of the polyethylene liner of a total shoulder arthroplasty system with a metal back glenoid was found to be more than twice as fast as that reported in total hip replacement with the acetabular liner made of the same type of polyethylene. For wear analysis a novel method, 3D scanning of ex vivo implants, using coherence scanning interferometry is proposed.

To conclude Hypothesis 2, the experiment failed to prove that non-central wear was faster than central wear.

6.0 Combined discussion of Hypotheses

The first modern total shoulder replacement system was designed by Neer in 1974.[27] Neer's glenoid was a cemented all-polyethylene keeled component with conforming humeral and glenoid radii of curvature.[212] Due to problems with loosening predominantly at the bone-cement interface, the glenoid component has undergone many modifications. One of these was the introduction of a metal back glenoid.

The Nottingham Total Shoulder System glenoid was developed to be a low-profile implant. The priority with the baseplate design was to keep the metal baseplate thin and the liner clip-on flanges small. This was to minimise potential metal-on-metal contact between the artificial head and the baseplate as the polyethylene liner wears away. The early baseplates were simply porous-coated at the back, but later they became hydroxyapatite-coated to improve osteointegration. Both models had a central peg and holes for screw fixation.

This design concept was somewhat similar to the design of Cofield, which also incorporated a metal backing with screw fixation and an exchangeable polyethylene liner.[213, 214] The potential benefits of a metal-backed design were the opportunity for isolated polyethylene exchange in a revision setting,[215] improved cementless "biological" fixation, and improved stress transfer between the implant and the bone.[114] Reports of poor survival, metallosis, osteolysis, loosening, and subsequent failure, however, overshadowed these implants.[169, 216-220]

For this reason, the next version of glenoid component design was again an all-polyethylene component where the keel was exchanged for several pegs.[205] The pegs intended to lessen glenoid loosening by resisting shear forces at the bone-cement-implant interface like studs on a football shoe.[221-223] Some clinical studies found that pegged glenoids performed better than keeled ones, but some reports stated that keeled implants were better for soft bone.[224-227]

The next generation of all-polyethylene pegged glenoid components involved pegs that were fitted with bone capture or bone ingrowth capability,[228-230] with improved bony fixation and pull out strength in early studies.[230] The weakness of this idea was that in vivo the porous metal – polyethylene combination due to the significantly different mechanical characteristics of the two materials often led to breakage.[128, 231, 232] Bone ingrowth, however, seemed promising.[232]

The conventional, or anatomical total shoulder replacement systems are still in use, both with metal-back glenoid components or with polyethylene glenoid components. Their popularity, however, seems to be decreasing as more reverse polarity shoulder replacement implants are being used.[2, 32]

The reverse polarity prosthetic shoulders, however, also use a metal-back glenoid component, and this has refocused interest on the anatomical metal-back glenoids.

As discussed before, the metal-back glenoids have inferior survival compared to cemented all polyethylene glenoids.[2, 217] Reverse total shoulders, however, in spite of the metal glenoid baseplate, have a survival rate that is comparable to anatomical shoulder replacement systems with a cemented glenoid.[2]

With the parallel use of anatomical and reverse systems, the need for compatible arthroplasty systems for revision surgery has arisen. For example, if an anatomical shoulder replacement fails due to rotator cuff insufficiency, but the humeral stem component and the metal back glenoid components are sound, it would make sense to keep those components and convert into a reverse system by just replacing the ball and socket components. This need also stresses the importance of understanding why and how metal back glenoid components fail.

Another rather interesting question is whether all polyethylene cemented glenoids really perform better, or there is a bias in the survival figures.

Streit et al. published valuable information about all-polyethylene cemented glenoid component micromovements.[166] In their study they used radiostereometric analysis (RSA) to follow glenoid component migration

with high accuracy. They followed eleven patients with all-polyethylene cemented glenoids for a minimum of 3 years. These patients had tantalum beads as points of reference implanted in their replaced shoulders, and special radiographs were taken to assess translation and rotational migration of the glenoid components.

Although the cohort had good clinical results throughout the duration of the study, the radiological findings were more worrying. Their results are summarised in Table 9.[166]

Table 2

Individual Component Motion in Translation and Rotation in Relation to the Appearance of Radiolucent Lines on Postoperative Radiographs[a]

Patient No./Sex/ Age, y	Side	RL Zone			Final Trans, mm			Final Rotation		
		1 y	2 y	3 y	x-axis	y-axis	z-axis	x-axis	y-axis	z-axis
1/F/66	R	0	0	0	-0.26	-0.03	-0.12	0.60°	-0.02°	-2.39°
2/M/50	L	0	0	1	-0.26	-0.36	0.10	2.14°	2.20°	2.45°
3/F/78	L	0	1	3	-0.25	-0.05	0.36	0.88°	-1.86°	0.85°
4/F/52	L	0	0	0	-0.15	-0.13	-0.16	-1.25°	-1.79°	1.8°
5/F/64	L	0	1	0	-0.29	-0.24	-0.74	2.71°	-2.14°	1.13°
6/M/52	R	0	1	1,2	1.51	-1.01	-1.09	4.63°	-1.70°	-8.54°
7/F/80	R	0	0	0	0.69	0.21	0.39	1.61°	0.08°	-1.32°
8/M/61	L	0	1	0	-0.08	-0.27	0.32	-0.14°	-0.83°	1.52°
9/M/52	R	0	3	0	-0.19	0.50	-0.15	0.45°	-1.54°	-1.98°
10/F/53	R	0	0	1	-0.15	-0.14	0.02	-3.76°	-0.07°	-0.42°
11/F/68	R	0	1	3	-0.55	-0.09	0.46	0.86°	0.11°	-7.45°

Abbreviations: F, female; L, left; M, male; R, right; RL, radiolucent lines; Trans, translation.
[a]All but one of the patients with radiolucencies at 3 years demonstrated rotation of greater than 2° at 3 years. The 5 greatest measured rotations from baseline at 3 years all occurred in patients with radiolucencies.

Table 9. Component motion in total shoulder arthroplasty. High migration and low migration groups can be identified.[166] Reproduced from Streit JJ, Shishani Y, Greene ME, Nebergall AK, Warner JP, Bragdon CR, et al. Radiostereometric and Radiographic Analysis of Glenoid Component Motion After Total Shoulder Arthroplasty. Orthopedics. 2015 Oct;38(10):e891-7.

No radiolucencies were detected around the implants at year 1, 6 components had radiolucencies around them at 2 years and 5 components had radiolucencies at 3 years (3 of which had lucencies at 2 years). Based on migration they observed two groups, the high migration group and the low migration group. In order to be listed as high migration, the glenoid had to move more that 1mm or 2 degrees. Four of the 6 patients in the high-motion group showed radiolucencies around the glenoid component at 3 years, whereas radiolucencies were visible around only 1 of the 5 components in the low-motion group.

This means that all polyethylene components may become loose much sooner than thought, but for some reason may remain clinically silent, or tolerable.

When assessing the Nottingham TSR cohort for osteolysis, some interesting observations were made. Some metal-back glenoids showed almost no osteolysis around them but they were clearly eroding the glenoid, migrating closer and closer to the spinoglenoid notch.

This observation led to the creation of the novel glenoid erosion score.[233]

The observations by Streit et al. suggested that an all-polyethylene liner may also become loose but may not be eroding the glenoid so quickly. More glenoid erosion was found to cause more pain.[233] Although this was speculative, it may suggest that all-polyethylene glenoids, although they become loose early, are revised later as they erode the glenoid more slowly.

One explanation could be that the all-polyethylene component is softer than a metal glenoid baseplate, and the destruction caused by a loose component is slower. One should note, however, that polyethylene wear particles are known to cause osteolysis.

To clarify the problem further, a correlation analysis was planned to quantify polyethylene wear in Nottingham shoulders and assess if polyethylene wear load correlated with osteolysis. Had a good correlation been found, it may have been concluded that direct mechanical damage by the baseplate was probably less important than polyethylene wear. Unfortunately this part of the work could not be completed due to lack of radiographs.

With a metal back glenoid system, the polyethylene liner needs to be thick to withstand deforming forces and stay attached to the baseplate. Cemented liners typically are thinner than Nottingham 3mm liner, which means that even if they are completely worn away, they will not create as much polyethylene debris. Once the artificial head has reached the bony glenoid the total shoulder replacement may act more like a hemiarthroplasty. If the live tissue debris is less osteolytic than the polyethylene debris, this phenomenon may contribute to better survival of cemented glenoids.

Another potential factor could be metal-on-metal wear. Upon inspection of the explanted glenoids, we noticed that both in the central and non-central wear group the metal baseplate was often damaged. Sometimes the clip-on mechanism of the baseplate was affected. Almost all polyethylene liners showed evidence of plastic deformation, mostly around the edges, and with wear they became a lot weaker. In our cohort, if a worn polyethylene liner becomes uncoupled from the baseplate the joint it gets revised very soon because of the mechanical problem.

Another interesting phenomenon to look at is the special distribution of osteolysis around the back of the metal glenoid baseplate and the all-polyethylene glenoid. Typically it is around the pegs, keel and/or screws. In the present work the vacuum phenomenon between components of an artificial shoulder joint is described. In the context of osteolysis, this has several implications. First if the loose glenoid moved in and out along an axis perpendicular to the surface of the bony glenoid, it can very efficiently pump synovial fluid to the inside of the bony glenoid, where the pegs are. If the synovial fluid carries polyethylene particles, it may cause extensive osteolysis.

The above idea could offer additional data as to why metal back reverse glenoids show a different type of osteolysis.[234]

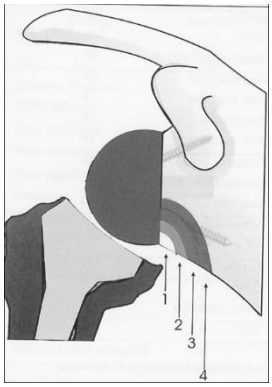


Figure 49. The Nerot-Sirveaux grading system for postoperative scapular notching.[234] Reproduced from Nicholson GP, Strauss EJ, Sherman SL. Scapular notching: Recognition and strategies to minimize clinical impact. Clinical orthopaedics and related research. 2011 Sep;469(9):2521-30.

Higher grades of erosion are hard to explain by purely mechanical contact of the humeral component on the glenoid (Figure 49). Another potential explanation could be that the vacuum forces initially loosen the caudal end of the metal baseplate and this movement pumps the synovial fluid along with polyethylene particles higher and higher towards the central peg.

Obviously direct contact has a very important role, as it is accountable for the increased debris production. This mechanism would also explain why newer reverse prosthesis designs still show notching but to a much lesser extent.

Polyethylene wear rate is a particularly important aspect of the survival of a total shoulder replacement. High wear rates were found in this current work, and the wear rates may be even higher as elements of the clip-on mechanism were not included in the wear analysis. The vacuum tests verified movement at this interface and there must be wear present here as well, so the polyethylene wear was probably underestimated in these measurements.

For decades, ultra-high-molecular-weight-polyethylene (UHMWPE) was used in many different types of arthroplasty. This material has its advantages. The dynamic mechanical properties UHMWPE such as fracture toughness and ultimate yield strength[154, 235, 236] compare well to highly crosslinked UHMWPE (HXL-UHMWPE). Humeral liners often undergo rim loading, and the brittleness of HXL UHMWPE may lead to failure.[154] This is the reason why the Nottingham Total Shoulder System had a UHMWPE glenoid liner throughout its life. However, HXL-UHMWPE has better wear characteristics, as evidenced by many studies mainly in conjunction with hip arthroplasty.[237-240]

Based on the results of this current study the wear rate of the glenoid liner in the Nottingham system was unacceptably high. The performance of HXL UHMWPE may have been better but due to its brittleness there may have been different problems.

The potential role of alternative bearing materials is discussed by Carpenter et al.[214] Ceramic hip replacement components have been on the market for decades,[241] but they are known for brittleness.[242, 243] Currently only one shoulder prosthesis system on the market offers a ceramic bearing option, but in that system the head is ceramic, not the glenoid component. This particular manufacturer has recalled the implant and modified the surgical technique due to the ceramic head becoming uncoupled from the stem. This could be another case where the designers overlooked the existence of vacuum forces, underlining the significance of Hypothesis 1.

Pyrolytic carbon (PyC) is another alternate bearing surface, which has been used for over 40 years in artificial heart valves.[244, 245] PyC has been utilized in hand surgery for small joint replacements, both as hemiarthroplasty or as total arthroplasty, usually with unfavourable results (high migration rate, pain and stiffness); also in radial head replacement with better results.[244-247] Small joint replacements were reported to have a high loosening and migration rate. The radial head prosthesis provided good functional mid-term results with significant osteolysis but no loosening. Some recent publications suggest that a PyC hemiarthroplasty may promote cartilage regeneration and bone repair.[214]

Overall, polyethylene has several disadvantages that would necessitate the imminent arrival of a potent replacement.

7.0 References

1. Matsen FA, Clinton J, Lynch J, Bertelsen A, Richardson ML. Glenoid component failure in total shoulder arthroplasty. J Bone Joint Surg Am. 2008 Apr;90(4):885-96.
2. Association AO. Annual Report 2015 - 2015 : AOANJRR - AOANJRR. 2016 [cited 2016 14.08.2016]; Available from: https://aoanjrr.sahmri.com/annual-reports-2015.
3. Rosenberg N, Neumann L, Modi A, Mersich IJ, Wallace AW. Improvements in survival of the uncemented Nottingham Total Shoulder prosthesis: a prospective comparative study. BMC Musculoskelet Disord. 2007;8:76.
4. Registry AOANJR. 2017 Annual Report. 2017 [cited 2018 10.04]; Available from: https://aoanjrr.sahmri.com/annual-reports-2017.
5. registry NJ. 14th Annual Report. 2017 [10.04.2018.]; Available from: http://www.njrcentre.org.uk/njrcentre/Reports,PublicationsandMinutes/Annualreports/tabid/86/Default.aspx.
6. Brand RA, Mont MA, Manring MM. Biographical sketch: Themistocles Gluck (1853-1942). Clin Orthop Relat Res. 2011 Jun;469(6):1525-7.
7. Emery R, Bankes M. Shoulder replacement: historical perspectives. In: Walch G, P B, editors. Shoulder Arthroplasty. Berlin: Springer-Verlag; 1999. p. 3–9.
8. Péan, J, E. Des moyens prothétiques destinés à obtenir la réparation des parties osseuses. Gaz. de Hôp.1894. p. 67:291-308.
9. KRUEGER FJ. A vitallium replica arthroplasty on the shoulder; a case report of aseptic necrosis of the proximal end of the humerus. Surgery. 1951 Dec;30(6):1005-11.
10. Richard, A. Malformation of unknown origin of the right humeral head; loss of function; resection and acrylic prosthesis. Mem Acad Chir1950. p. 76(28-9): 821-3. .
11. A R, R J, L R. Reconstruction prothétique acrylique de l'extrémité supérieure de l'humérus spécialement au cours des fracturesluxations. Paris: J Chir; 1952. p. 68(8-9): 537-47. .
12. MacAusland WR. Nylon prosthesis in lesions of the shoulder, elbow and finger. The American Journal of Surgery; 1953. p. 164 - 73
13. Ross AC, Wilson JN, Scales JT. Endoprosthetic replacement of the proximal humerus. J Bone Joint Surg Br. 1987 Aug;69(4):656-61.
14. Burrows H. Major prosthetic replacement of bone: lessons learnt in seventeen years.: J Bone Joint Surg; 1968. p. 50B: 225-6.
15. Neer CS. The classic: Articular replacement for the humeral head. 1955. Clin Orthop Relat Res. 2011 Sep;469(9):2409-21.
16. Neer CS, Watson KC, Stanton FJ. Recent experience in total shoulder replacement. J Bone Joint Surg Am. 1982 Mar;64(3):319-37.
17. Lettin AW, Copeland SA, Scales JT. The Stanmore total shoulder replacement. J Bone Joint Surg Br. 1982;64(1):47-51.
18. Boileau P, Sinnerton RJ, Chuinard C, Walch G. Arthroplasty of the shoulder. J Bone Joint Surg Br. 2006 May;88(5):562-75.
19. Boileau P, Walch G. The three-dimensional geometry of the proximal humerus. Implications for surgical technique and prosthetic design. J Bone Joint Surg Br. 1997 Sep;79(5):857-65.
20. Roberts SN, Foley AP, Swallow HM, Wallace WA, Coughlan DP. The geometry of the humeral head and the design of prostheses. J Bone Joint Surg Br. 1991 Jul;73(4):647-50.
21. Wallace AL, Phillips RL, MacDougal GA, Walsh WR, Sonnabend DH. Resurfacing of the glenoid in total shoulder arthroplasty. A comparison, at a mean of five years, of prostheses inserted with and without cement. J Bone Joint Surg Am. 1999 Apr;81(4):510-8.
22. Takase K, Imakiire A, Burkhead WZ. Radiographic study of the anatomic relationships of the greater tuberosity. J Shoulder Elbow Surg. 2002 2002 Nov-Dec;11(6):557-61.
23. Takase K, Yamamoto K, Imakiire A, Burkhead WZ. The radiographic study in the relationship of the glenohumeral joint. J Orthop Res. 2004 Mar;22(2):298-305.
24. Pearl ML, Kurutz S. Geometric analysis of commonly used prosthetic systems for proximal humeral replacement. J Bone Joint Surg Am. 1999 May;81(5):660-71.
25. Levy O, Copeland SA. Cementless surface replacement arthroplasty of the shoulder. 5- to 10-year results with the Copeland mark-2 prosthesis. J Bone Joint Surg Br. 2001 Mar;83(2):213-21.

26. Robinson WA, Wagner ER, Cofield R, Sanchez-Sotelo J, Sperling JW. Long-term outcomes of humeral head replacement for the treatment of osteoarthritis; a report of 44 arthroplasties with minimum 10-year follow-up. J Shoulder Elbow Surg. 2017 Dec. Epub 2017/12/18.
27. Neer CS. Replacement arthroplasty for glenohumeral osteoarthritis. J Bone Joint Surg Am. 1974 Jan;56(1):1-13.
28. Cofield RH. Uncemented total shoulder arthroplasty. A review. Clin Orthop Relat Res. 1994 Oct(307):86-93.
29. Fox TJ, Cil A, Sperling JW, Sanchez-Sotelo J, Schleck CD, Cofield RH. Survival of the glenoid component in shoulder arthroplasty. J Shoulder Elbow Surg. United States2009. p. 859-63.
30. Rockwood C, A. A century of shoulder arthroplasty innovations and discoveries. Orthopaedicstoday: Healio; 2000 [cited 2018 17.02.2018.]; Available from: https://www.healio.com/orthopedics/shoulder-elbow/news/online/%7Bfc5b917e-0d24-4e92-919d-d81a1a113c57%7D/a-century-of-shoulder-arthroplasty-innovations-and-discoveries.
31. Rasmussen JV, Brorson S, Hallan G, Dale H, Äärimaa V, Mokka J, et al. Is it feasible to merge data from national shoulder registries? A new collaboration within the Nordic Arthroplasty Register Association. J Shoulder Elbow Surg. 2016 Dec;25(12):e369-e77. Epub 2016/04/20.
32. Australian Orthopaedic Association National Joint replacement Registry Annual Report 2013. 2013 [cited 2014 10-10-2014]; Available from: https://aoanjrr.dmac.adelaide.edu.au/annual-reports-2013.
33. Abu-Amer Y, Darwech I, Clohisy JC. Aseptic loosening of total joint replacements: mechanisms underlying osteolysis and potential therapies. Arthritis research & therapy. 2007;9 Suppl 1:S6.
34. Rossi P, Marmotti A, Castoldi F, Rossi R. Periprosthetic osteolysis: Biological or mechanical problem?. [Italian] Osteolisi periprotesica: Problema biologico o meccanico? Minerva Ortopedica e Traumatologica. 2005;56(4):199-207.
35. Archibeck MJ, Jacobs JJ, Black J. Alternate bearing surfaces in total joint arthroplasty: Biologic considerations. Clinical Orthopaedics and Related Research. 2000 (379):12-21.
36. Atkins GJ, Welldon KJ, Holding CA, Haynes DR, Howie DW, Findlay DM. The induction of a catabolic phenotype in human primary osteoblasts and osteocytes by polyethylene particles. Biomaterials. 2009 Aug;30(22):3672-81.
37. Beck RT, Illingworth KD, Saleh KJ. Review of periprosthetic osteolysis in total joint arthroplasty: An emphasis on host factors and future directions. Journal of Orthopaedic Research. 2012 April;30(4):541-6.
38. Bi Y, Seabold JM, Kaar SG, Ragab AA, Goldberg VM, Anderson JM, et al. Adherent endotoxin on orthopedic wear particles stimulates cytokine production and osteoclast differentiation. Journal of Bone and Mineral Research. 2001;16(11):2082-91.
39. Bi Y, Collier TO, Goldberg VM, Anderson JM, Greenfield EM. Adherent endotoxin mediates biological responses of titanium particles without stimulating their phagocytosis. Journal of Orthopaedic Research. 2002;20(4):696-703.
40. Morra M, Cassinelli C, Cascardo G, Bollati D. Before talking of coatings, what really is the surface of orthopaedic implant devices? Journal of Orthopaedics and Traumatology. 2011 October;12:S113-S4.
41. Greenfield EM, Bi Y, Ragab AA, Goldberg VM, Nalepka JL, Seabold JM. Does endotoxin contribute to aseptic loosening of orthopedic implants? Journal of Biomedical Materials Research - Part B Applied Biomaterials. 2005 15 Jan;72(1):179-85.
42. Greenfield EM, Beidelschies MA, Tatro JM, Goldberg VM, Hise AG. Bacterial pathogen-associated molecular patterns stimulate biological activity of orthopaedic wear particles by activating cognate toll-like receptors. Journal of Biological Chemistry. 2010 15 Oct;285(42):32378-84.
43. Polyzois I, Nikolopoulos D, Michos I, Patsouris E, Theocharis S. Local and systemic toxicity of nanoscale debris particles in total hip arthroplasty. Journal of Applied Toxicology. 2012 April;32(4):255-69.
44. Bowsher JG, Hussain A, Williams PA, Shelton JC. Metal-on-metal hip simulator study of increased wear particle surface area due to 'severe' patient activity. Proc Inst Mech Eng H. 2006 Feb;220(2):279-87.
45. Billi F, Campbell P. Nanotoxicology of metal wear particles in total joint arthroplasty: a review of current concepts. J Appl Biomater Biomech. 2010 2010 Jan-Apr;8(1):1-6.

46. Billi F, Benya P, Kavanaugh A, Adams J, Ebramzadeh E, McKellop H. The John Charnley Award: an accurate and sensitive method to separate, display, and characterize wear debris: part 1: polyethylene particles. Clin Orthop Relat Res. 2012 Feb;470(2):329-38.
47. Lewis AC, Heard PJ. The effects of calcium phosphate deposition upon corrosion of CoCr alloys and the potential for implant failure. J Biomed Mater Res A. 2005 Nov;75(2):365-73.
48. Yan Y, Neville A, Dowson D. Understanding the role of corrosion in the degradation of metal-on-metal implants. Proc Inst Mech Eng H. 2006 Feb;220(2):173-81.
49. Caicedo MS, Desai R, McAllister K, Reddy A, Jacobs JJ, Hallab NJ. Soluble and particulate Co-Cr-Mo alloy implant metals activate the inflammasome danger signaling pathway in human macrophages: a novel mechanism for implant debris reactivity. J Orthop Res. 2009 Jul;27(7):847-54.
50. Antoniou J, Zukor DJ, Mwale F, Minarik W, Petit A, Huk OL. Metal ion levels in the blood of patients after hip resurfacing: a comparison between twenty-eight and thirty-six-millimeter-head metal-on-metal prostheses. J Bone Joint Surg Am. 2008 Aug;90 Suppl 3:142-8.
51. Daniel J, Ziaee H, Pradhan C, McMinn DJ. Six-year results of a prospective study of metal ion levels in young patients with metal-on-metal hip resurfacings. J Bone Joint Surg Br. 2009 Feb;91(2):176-9.
52. Langton DJ, Sprowson AP, Joyce TJ, Reed M, Carluke I, Partington P, et al. Blood metal ion concentrations after hip resurfacing arthroplasty: a comparative study of articular surface replacement and Birmingham Hip Resurfacing arthroplasties. J Bone Joint Surg Br. 2009 Oct;91(10):1287-95.
53. Sauvé P, Mountney J, Khan T, De Beer J, Higgins B, Grover M. Metal ion levels after metal-on-metal Ring total hip replacement: a 30-year follow-up study. J Bone Joint Surg Br. 2007 May;89(5):586-90.
54. Krewski D, Yokel RA, Nieboer E, Borchelt D, Cohen J, Harry J, et al. Human health risk assessment for aluminium, aluminium oxide, and aluminium hydroxide. J Toxicol Environ Health B Crit Rev. 2007;10 Suppl 1:1-269.
55. Hallab NJ, Jacobs JJ. Biologic effects of implant debris. Bull NYU Hosp Jt Dis. 2009;67(2):182-8.
56. Jacobs JJ, Urban RM, Hallab NJ, Skipor AK, Fischer A, Wimmer MA. Metal-on-metal bearing surfaces. J Am Acad Orthop Surg. 2009 Feb;17(2):69-76.
57. Chithrani BD, Ghazani AA, Chan WC. Determining the size and shape dependence of gold nanoparticle uptake into mammalian cells. Nano Lett. 2006 Apr;6(4):662-8.
58. Gratton SE, Ropp PA, Pohlhaus PD, Luft JC, Madden VJ, Napier ME, et al. The effect of particle design on cellular internalization pathways. Proc Natl Acad Sci U S A. 2008 Aug;105(33):11613-8.
59. Papageorgiou I, Brown C, Schins R, Singh S, Newson R, Davis S, et al. The effect of nano- and micron-sized particles of cobalt-chromium alloy on human fibroblasts in vitro. Biomaterials. 2007 July;28(19):2946-58.
60. Wang ML, Tuli R, Manner PA, Sharkey PF, Hall DJ, Tuan RS. Direct and indirect induction of apoptosis in human mesenchymal stem cells in response to titanium particles. J Orthop Res. 2003 Jul;21(4):697-707.
61. Wang ML, Sharkey PF, Tuan RS. Particle bioreactivity and wear-mediated osteolysis. J Arthroplasty. 2004 Dec;19(8):1028-38.
62. Caicedo MS, Pennekamp PH, McAllister K, Jacobs JJ, Hallab NJ. Soluble ions more than particulate cobalt-alloy implant debris induce monocyte costimulatory molecule expression and release of proinflammatory cytokines critical to metal-induced lymphocyte reactivity. J Biomed Mater Res A. 2010 Jun;93(4):1312-21.
63. Hallab NJ, Caicedo M, Finnegan A, Jacobs JJ. Th1 type lymphocyte reactivity to metals in patients with total hip arthroplasty. J Orthop Surg Res. 2008 Feb;3:6.
64. Willert HG, Buchhorn GH, Fayyazi A, Flury R, Windler M, Köster G, et al. Metal-on-metal bearings and hypersensitivity in patients with artificial hip joints. A clinical and histomorphological study. J Bone Joint Surg Am. 2005 Jan;87(1):28-36.
65. Ani M, Moshtaghie AA. The effect of chromium on parameters related to iron metabolism. Biol Trace Elem Res. 1992 1992 Jan-Mar;32:57-64.
66. Moshtaghie AA, Ani M, Bazrafshan MR. Comparative binding study of aluminum and chromium to human transferrin. Effect of iron. Biol Trace Elem Res. 1992 1992 Jan-Mar;32:39-46.

67. Bregoli L, Chiarini F, Gambarelli A, Sighinolfi G, Gatti AM, Santi P, et al. Toxicity of antimony trioxide nanoparticles on human hematopoietic progenitor cells and comparison to cell lines. Toxicology. 2009 Aug;262(2):121-9.
68. Peters K, Unger RE, Gatti AM, Sabbioni E, Tsaryk R, Kirkpatrick CJ. Metallic nanoparticles exhibit paradoxical effects on oxidative stress and pro-inflammatory response in endothelial cells in vitro. Int J Immunopathol Pharmacol. 2007 2007 Oct-Dec;20(4):685-95.
69. Singh N, Manshian B, Jenkins GJ, Griffiths SM, Williams PM, Maffeis TG, et al. NanoGenotoxicology: the DNA damaging potential of engineered nanomaterials. Biomaterials. 2009 Aug;30(23-24):3891-914.
70. Vittori D, Nesse A, Pérez G, Garbossa G. Morphologic and functional alterations of erythroid cells induced by long-term ingestion of aluminium. J Inorg Biochem. 1999 Aug;76(2):113-20.
71. Hart AJ, Skinner JA, Winship P, Faria N, Kulinskaya E, Webster D, et al. Circulating levels of cobalt and chromium from metal-on-metal hip replacement are associated with CD8+ T-cell lymphopenia. J Bone Joint Surg Br. 2009 Jun;91(6):835-42.
72. Hart AJ, Sabah S, Henckel J, Lewis A, Cobb J, Sampson B, et al. The painful metal-on-metal hip resurfacing. J Bone Joint Surg Br. 2009 Jun;91(6):738-44.
73. Ferreira ME, de Lourdes Pereira M, Garcia e Costa F, Sousa JP, de Carvalho GS. Comparative study of metallic biomaterials toxicity: a histochemical and immunohistochemical demonstration in mouse spleen. J Trace Elem Med Biol. 2003;17(1):45-9.
74. Cho DR, Shanbhag AS, Hong CY, Baran GR, Goldring SR. The role of adsorbed endotoxin in particle-induced stimulation of cytokine release. Journal of Orthopaedic Research. 2002;20(4):704-13.
75. Shanbhag A, Yang J, Lilien J, Black J. Decreased neutrophil respiratory burst on exposure to cobalt-chrome alloy and polystyrene in vitro. J Biomed Mater Res. 1992 Feb;26(2):185-95.
76. Yang J, Shanbhag A, Lilien J, Black J. Human neutrophil response to short-term exposure to F-75 cobalt-based alloy. J Biomed Mater Res. 1992 Sep;26(9):1217-30.
77. Huk OL, Catelas I, Mwale F, Antoniou J, Zukor DJ, Petit A. Induction of apoptosis and necrosis by metal ions in vitro. J Arthroplasty. 2004 Dec;19(8 Suppl 3):84-7.
78. Hatton A, Nevelos JE, Nevelos AA, Banks RE, Fisher J, Ingham E. Alumina-alumina artificial hip joints. Part I: a histological analysis and characterisation of wear debris by laser capture microdissection of tissues retrieved at revision. Biomaterials. 2002 Aug;23(16):3429-40.
79. Walch G, Badet R, Boulahia A, Khoury A. Morphologic study of the glenoid in primary glenohumeral osteoarthritis. J Arthroplasty. 1999 Sep;14(6):756-60.
80. Pape G, Bruckner T, Loew M, Zeifang F. Treatment of severe cuff tear arthropathy with the humeral head resurfacing arthroplasty: two-year minimum follow-up. J Shoulder Elbow Surg. 2013 Jan;22(1):e1-7.
81. Kappe T, Cakir B, Reichel H, Elsharkawi M. Reliability of radiologic classification for cuff tear arthropathy. J Shoulder Elbow Surg. 2011 Jun;20(4):543-7.
82. Ekelund A, Seebaue L. Advanced Evaluation and Management of Glenohumeral Arthritisin the Cuff-Deficient Shoulder. In: Rockwood C, Matsen F, editors. Rockwood and Matsen's The Shoulder. IV ed. Philadelphia: Saunders; 2009. p. 1247-76.
83. Ilg A, Bankes MJ, Emery RJ. The intra- and inter-observer reliability of the Samilson and Prieto grading system of glenohumeral arthropathy. Knee Surg Sports Traumatol Arthrosc. 2001 May;9(3):187-90.
84. Buscayret F, Edwards TB, Szabo I, Adeleine P, Coudane H, Walch G. Glenohumeral arthrosis in anterior instability before and after surgical treatment: incidence and contributing factors. Am J Sports Med. 2004 Jul-Aug;32(5):1165-72. Epub 2004/07/21.
85. Walch G, Boileau P. Shoulder Arthroplasty. First ed. Berlin: Springer-Verlag; 1998. 444 p.
86. Badet R, Boulahia A, Walch G. CT scan measurement of the humeral head subluxation in a saggittal plane method and application in primary gleno humeral osteoarthritis without humeral head elevation. [French] Mesure tomodensitometrique de la subluxation humerale antero-posterieure: Proposition d'une methode. Application a l'omarthrose centree. Revue de Chirurgie Orthopedique et Reparatrice de l'Appareil Moteur. 1998;84(6):508-14.
87. Friedman RJ. Glenohumeral translation after total shoulder arthroplasty. J Shoulder Elbow Surg. 1992 Nov;1(6):312-6.

88. Rouleau DM, Kidder JF, Pons-Villanueva J, Dynamidis S, Defranco M, Walch G. Glenoid version: How to measure it? Validity of different methods in two-dimensional computed tomography scans. Journal of Shoulder and Elbow Surgery. 2010 December;19(8):1230-7.
89. Amadi HO, Hansen UN, Wallace AL, Bull AM. A scapular coordinate frame for clinical and kinematic analyses. J Biomech. 2008 Jul;41(10):2144-9. Epub 2008/06/13.
90. Friedman RJ, Hawthorne KB, Genez BM. The use of computerized tomography in the measurement of glenoid version. J Bone Joint Surg Am. 1992 Aug;74(7):1032-7. Epub 1992/08/01.
91. Churchill RS, Brems JJ, Kotschi H. Glenoid size, inclination, and version: an anatomic study. J Shoulder Elbow Surg. 2001 2001 Jul-Aug;10(4):327-32.
92. Codsi MJ, Bennetts C, Gordiev K, Boeck DM, Kwon Y, Brems J, et al. Normal glenoid vault anatomy and validation of a novel glenoid implant shape. J Shoulder Elbow Surg. 2008 2008 May-Jun;17(3):471-8. Epub 2008/03/07.
93. Kwon YW, Powell KA, Yum JK, Brems JJ, Iannotti JP. Use of three-dimensional computed tomography for the analysis of the glenoid anatomy. J Shoulder Elbow Surg. 2005 2005 Jan-Feb;14(1):85-90.
94. Ganapathi A, McCarron JA, Chen X, Iannotti JP. Predicting normal glenoid version from the pathologic scapula: A comparison of 4 methods in 2- and 3-dimensional models. Journal of Shoulder and Elbow Surgery. 2011 March;20(2):234-44.
95. Habermeyer P, Magosch P, Luz V, Lichtenberg S. Three-dimensional glenoid deformity in patients with osteoarthritis: A radiographic analysis. Journal of Bone and Joint Surgery - Series A. 2006 June;88(6):1301-7.
96. Bryce CD, Davison AC, Okita N, Lewis GS, Sharkey NA, Armstrong AD. A biomechanical study of posterior glenoid bone loss and humeral head translation. Journal of Shoulder and Elbow Surgery. 2010 October;19(7):994-1002.
97. Farron A, Terrier A, Buchler P. Risks of loosening of a prosthetic glenoid implanted in retroversion. Journal of Shoulder and Elbow Surgery. 2006 July/August;15(4):521-6.
98. Nguyen D, Kippe M, Bigliani LU. Osteoarthritis: Overcoming the Slippery Slope. Seminars in Arthroplasty. 2008 March;19(1):23-9.
99. Shapiro TA, McGarry MH, Gupta R, Lee YS, Lee TQ. Biomechanical effects of glenoid retroversion in total shoulder arthroplasty. Journal of Shoulder and Elbow Surgery. 2007 May/June;16(3 SUPPL.):S90-S5.
100. Walch G, Ascani C, Boulahia A, Nove-Josserand L, Edwards TB. Static posterior subluxation of the humeral head: an unrecognized entity responsible for glenohumeral osteoarthritis in the young adult. Journal of shoulder and elbow surgery / American Shoulder and Elbow Surgeons 2002 2002;[et al.]. 11(4):309-14.
101. Spencer Jr EE, Valdevit A, Kambic H, Brems JJ, Iannotti JP. The effect of humeral component anteversion on shoulder stability with glenoid component retroversion. Journal of Bone and Joint Surgery - Series A. 2005 April;87(4):808-14.
102. Gregush RV, Galatz LM. Dealing with posterior glenoid wear: A slippery slope. Seminars in Arthroplasty. 2005 December;16(4):301-5.
103. Sears BW, Johnston PS, Ramsey ML, Williams GR. Glenoid bone loss in primary total shoulder arthroplasty: evaluation and management. The Journal of the American Academy of Orthopaedic Surgeons. 2012 Sep;20(9):604-13.
104. Rice RS, Sperling JW, Miletti J, Schleck C, Cofield RH. Augmented glenoid component for bone deficiency in shoulder arthroplasty. Clinical orthopaedics and related research. 2008 Mar;466(3):579-83.
105. Gregory T, Hansen U, Emery R, Amis AA, Mutchler C, Taillieu F, et al. Total shoulder arthroplasty does not correct the orientation of the eroded glenoid. Acta Orthop. 2012 Oct;83(5):529-35.
106. Hennigan SP, Iannotti JP. Instability after prosthetic arthroplasty of the shoulder. Orthop Clin North Am. 2001 Oct;32(4):649-59, ix.
107. Hasan SS, Leith JM, Campbell B, Kapil R, Smith KL, Matsen FA. Characteristics of unsatisfactory shoulder arthroplasties. J Shoulder Elbow Surg. 2002 2002 Sep-Oct;11(5):431-41.
108. Iannotti JP, Spencer EE, Winter U, Deffenbaugh D, Williams G. Prosthetic positioning in total shoulder arthroplasty. J Shoulder Elbow Surg. 2005 2005 Jan-Feb;14(1 Suppl S):111S-21S.

109. Spencer EE, Valdevit A, Kambic H, Brems JJ, Iannotti JP. The effect of humeral component anteversion on shoulder stability with glenoid component retroversion. J Bone Joint Surg Am. 2005 Apr;87(4):808-14.
110. Gregory T, Hansen U, Emery RJ, Augereau B, Amis AA. Developments in shoulder arthroplasty. Proc Inst Mech Eng H. 2007 Jan;221(1):87-96.
111. Terrier A, Büchler P, Farron A. Influence of glenohumeral conformity on glenoid stresses after total shoulder arthroplasty. J Shoulder Elbow Surg. 2006 2006 Jul-Aug;15(4):515-20.
112. Jong I-C, Rogers B, Springer W. Teaching von Mises stress: from principal axes to non-principal axes. 2009 [cited 2019 24/02/2019]; Available from: https://www.researchgate.net/publication/237586805_AC_2009-1437_TEACHING_VON_MISES_STRESS_FROM_PRINCIPAL_AXES_TO_NON-PRINCIPAL_AXES.
113. Dye D. Mechanical Behaviour Continuum Mechanics (Stress Tensors). 2013 [cited 2019 24/02/2019]; Available from: https://dyedavid.files.wordpress.com/2014/01/203b-stresstensors-dd-notes.pdf.
114. Stone KD, Grabowski JJ, Cofield RH, Morrey BF, An KN. Stress analyses of glenoid components in total shoulder arthroplasty. J Shoulder Elbow Surg. 1999 1999 Mar-Apr;8(2):151-8.
115. Hopkins AR, Hansen UN, Amis AA, Emery R. The effects of glenoid component alignment variations on cement mantle stresses in total shoulder arthroplasty. J Shoulder Elbow Surg. 2004 2004 Nov-Dec;13(6):668-75.
116. Anglin C, Wyss UP, Pichora DR. Glenohumeral contact forces. Proc Inst Mech Eng H. 2000;214(6):637-44.
117. Bergmann G, Graichen F, Bender A, Kääb M, Rohlmann A, Westerhoff P. In vivo glenohumeral contact forces--measurements in the first patient 7 months postoperatively. J Biomech. 2007;40(10):2139-49.
118. Westerhoff P, Graichen F, Bender A, Halder A, Beier A, Rohlmann A, et al. Measurement of shoulder joint loads during wheelchair propulsion measured in vivo. Clin Biomech (Bristol, Avon). 2011 Dec;26(10):982-9. Epub 2011/06/29.
119. Anglin C, Wyss UP, Pichora DR. Mechanical testing of shoulder prostheses and recommendations for glenoid design. J Shoulder Elbow Surg. 2000 2000 Jul-Aug;9(4):323-31.
120. Hill AM, Bull AM, Wallace AL, Johnson GR. Qualitative and quantitative descriptions of glenohumeral motion. Gait Posture. 2008 Feb;27(2):177-88. Epub 2007/05/16.
121. Prinold JA, Masjedi M, Johnson GR, Bull AM. Musculoskeletal shoulder models: a technical review and proposals for research foci. Proc Inst Mech Eng H. 2013 Oct;227(10):1041-57. Epub 2013/07/12.
122. Hopkins AR, Hansen UN, Amis AA, Taylor M, Gronau N, Anglin C. Finite element modelling of glenohumeral kinematics following total shoulder arthroplasty. J Biomech. 2006;39(13):2476-83. Epub 2005/09/30.
123. Geraldes DM, Hansen U, Amis AA. Parametric analysis of glenoid implant design and fixation type. J Orthop Res. 2017 Apr;35(4):775-84. Epub 2016/06/20.
124. Gagliano JR, Helms SM, Colbath GP, Przestrzelski BT, Hawkins RJ, DesJardins JD. A comparison of onlay versus inlay glenoid component loosening in total shoulder arthroplasty. J Shoulder Elbow Surg. 2017 Jul;26(7):1113-20. Epub 2017/03/27.
125. Braman JP, Falicov A, Boorman R, Matsen FA. Alterations in surface geometry in retrieved polyethylene glenoid component. J Orthop Res. 2006 Jun;24(6):1249-60.
126. Scarlat MM, Matsen IFA. Observations on retrieved polyethylene glenoid components. Journal of Arthroplasty. 2001;16(6):795-801.
127. Walch G, Young AA, Boileau P, Loew M, Gazielly D, Molé D. Patterns of loosening of polyethylene keeled glenoid components after shoulder arthroplasty for primary osteoarthritis: results of a multicenter study with more than five years of follow-up. J Bone Joint Surg Am. 2012 Jan;94(2):145-50.
128. Fucentese SF, Costouros JG, Kuhnel SP, Gerber C. Total shoulder arthroplasty with an uncemented soft-metal-backed glenoid component. Journal of Shoulder and Elbow Surgery. 2010 June;19(4):624-31.
129. Bonnevialle N, Melis B, Neyton L, Favard L, Mole D, Walch G, et al. Aseptic glenoid loosening or failure in total shoulder arthroplasty: revision with glenoid reimplantation. J Shoulder Elbow Surg. 2012 Oct 30.

130. Enneking WF, Campanacci DA. Retrieved human allografts. A clinicopathological study. Journal of Bone and Joint Surgery - Series A. 2001;83(7):971-86.
131. Steinmann SP, Cofield RH. Bone grafting for glenoid deficiency in total shoulder replacement. Journal of shoulder and elbow surgery / American Shoulder and Elbow Surgeons 2000 2000;[et al.]. 9(5):361-7.
132. Matsen FA, 3rd, Bicknell RT, Lippitt SB. Shoulder arthroplasty: the socket perspective. J Shoulder Elbow Surg. 2007 Sep-Oct;16(5 Suppl):S241-7.
133. Pritchett JW. Long-term results and patient satisfaction after shoulder resurfacing. Journal of Shoulder and Elbow Surgery. 2011 July;20(5):771-7.
134. Weldon IEJ, Boorman RS, Parsons IIM, Matsen IFA. "Ream and run": The principles and procedures of non-prosthetic glenoid arthroplasty with prosthetic humeral hemiarthroplasty. Techniques in Shoulder and Elbow Surgery. 2004 June;5(2):76-89.
135. Themistocleous GS, Zalavras CG, Zachos VC, Itamura JM. Biologic resurfacing of the glenoid using a meniscal allograft. Techniques in Hand and Upper Extremity Surgery. 2006 September;10(3):145-9.
136. Ellenbecker TS, Bailie DS, Lamprecht D. Humeral resurfacing hemiarthroplasty with meniscal allograft in a young patient with glenohumeral osteoarthritis. J Orthop Sports Phys Ther. 2008 May;38(5):277-86.
137. Nicholson GP, Goldstein JL, Romeo AA, Cole BJ, Hayden JK, Twigg SL, et al. Lateral meniscus allograft biologic glenoid arthroplasty in total shoulder arthroplasty for young shoulders with degenerative joint disease. Journal of Shoulder and Elbow Surgery. 2007 September/October;16(5 SUPPL.):S261-S6.
138. Krishnan SG, Nowinski RJ, Harrison D, Burkhead WZ. Humeral hemiarthroplasty with biologic resurfacing of the glenoid for glenohumeral arthritis: Two to fifteen-year outcomes. Journal of Bone and Joint Surgery - Series A. 2007 April;89(4):727-34.
139. Parsons IIM, Millett PJ, Warner JJP. Glenoid Wear after Shoulder Hemiarthroplasty: Quantitative Radiographic Analysis. Clinical Orthopaedics and Related Research. 2004 April(421):120-5.
140. Parsons IIM, Weldon IEJ, Matsen IFA. Spherical glenoid reaming with humeral hemiarthroplasty: A nonprosthetic, orthobiologic approach to shoulder arthroplasty. Techniques in Orthopaedics. 2007 March;22(1):62-70.
141. Cil A, Veillette CJ, Sanchez-Sotelo J, Sperling JW, Schleck CD, Cofield RH. Survivorship of the humeral component in shoulder arthroplasty. J Shoulder Elbow Surg. 2010 Jan;19(1):143-50.
142. Muratoglu OK, Ruberti J, Melotti S, Spiegelberg SH, Greenbaum ES, Harris WH. Optical analysis of surface changes on early retrievals of highly cross-linked and conventional polyethylene tibial inserts. J Arthroplasty. 2003 Oct;18(7 Suppl 1):42-7.
143. McKellop HA. The lexicon of polyethylene wear in artificial joints. Biomaterials. 2007 Dec;28(34):5049-57.
144. McKellop H, Shen FW, Lu B, Campbell P, Salovey R. Development of an extremely wear-resistant ultra high molecular weight polyethylene for total hip replacements. J Orthop Res. 1999 Mar;17(2):157-67.
145. Liao YS, Benya PD, McKellop HA. Effect of protein lubrication on the wear properties of materials for prosthetic joints. J Biomed Mater Res. 1999;48(4):465-73.
146. Hopkins AR, Hansen UN, Amis AA. Finite element models of total shoulder replacement: application of boundary conditions. Comput Methods Biomech Biomed Engin. 2005 Feb;8(1):39-44. Epub 2005/09/13.
147. Goreham-Voss CM, Hyde PJ, Hall RM, Fisher J, Brown TD. Cross-shear implementation in sliding-distance-coupled finite element analysis of wear in metal-on-polyethylene total joint arthroplasty: intervertebral total disc replacement as an illustrative application. J Biomech. 2010 Jun;43(9):1674-81.
148. Quental C, Folgado J, Fernandes PR, Monteiro J. Computational analysis of polyethylene wear in anatomical and reverse shoulder prostheses. Med Biol Eng Comput. 2015 Feb;53(2):111-22. Epub 2014/11/02.
149. Ribeiro NS, Folgado J, Fernandes PR, Monteiro J. Wear analysis in anatomical and reversed shoulder prostheses. Comput Methods Biomech Biomed Engin. 2011 Oct;14(10):883-92. Epub 2011/06/21.

150. Haggart J, Newton MD, Hartner S, Ho A, Baker KC, Kurdziel MD, et al. Neer Award 2017: wear rates of 32-mm and 40-mm glenospheres in a reverse total shoulder arthroplasty wear simulation model. J Shoulder Elbow Surg. 2017 Sep. Epub 2017/09/08.
151. Braun S, Schroeder S, Mueller U, Sonntag R, Buelhoff M, Kretzer JP. Influence of joint kinematics on polyethylene wear in anatomic shoulder joint arthroplasty. J Shoulder Elbow Surg. 2018 Apr. Epub 2018/04/23.
152. Tempelaere C, Pierrart J, Lefèvre-Colau MM, Vuillemin V, Cuénod CA, Hansen U, et al. Dynamic Three-Dimensional Shoulder Mri during Active Motion for Investigation of Rotator Cuff Diseases. PLoS One. 2016;11(7):e0158563. Epub 2016/07/19.
153. Mueller U, Braun S, Schroeder S, Schroeder M, Sonntag R, Jaeger S, et al. Influence of humeral head material on wear performance in anatomic shoulder joint arthroplasty. J Shoulder Elbow Surg. 2017 Oct;26(10):1756-64. Epub 2017/07/06.
154. Nam D, Kepler CK, Nho SJ, Craig EV, Warren RF, Wright TM. Observations on retrieved humeral polyethylene components from reverse total shoulder arthroplasty. Journal of Shoulder and Elbow Surgery. 2010 October;19(7):1003-12.
155. Nho SJ, Ala OL, Dodson CC, Figgie MP, Wright TM, Craig EV, et al. Comparison of conforming and nonconforming retrieved glenoid components. Journal of Shoulder and Elbow Surgery. 2008 November 2008/December;17(6):914-20.
156. Swieszkowski W, Frankle M, Bersee Harald EN, Kurzydlowski Krzysztof J. In vivo wear of polyethylene glenoid components in total shoulder arthroplasty. e-Polymers2005.
157. Terrier A, Merlini F, Pioletti DP, Farron A. Comparison of polyethylene wear in anatomical and reversed shoulder prostheses. J Bone Joint Surg Br. 2009 Jul;91(7):977-82.
158. Coley B, Jolles BM, Farron A, Aminian K. Arm position during daily activity. Gait Posture. 2008 Nov;28(4):581-7. Epub 2008/06/10.
159. Coley B, Jolles BM, Farron A, Pichonnaz C, Bassin JP, Aminian K. Estimating dominant upper-limb segments during daily activity. Gait Posture. 2008 Apr;27(3):368-75. Epub 2007/06/19.
160. Coley B, Jolles BM, Farron A, Aminian K. Detection of the movement of the humerus during daily activity. Med Biol Eng Comput. 2009 May;47(5):467-74. Epub 2009/03/10.
161. Patel RJ, Wright TM, Gao Y. Load transfer after cemented total shoulder arthroplasty. J Shoulder Elbow Surg. 2014 Oct;23(10):1553-62. Epub 2014/04/18.
162. Junaid S, Gupta S, Sanghavi S, Anglin C, Emery R, Amis A, et al. Failure mechanism of the all-polyethylene glenoid implant. Journal of Biomechanics. 2010 10/05/accepted;43(4):714-9.
163. Gregory T, Hansen U, Taillieu F, Baring T, Brassart N, Mutchler C, et al. Glenoid loosening after total shoulder arthroplasty: an in vitro CT-scan study. J Orthop Res. 2009 Dec;27(12):1589-95.
164. Franklin JL, Barrett WP, Jackins SE, Matsen FA. Glenoid loosening in total shoulder arthroplasty. Association with rotator cuff deficiency. J Arthroplasty. 1988;3(1):39-46.
165. Gregory T. Glenoid failure in Total Shoulder Arthroplasty London: Imperial College; 2010.
166. Streit JJ, Shishani Y, Greene ME, Nebergall AK, Wanner JP, Bragdon CR, et al. Radiostereometric and Radiographic Analysis of Glenoid Component Motion After Total Shoulder Arthroplasty. Orthopedics. 2015 Oct;38(10):e891-7.
167. Administration AGDoHTG. Hazard alert on Affinis Fracture Ceramic Head. 2014 [cited 2016 01/11/2016]; Available from: https://www.tga.gov.au/alert/affinis-fracture-ceramic-head-used-shoulder-replacements.
168. Driessnack RP, Ferlic DC, Wiedel JD. Dissociation of the glenoid component in the Macnab/English total shoulder arthroplasty. J Arthroplasty. 1990 Mar;5(1):15-8.
169. Papadonikolakis A, Matsen FA. Metal-Backed Glenoid Components Have a Higher Rate of Failure and Fail by Different Modes in Comparison with All-Polyethylene Components: A Systematic Review. J Bone Joint Surg Am. 2014 Jun;96(12):1041-7.
170. Valenti P, Valle P, Sauzieres P, Boughebri O, Moraiti T, Maqdes A, et al. Uncemented metal-back glenoid component in revision of aseptic glenoid loosening: a prospective study of 10 cases with a minimum follow-up of 2 years. Arch Orthop Trauma Surg. 2014 Jun;134(6):785-91.
171. Levy O, Copeland SA. Rotational dissociation of glenoid components in a total shoulder prosthesis: an indication that sagittal torque forces may be important in glenoid component design. J Shoulder Elbow Surg. 2001 2001 Mar-Apr;10(2):197.
172. Kirk PG, Sorger J. Failure of an implant after total shoulder arthroplasty. A case report. J Bone Joint Surg Am. 1997 Apr;79(4):597-8.

173. Sarah J, Sanjay G, Sanjay S, Carolyn A, Emery R, Andrew A, et al. Failure mechanism of the all-polyethylene glenoid implant. Journal of Biomechanics. 2010 10/05/accepted;43(4):714-9.
174. Habermeyer P, Schuller U. [Significance of the glenoid labrum for stability of the glenohumeral joint. An experimental study]. Unfallchirurg. 1990 Jan;93(1):19-26.
175. Itoi E. Pathophysiology and treatment of atraumatic instability of the shoulder. J Orthop Sci. 2004;9(2):208-13.
176. Kumar VP, Balasubramaniam P. The role of atmospheric pressure in stabilising the shoulder. An experimental study. J Bone Joint Surg Br. 1985 Nov;67(5):719-21.
177. Heinlein SA, Cosgarea AJ. Biomechanical Considerations in the Competitive Swimmer's Shoulder. Sports Health. 2010 Nov;2(6):519-25.
178. Johnson CD, McHugh MP, Wood T, Kibler B. Performance demands of professional male tennis players. Br J Sports Med. 2006 Aug;40(8):696-9; discussion 9.
179. Habermeyer P, Schuller U, Wiedemann E. The intra-articular pressure of the shoulder: an experimental study on the role of the glenoid labrum in stabilizing the joint. Arthroscopy. 1992;8(2):166-72.
180. Martin-Alarcon L, Schmidt TA. Rheological effects of macromolecular interactions in synovial fluid. Biorheology. 2016 Jul;53(2):49-67.
181. Schurz J, Ribitsch V. Rheology of synovial fluid. Biorheology. 1987;24(4):385-99.
182. Oates KM, Krause WE, Jones RL, Colby RH. Rheopexy of synovial fluid and protein aggregation. J R Soc Interface. 2006 Feb;3(6):167-74.
183. Haward SJ. Characterization of hyaluronic acid and synovial fluid in stagnation point elongational flow. Biopolymers. 2014 Mar;101(3):287-305.
184. Zhang Z, Barman S, Christopher GF. The role of protein content on the steady and oscillatory shear rheology of model synovial fluids. Soft Matter. 2014 Aug;10(32):5965-73.
185. Bingöl A, Lohmann D, Püschel K, Kulicke WM. Characterization and comparison of shear and extensional flow of sodium hyaluronate and human synovial fluid. Biorheology. 2010;47(3-4):205-24.
186. Jay GD, Waller KA. The biology of lubricin: near frictionless joint motion. Matrix Biol. 2014 Oct;39:17-24. Epub 2014/08/27.
187. Liang J. Investigation of Synthetic and Natural Lubricants: North Carolina State University; 2008.
188. Heuberger MP, Widmer MR, Zobeley E, Glockshuber R, Spencer ND. Protein-mediated boundary lubrication in arthroplasty. Biomaterials. 2005 Apr;26(10):1165-73.
189. Chandran Suja V, Barakat AI. A Mathematical Model for the Sounds Produced by Knuckle Cracking. Sci Rep. 2018 Mar;8(1):4600. Epub 2018/03/29.
190. International A. ASTM F2028 - 14 Standard Test Methods for Dynamic Evaluation of Glenoid Loosening or Disassociation. 2017 [cited 2017 07.01.2017]; Available from: https://www.astm.org/Standards/F2028.htm.
191. Wirth MA, Klotz C, Deffenbaugh DL, McNulty D, Richards L, Tipper JL. Cross-linked glenoid prosthesis: A wear comparison to conventional glenoid prosthesis with wear particulate analysis. Journal of Shoulder and Elbow Surgery. 2009 January 2009/February;18(1):130-7.
192. Kohut G, Dallmann F, Irlenbusch U. Wear-induced loss of mass in reversed total shoulder arthroplasty with conventional and inverted bearing materials. J Biomech. 2012 Feb;45(3):469-73. Epub 2011/12/27.
193. Adam P, Farizon F, Fessy MH. Dual mobility retentive acetabular liners and wear: surface analysis of 40 retrieved polyethylene implants. Orthop Traumatol Surg Res. 2014 Feb;100(1):85-91.
194. Chuter GS, Cloke DJ, Mahomed A, Partington PF, Green SM. Wear analysis of failed acetabular polyethylene: a comparison of analytical methods. J Bone Joint Surg Br. 2007 Feb;89(2):273-9.
195. Teeter MG, Naudie DD, Charron KD, Holdsworth DW. Three-dimensional surface deviation maps for analysis of retrieved polyethylene acetabular liners using micro-computed tomography. J Arthroplasty. 2010 Feb;25(2):330-2.
196. Teeter MG, Naudie DD, McErlain DD, Brandt JM, Yuan X, Macdonald SJ, et al. In vitro quantification of wear in tibial inserts using microcomputed tomography. Clin Orthop Relat Res. 2011 Jan;469(1):107-12.
197. Teeter MG, Parikh A, Taylor M, Sprague J, Naudie DD. Wear and creep behavior of total knee implants undergoing wear testing. J Arthroplasty. 2015 Jan;30(1):130-4.
198. Phasevision. 2016 [cited 2016 29-08-2016]; Products].

199. Bitar D, Parvizi J. Biological response to prosthetic debris. World J Orthop. 2015 Mar;6(2):172-89.
200. Ingham E, Fisher J. Biological reactions to wear debris in total joint replacement. Proc Inst Mech Eng H. 2000;214(1):21-37.
201. Goodman SB, Gibon E, Yao Z. The basic science of periprosthetic osteolysis. Instr Course Lect. 2013;62:201-6.
202. Harris WH. Wear and periprosthetic osteolysis: the problem. Clin Orthop Relat Res. 2001 Dec(393):66-70.
203. Hallab NJ, Jacobs JJ. Biologic effects of implant debris. Bulletin of the NYU Hospital for Joint Diseases. 2009;67(2):182-8.
204. Lewicki KA, Bell JE, Van Citters DW. Analysis of polyethylene wear of reverse shoulder components: A validated technique and initial clinical results. J Orthop Res. 2016 Jun.
205. Carpenter S, Pinkas D, Newton MD, Kurdziel MD, Baker KC, Wiater JM. Wear rates of retentive versus nonretentive reverse total shoulder arthroplasty liners in an in vitro wear simulation. J Shoulder Elbow Surg. 2015 Sep;24(9):1372-9.
206. | VDI/VDE 2634 Blatt 1. Deutsch; 2002-05; Available from: http://www.vdi.eu/guidelines/vdivde_2634_blatt_1-optische_3d_messsysteme_bildgebende_systeme_mit_punktfoermiger_antastung/.
207. Swieszkowski W, Frankle M, Bersee Harald EN, Kurzydlowski Krzysztof J. In vivo wear of polyethylene glenoid components in total shoulder arthroplasty. e-Polymers2005.
208. Samujh C, Bhimani S, Smith L, Malkani AL. Wear Analysis of Second-generation Highly Cross-Linked Polyethylene in Primary Total Hip Arthroplasty. Orthopedics. 2016 Aug:1-5.
209. Garvin KL, White TC, Dusad A, Hartman CW, Martell J. Low wear rates seen in THAs with highly crosslinked polyethylene at 9 to 14 years in patients younger than age 50 years. Clin Orthop Relat Res. 2015 Dec;473(12):3829-35.
210. Pourzal R, Knowlton CB, Hall DJ, Laurent MP, Urban RM, Wimmer MA. How Does Wear Rate Compare in Well-functioning Total Hip and Knee Replacements? A Postmortem Polyethylene Liner Study. Clin Orthop Relat Res. 2016 Feb.
211. Selvarajah E, Hooper G, Grabowski K, Frampton C, Woodfield TB, Inglis G. The rates of wear of X3 highly cross-linked polyethylene at five years when coupled with a 36 mm diameter ceramic femoral head in young patients. Bone Joint J. 2015 Nov;97-B(11):1470-4.
212. Williams GR, Abboud JA. Total shoulder arthroplasty: glenoid component design. J Shoulder Elbow Surg. 2005 2005 Jan-Feb;14(1 Suppl S):122S-8S.
213. Churchill RS. Trends in glenoid component design in unconstrained shoulder arthroplasty. J Shoulder Elbow Surg. 2011 Mar;20(2 Suppl):S41-6.
214. Carpenter SR, Urits I, Murthi AM. Porous metals and alternate bearing surfaces in shoulder arthroplasty. Curr Rev Musculoskelet Med. 2016 Mar;9(1):59-66.
215. Cheung EV, Sperling JW, Cofield RH. Polyethylene insert exchange for wear after total shoulder arthroplasty. Journal of Shoulder and Elbow Surgery. 2007 September;16(5):574-8.
216. Boileau P, Avidor C, Krishnan SG, Walch G, Kempf JF, Mole D. Cemented polyethylene versus uncemented metal-backed glenoid components in total shoulder arthroplasty: a prospective, double-blind, randomized study. Journal of shoulder and elbow surgery / American Shoulder and Elbow Surgeons 2002 2002;[et al.]. 11(4):351-9.
217. Boileau P, Moineau G, Morin-Salvo N, Avidor C, Godenèche A, Lévigne C, et al. Metal-backed glenoid implant with polyethylene insert is not a viable long-term therapeutic option. J Shoulder Elbow Surg. 2015 Oct;24(10):1534-43.
218. Papadonikolakis A, Neradilek MB, Matsen FA. Failure of the glenoid component in anatomic total shoulder arthroplasty: a systematic review of the English-language literature between 2006 and 2012. J Bone Joint Surg Am. 2013 Dec;95(24):2205-12.
219. Tammachote N, Sperling JW, Vathana T, Cofield RH, Harmsen WS, Schleck CD. Long-term results of cemented metal-backed glenoid components for osteoarthritis of the shoulder. Journal of Bone and Joint Surgery - Series A. 2009 01 Jan;91(1):160-6.
220. Taunton MJ, McIntosh AL, Sperling JW, Cofield RH. Total shoulder arthroplasty with a metal-backed, bone-ingrowth glenoid component. Medium to long-term results. J Bone Joint Surg Am. United States2008. p. 2180-8.
221. Giori NJ, Beaupré GS, Carter DR. The influence of fixation peg design on the shear stability of prosthetic implants. J Orthop Res. 1990 Nov;8(6):892-8.

222. Pomwenger W, Entacher K, Resch H, Schuller-Götzburg P. Multi-patient finite element simulation of keeled versus pegged glenoid implant designs in shoulder arthroplasty. Med Biol Eng Comput. 2015 Sep;53(9):781-90.
223. Lacroix D, Murphy LA, Prendergast PJ. Three-dimensional finite element analysis of glenoid replacement prostheses: a comparison of keeled and pegged anchorage systems. J Biomech Eng. 2000 Aug;122(4):430-6.
224. Anglin C, Wyss UP, Nyffeler RW, Gerber C. Loosening performance of cemented glenoid prosthesis design pairs. Clin Biomech (Bristol, Avon). 2001 Feb;16(2):144-50.
225. Edwards TB, Labriola JE, Stanley RJ, O'Connor DP, Elkousy HA, Gartsman GM. Radiographic comparison of pegged and keeled glenoid components using modern cementing techniques: a prospective randomized study. J Shoulder Elbow Surg. 2010 Mar;19(2):251-7.
226. Gartsman GM, Elkousy HA, Warnock KM, Edwards TB, O'Connor DP. Radiographic comparison of pegged and keeled glenoid components. J Shoulder Elbow Surg. 2005 2005 May-Jun;14(3):252-7.
227. Lazarus MD, Jensen KL, Southworth C, Matsen FA. The radiographic evaluation of keeled and pegged glenoid component insertion. J Bone Joint Surg Am. 2002 Jul;84-A(7):1174-82.
228. Arnold RM, High RR, Grosshans KT, Walker CW, Fehringer EV. Bone presence between the central peg's radial fins of a partially cemented pegged all poly glenoid component suggest few radiolucencies. J Shoulder Elbow Surg. 2011 Mar;20(2):315-21.
229. Churchill RS, Zellmer C, Zimmers HJ, Ruggero R. Clinical and radiographic analysis of a partially cemented glenoid implant: five-year minimum follow-up. J Shoulder Elbow Surg. 2010 Oct;19(7):1091-7.
230. Wirth MA, Korvick DL, Basamania CJ, Toro F, Aufdemorte TB, Rockwood CA. Radiologic, mechanical, and histologic evaluation of 2 glenoid prosthesis designs in a canine model. J Shoulder Elbow Surg. 2001 2001 Mar-Apr;10(2):140-8.
231. Budge MD, Kurdziel MD, Baker KC, Wiater JM. A biomechanical analysis of initial fixation options for porous-tantalum-backed glenoid components. J Shoulder Elbow Surg. 2013 May;22(5):709-15.
232. Budge MD, Nolan EM, Heisey MH, Baker K, Wiater JM. Results of total shoulder arthroplasty with a monoblock porous tantalum glenoid component: a prospective minimum 2-year follow-up study. J Shoulder Elbow Surg. 2013 Apr;22(4):535-41.
233. Kocsis G, Thyagarajan DS, Fairbairn KJ, Wallace WA. A new classification of glenoid bone loss to help plan the implantation of a glenoid component before revision arthroplasty of the shoulder. Bone Joint J. 2016 Mar;98-B(3):374-80.
234. Nicholson GP, Strauss EJ, Sherman SL. Scapular notching: Recognition and strategies to minimize clinical impact. Clinical orthopaedics and related research. 2011 Sep;469(9):2521-30.
235. Gomoll A, Wanich T, Bellare A. J-integral fracture toughness and tearing modulus measurement of radiation cross-linked UHMWPE. J Orthop Res. 2002 Nov;20(6):1152-6.
236. Nho SJ, Nam D, Ala OL, Craig EV, Warren RF, Wright TM. Observations on retrieved glenoid components from total shoulder arthroplasty. Journal of Shoulder and Elbow Surgery. 2009 May 2009/June;18(3):371-8.
237. Reynolds SE, Malkani AL, Ramakrishnan R, Yakkanti MR. Wear analysis of first-generation highly cross-linked polyethylene in primary total hip arthroplasty: an average 9-year follow-up. J Arthroplasty. 2012 Jun;27(6):1064-8.
238. Geerdink CH, Grimm B, Vencken W, Heyligers IC, Tonino AJ. Cross-linked compared with historical polyethylene in THA: an 8-year clinical study. Clin Orthop Relat Res. 2009 Apr;467(4):979-84.
239. Sato T, Nakashima Y, Akiyama M, Yamamoto T, Mawatari T, Itokawa T, et al. Wear resistant performance of highly cross-linked and annealed ultra-high molecular weight polyethylene against ceramic heads in total hip arthroplasty. J Orthop Res. 2012 Dec;30(12):2031-7.
240. Saikko V, Calonius O, Keränen J. Wear of conventional and cross-linked ultra-high-molecular-weight polyethylene acetabular cups against polished and roughened CoCr femoral heads in a biaxial hip simulator. J Biomed Mater Res. 2002;63(6):848-53.
241. Williams GR, Iannotti JP. Alternative bearing surfaces--do we need them? Am J Orthop (Belle Mead NJ). 2007 Dec;36(12 Suppl 1):15-7.
242. Fritsch EW, Gleitz M. Ceramic femoral head fractures in total hip arthroplasty. Clin Orthop Relat Res. 1996 Jul(328):129-36.

243. Cuckler JM, Bearcroft J, Asgian CM. Femoral head technologies to reduce polyethylene wear in total hip arthroplasty. Clin Orthop Relat Res. 1995 Aug(317):57-63.
244. Gauci MO, Winter M, Dumontier C, Bronsard N, Allieu Y. Clinical and radiologic outcomes of pyrocarbon radial head prosthesis: midterm results. J Shoulder Elbow Surg. 2016 Jan;25(1):98-104.
245. Dickson DR, Nuttall D, Watts AC, Talwalkar SC, Hayton M, Trail IA. Pyrocarbon Proximal Interphalangeal Joint Arthroplasty: Minimum Five-Year Follow-Up. J Hand Surg Am. 2015 Nov;40(11):2142-8.e4.
246. Houdek MT, Wagner ER, Rizzo M, Moran SL. Metacarpophalangeal Joint Arthroplasty in the Setting of Trauma. J Hand Surg Am. 2015 Dec;40(12):2416-20.
247. Reissner L, Schindele S, Hensler S, Marks M, Herren DB. Ten year follow-up of pyrocarbon implants for proximal interphalangeal joint replacement. J Hand Surg Eur Vol. 2014 Jul;39(6):582-6.